DYNAMIC RESPONSE OF ASYMMETRIC SHEAR WALL-FRAME BUILDING STRUCTURES

DYNAMIC RESPONSE OF ASYMMETRIC SHEAR WALL-FRAME BUILDING STRUCTURES

By

M.F. ISHAC, B.Sc. (Civil)

A Thesis

Submitted to the School of Graduate Studies

in Partial Fulfilment of the Requirements

for the Degree

Master of Engineering

McMaster University

December, 1975

MASTER OF ENGINEERING (1975) McMASTER UNIVERSITY
(Civil Engineering) Hamilton, Ontario

TITLE: Dynamic Response of Asymmetric Shear Wall-Frame Building Structures

AUTHOR: M.F. Ishac, B.Sc. (Cairo Univeristy) Cairo, Egypt

SUPERVISOR: Dr. A.C. Heidebrecht

NUMBER OF PAGES: x, 135

SCOPE AND CONTENTS:

A mathematical model to compute the dynamic response of asymmetric shear wall-frame building structures is presented. The formulation is developed in detail for the case of one axis of symmetry. Also, the method is derived for the case of relatively uniform stiffining element with respect to height and it is based on the continuous approach. The lateral load resisting elements, as elastic continua, are combined by using the equilibrium and compatibility conditions to yield a coupled set of partial differential equations. Eigenvalues and eigenvectors are determined using numerical procedures and results are presented to show the natural periods and mode shapes for several practical structures. The total dynamic response of such structures subjected to earthquake ground motions is determined and results are presented for excitation due to several different earthquakes. The response results are compared with those obtained by using a static analysis with the objective of evaluating the adequacy of such static loading provisions and developing guidelines to define situations for which a detailed dynamic response computation is required.

ACKNOWLEDGEMENTS

I would like to express my sincere appreciation to my research supervisor, Dr. A.C. Heidebrecht, for his guidance, interest and encouragement during every stage of the research work.

I am thankful to the National Research Council of Canada for providing the financial support for this investigation and the Computer Centre of McMaster University for making possible the computations involved in this work.

I would also like to thank the following individuals

(i) Dr. W.K. Tso, Professor, for making useful suggestions from time to time.

(ii) Dr. A. Rutenberg, Visiting Associate Professor, for helping me on various occasions.

(iii) Dr. A.C. Heidebrecht, Chairman, for making available to me the departmental teaching assistantship.

(iv) Miss Susan Baker, Secretary, for making this thesis presentable.

And finally, and personally most important, for their understanding and encouragement, this thesis is dedicated to my parents.

TABLE OF CONTENTS

		Page
CHAPTER I -	INTRODUCTION	1
	1. Interaction of Shear Walls and Frames in Multistory Structures	1
	2. Review of Methods of Analysis of Wall-Frame Building Structures	3
	3. Scope of Present Study	7
CHAPTER II -	DYNAMIC ANALYSIS OF ASYMMETRIC WALL-FRAME STRUCTURES	9
	1. Introduction	9
	2. Equation of Motion of Asymmetric Wall-Frame Structures	10
	3. Exact Treatment for Natural Frequencies and Mode Shapes for a 2-Dimensional Wall-Frame Structure	15
	4. Special Case of a Single Wall-Frame System	43
CHAPTER III -	RESPONSE ANALYSIS	63
	1. Introduction	63
	2. Treatment for Normalized Mode Shapes	63
	3. Centre of Mass Response due to a Sinusoidal Base Motion	67
	4. Centre of Mass Response due to Seismic Ground Motion	71
CHAPTER IV -	RESPONSE PARAMETERS FOR ASYMMETRIC WALL-FRAME STRUCTURES SUBJECTED TO SEISMIC GROUND MOTIONS	80
	1. Introduction	80
	2. Response Parameters	81
	3. Example Wall-Frame Structure subjected to different Earthquake loading	86
	4. Amplification Parameters	88

Page

CHAPTER V - CONCLUSIONS 122

REFERENCES 126

APPENDICES 131

1. List of FØRTRAN IV Computer Programmes 131
2. List of Symbols 132
3. Response Comparison 135

LIST OF FIGURES

Figure	Title	Page
1	Typical Deflected Shapes	2
1-a	Free Frame	2
1-b	Free Wall	2
1-c	Combined Frame and Wall	2
2	Coordinate System for a Typical Cross-Section of Asymmetric Wall-Frame Structure	11
3	Coordinate System for a Typical Cross-Section of a 2-Dimensional Wall-Frame Structure.	17
4	Floor Plan for Example Structure I	26
5	The Coupled Flexural-Torsional Mode Shapes - Example Structure I	31
6	Floor Plan for Example Structure II	35
7-a	The Coupled Flexural-Torsional Mode Shapes - Building 2 of Example Structure II	46
7-b	The Coupled Flexural-Torsional Mode Shapes - Building 3 of Example Structure II	49
7-c	The Coupled Flexural-Torsional Mode Shapes - Building 4 of Example Structure II	52
8	Coordinate System for a Typical Cross-Section of a Single Wall-Frame System	55
9	Earthquake Record of EL CENTRO *W-E* - May 18, 1940	87
10-a	Variation of Top Displacement $\bar{Y}$ with Time EL CENTRO *W-E* - Example Structure I	89
10-b	Variation of Top Rotation $\bar{\theta}$ with Time EL CENTRO *W-E* - Example Structure I	90
10-c	Variation of Base Moment M_W with Time EL CENTRO *W-E* - Example Structure I	91

Figure	Title	Page
10-d	Variation of Base Shear S_W with Time EL CENTRO *W-E* - Example Structure I	92
10-e	Variation of Base Bimoment B_W with Time EL CENTRO *W-E* - Example Structure I	93
10-f	Variation of Base Torsion T_W with Time EL CENTRO *W-E* - Example Structure I	94
11	Earthquake Record of EL CENTRO *N-S*, May 18, 1940	96
12	Earthquake Record of TAFT *N21E*, July 21, 1952	97
13	Earthquake Record of SAN FRANCISCO *N10E*, March 22, 1957	98
14-a	Variation of Top Displacement $\bar{Y}$ with Time EL CENTRO *N-S* - Example Structure I	99
14-b	Variation of Top Rotation $\bar{\theta}$ with Time EL CENTRO *N-S* - Example Structure I	100
14-c	Variation of Base Moment M_W with Time EL CENTRO *N-S* - Example Structure I	101
14-d	Variation of Base Shear S_W with Time EL CENTRO *N-S* - Example Structure I	102
14-e	Variation of Base Bimoment B_W with Time EL CENTRO *N-S* - Example Structure I	103
14-f	Variation of Base Torsion T_W with Time EL CENTRO *N-S* - Example Structure I	104
15-a	Variation of Top Displacement $\bar{Y}$ with Time TAFT *N21E* - Example Structure I	105
15-b	Variation of Top Rotation $\bar{\theta}$ with Time TAFT *N21E* - Example Structure I	106
15-c	Variation of Base Moment M_W with Time TAFT *N21E* - Example Structure I	107

Figure	Title	Page
15-d	Variation of Base Shear S_W with Time TAFT *N21E* - Example Structure I	108
15-e	Variation of Base Bimoment B_W with Time TAFT *N21E* - Example Structure I	109
15-f	Variation of Base Torsion T_W with Time TAFT *N21E* - Example Structure I	110
16-a	Variation of Top Displacement $\bar{Y}$ with Time SAN FRANCISCO *N10E* - Example Structure I	111
16-b	Variation of Top Rotation $\bar{\theta}$ with Time SAN FRANCISCO *N10E* - Example Structure I	112
16-c	Variation of Base Moment M_W with Time SAN FRANCISCO *N10E* - Example Structure I	113
16-d	Variation of Base Shear S_W with Time SAN FRANCISCO *N10E* - Example Structure I	114
16-e	Variation of Base Bimoment B_W with Time SAN FRANCISCO *N10E* - Example Structure I	115
16-f	Variation of Base Torsion T_W with Time SAN FRANCISCO *N10E* - Example Structure I	116

LIST OF TABLES

Table	Title	Page
1.a	Physical and Geometrical Properties of Walls - Example Structure I	27
1.b	Physical and Geometrical Properties of Frames - Example Structure I	28
2	Natural Periods of Vibration in Example Structure I - Comparison of Results	30
3	The Predominant Motion for each Mode of Vibration - Example Structure I	30
4.a	Stiffness Properties of the Core - Example Structure II	36
4.b	Shear Stiffnesses of the Frames - Example Structure II	36
4.c	Geometrical Properties of the Columns - Example Structure II	37
4.d	The Basic Parameters associated with the Dynamic Properties of the four Buildings - Example Structure II	38
5.a	Natural Periods of Vibration in Building 1 of Example Structure II - Comparison of Results	39
5.b	Natural Periods of Vibration in Building 2 of Example Structure II - Comparison of Results	40
5.c	Natural Periods of Vibration in Building 3 of Example Structure II - Comparison of Results	41
5.d	Natural Periods of Vibration in Building 4 of Example Structure II - Comparison of Results	42
6.a	Effect of Core Eccentricity on the Natural Periods - Example Structure II	44
6.b	Effect of Core Eccentricity on the ratio δ_θ / δ_Y - Example Structure II	45

Table	Title	Page
7	Comparison of Exact and Approximate Natural Periods for Building 4 of Example Structure II	62
8	Variation of the Modal Participation Factor with the Modes of Vibration - Example Structure I	76
9	Variation of the Modal Participation Factor with the Modes of Vibration - Example Structure II	77
10	Maximum Response Parameters due to the *W-E* Component of EL CENTRO Earthquake - Example Structure I	95
11	Maximum Response Parameters due to various Earthquake Records applied to Example Structure I - Comparison of Results	117
12	Comparison between the Dynamic Response Analysis and the Static Analysis of the 1975 NBC code - Example Structure I	120
13	Comparison between the Dynamic Response Analysis and the Static Analysis of reference (24) - Example Structure I	121
14	Comparison between the maximum response parameters obtained from the Dynamic Response Analysis and those computed by the Response Spectrum Technique	135

CHAPTER I

INTRODUCTION

1. Interaction of Shear Walls and Frames in Multistory Structures

The interaction of shear walls with frames in multistory structures has been studied in recent years and several methods of analysis have been proposed. This interaction is a special case of indeterminancy, in which two basically different components are tied together to produce one structure. As buildings increase in height, it becomes more important to ensure adequate lateral stiffness to resist loads which may arise due to wind, seismic or blast effects. If the frame alone is considered to take the full lateral load, it would develop moments in columns and beams to resist the total shear at each storey and as a result it would deflect as in Figure 1-a. If a shear wall, on the other hand, is considered to resist all the lateral loads, it would develop moments at each floor equal to the overturning moment at that level and it would deflect as in Figure 1-b. By comparing these two figures, it can be seen that a rigid frame deflects predominantly in a shear mode and a shear wall deflects predominantly in a bending mode. If a shear wall and a frame interact in a building, each one will try to obstruct the other from taking its natural free deflected shape, and as a result a redistribution of forces between the two would be expected. As shown in Figure 1-c the frame will restrain or pull the shear wall back in the upper stories, while in the lower regions the opposite will occur. A

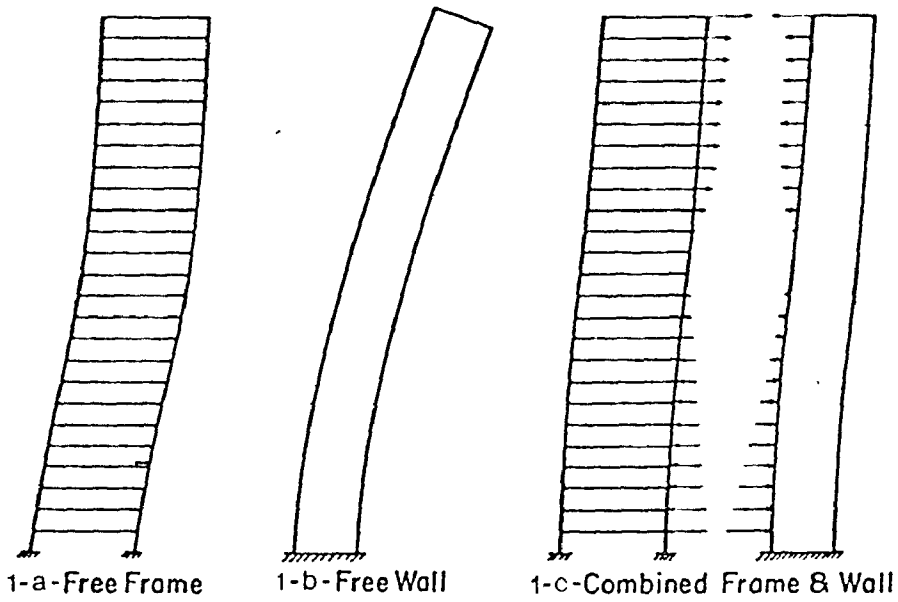

FIGURE 1 TYPICAL DEFLECTED SHAPES

considerable amount of research work has been published on this interaction of shear walls with frames and the static and dynamic analysis of this particular class of building structures have been widely treated in recent years.

2. Review of Methods of Analysis of Wall-Frame Building Structures

In 1972, a report describing the current numerical methods of three-dimensional analysis of tall buildings under the action of static horizontal loads was presented by Stamato (26). The various methods of three-dimensional analysis may be classified according to two different criteria. The first refers to the stiffness of the floor slabs and the second deals with the treatment by continuous or discrete methods. In the first classification criterion, the majority of the current methods assume the floor slabs as being completely flexible transversally and infinitely rigid in their own planes. The other methods consider the actual values of the floor stiffness by finite element techniques. For the second classification criterion, in the continuous methods the horizontal elements which connect the vertical resistant elements are substituted by a continuous medium of equivalent stiffness distributed along the height of the building. These methods lead to a system of differential equations which, after being integrated, supply the displacements and internal forces in the whole structure. In the discrete methods the matrix techniques are used and these methods lead to a system of many linear equations which, after being solved, supply the displacements and internal forces in the whole structure.

The dynamic analysis is treated as an extension of static analysis.

The formulation of the static problem being determined, that of the dynamic problem can be obtained by including the inertial forces of the building structure. The governing equation of motion is used to determine the dynamic properties of the entire structure. These dynamic properties are the natural frequencies of vibration and the corresponding mode shapes.

Using the stiffness matrix method, Clough, King and Wilson (4) presented an efficient digital computer method for structural analysis of large multistorey buildings laid out in a rectangular grid pattern containing shear walls and frames and subjected to both vertical and lateral loading. It is assumed that floor slabs are rigid in their own planes. The method is based on the development of a tri-diagonal stiffness matrix of each frame in the building, its reduction by recursion relationships to the lateral frame stiffness, and finally the superposition of the lateral frame stiffnesses to obtain the total building stiffness. This method can be extended for dynamic analysis of this type of structure.

In the analysis by Rosman (23), the continuous method is used and the floors are assumed to be infinitely rigid in their own planes, as compared to the walls and frames, while they are sufficiently flexible out of their planes. The different vertical settlements of walls and frames do not affect the internal forces due to the lateral loading and the axial deformations of the columns have no influence on the load distribution. Solutions are obtained when the walls and

frames are in different planes or in the same plane using approximate method or by exact integration of the differential equations.

Adopting Rosman's way of analysing a shear wall-frame structure as a combination of flexural and shear cantilever beams, Heidebrecht and Stafford Smith (12) presented a simple hand method for analysis of uniform wall-frame structures. In this method, a fourth-order differential equation is derived with the lateral deflection of the structure as the unknown. The solution of the differential equation yields the lateral deflection and hence the force components. The three common types of loadings are considered and design curves for deflection, moment, shearing force and horizontal interaction force are included. The method is extended for dynamic analysis and the basic mathematical model of the shear-flexure beam is used to determine the dynamic properties of such tall building structures.

Gluck (8) presented a three-dimensional continuous method for structures consisting of simple or coupled, prismatic or non-prismatic, shear walls and frames arranged asymmetrically in the floor plan. Based on the compatibility and equilibrium conditions, a set of coupled differential equations is derived with the translational and rotational displacement functions as the unknowns. This analysis, however, does not include the effect of axial deformations of the walls and columns. The method is extended for dynamic analysis (1) and the problem is reduced to an eigenvalue problem of order 12 independent of the number of stories. Allowing different foundation conditions, the method is worked out for full restraint of the structure at the base

or a rigid raft foundation on an elastic subgrade; the normal modes are determined for each case.

The analysis of the elastic earthquake response of non-symmetric multistory structures is presented by Mendelson and Baruch (19). The analysis is based on the continuous connection method, using the normal modes of the structure and taking into consideration the partial restraint of the structure in the subgrade. The method consists, in principle, in resolving the structure into two subsystems: the shear walls, which are cantilevers fixed in the base, and the frames and connecting beams, whose shear resistance is proportional to the first derivative of the displacement. The displacements and internal forces are obtained as continuous functions along the vertical axis.

Using the same continuous approach, Stamato and Mancini (27) have presented a three-dimensional interaction of walls and frames. The unknowns of this analysis are the lateral displacements in the X and Y directions and the rotational deformation about the Z axis. Rutenberg and Heidebrecht (24) reduced this problem to relatively simple hand method for the static analysis of uniform asymmetric flexural wall-frame structures subjected to lateral loads. This static analysis is extended and an approximate method for evaluation of the dynamic properties of such structures is proposed by Rutenberg, Tso and Heidebrecht (25). An exact solution is first given for the case in which the coefficient matrix of the dynamic equilibrium equations satisfies certain conditions. Using perturbation analysis, the method is then applied to the more general case in which these

conditions are only approximately satisfied.

The dynamic analysis of assymmetric wall-frame buildings has been developed by Heidebrecht (14) and an approximate method for the computation of coupled dynamic frequencies and mode shapes for uniform tall building structures is described.

3. Scope of Present Study

The purpose of this thesis is to develop a mathematical model to compute the dynamic response of asymmetric shear wall-frame building structures. This particular class of building structure includes those whose lateral load resisting system is made up of an asymmetrically arranged grouping of flexural type (shear walls) and shear type (frames) elements. These elements may be located in any asymmetric fashion, but for the purpose of comparison with normal static planar loading procedures, the method is developed in detail for the case of one axis of symmetry. Also, the method is derived for the case of relatively uniform stiffining elements with respect to height and it is based on the continuous approach. Each element is modelled as an elastic continuum, i.e. either as a shear or flexural beam. The elements are combined by using the equilibrium and compatibility conditions to yield a coupled set of partial differential equations. Eigenvalues and eigenvectors can be determined using numerical procedures. Results are presented to show the natural periods and mode shapes for several practical structures. A numerical integration procedure is used to determine the total dynamic response of such structures subjected to earthquake ground motions and results are

presented for excitation due to several different earthquakes. The response results are analysed to consider the influence of the flexural-torsional coupling on the dynamic amplification of the various response parameters. Results are also compared with those obtained by using a static analysis with the objective of evaluating the adequacy of such static loading provisions and developing guidelines to define situations for which a detailed dynamic response computation is required.

CHAPTER II

DYNAMIC ANALYSIS OF ASYMMETRIC WALL-FRAME STRUCTURES

1. Introduction

The dynamic analysis of multistory structures has been widely treated in recent years. Heidebrecht (14) has presented a method for the dynamic analysis of uniform tall building structures containing both flexural and shear type resisting elements. This method permits the determination of the coupled dynamic properties by hand computation using either slide rule or desk calculator.

In this chapter, a study of the coupled dynamic behaviour of a wall-frame structure is presented. The continuous method is used for analysis. The governing equations of motion with appropriate boundary conditions are given. An exact treatment for determining natural frequencies and coupled flexural-torsional modes of vibration for a two-dimensional wall-frame structure is presented. A special case of a single wall-frame system is studied.

The dynamic analysis of the wall-frame system depends upon the following assumptions:

(i) The floors act as rigid diaphragms in their own planes.

(ii) The lateral load resisting elements have the same relative cross-sectional position at all floor levels.

(iii) The vertical forces acting on the lateral load resisting elements

are negligible.

(iv) All the lateral load resisting elements are either flexural or shear type elements.

(v) The geometric properties of the lateral load resisting elements are vertically uniform for the entire height of the building.

(vi) The structure is fully restrained at the base.

Figure 2 shows the coordinate system for a typical cross section of the structure. The X-Y coordinate system coincides in direction with the principal axes of the structural components. The coordinate Z axis, positive upwards, is located at the centre of mass.

2. Equation of Motion of Asymmetric Wall-Frame Structures

The differential equations for the statical equilibrium of a shear wall i whose centroid is located at the coordinate position (e_{Xi}, e_{Yi}) are given by

$$w_{Xi}(Z) = EI_{Xi} \frac{d^4 X_i}{dZ^4} \tag{2.1a}$$

$$w_{Yi}(Z) = EI_{Yi} \frac{d^4 Y_i}{dZ^4} \tag{2.1b}$$

$$w_{\theta i}(Z) = EI_{\omega i} \frac{d^4 \theta_i}{dZ^4} - GJ_i \frac{d^2 \theta_i}{dZ^2} \tag{2.1c}$$

in which w_{Xi} and w_{Yi} are the lateral loads applied to the unit height of wall in the X and Y directions respectively, $w_{\theta i}$ is the external applied torsional moment per unit height of wall, EI_{Xi} and EI_{Yi} are the flexural stiffnesses in the X and Y directions respectively, $EI_{\omega i}$ is the warping torsional stiffness, GJ_i is the St. Venant torsional stiffness, X_i and Y_i are the lateral

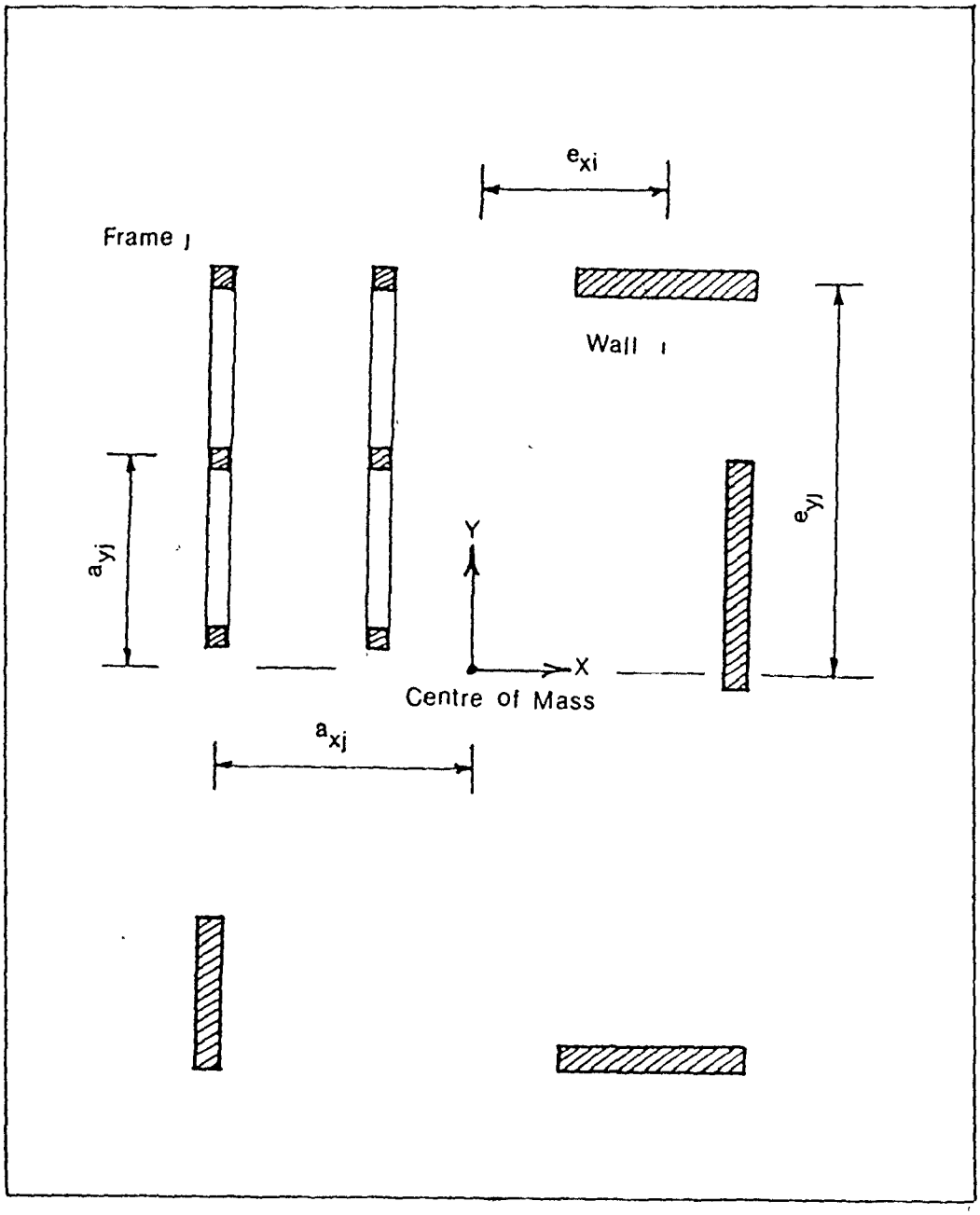

FIGURE 2 COORDINATE SYSTEM FOR A TYPICAL CROSS-SECTION OF ASYMMETRIC WALL-FRAME STRUCTURE

displacements in the X and Y directions respectively, θ_i is the rotational deformation, and Z is the height above the foundation.

Similarly the differential equations for the statical equilibrium of a frame j whose centroid is located at the coordinate position (a_{Xj}, a_{Yj}) are given by

$$w_{Xj}(Z) = -GA_{Xj}\frac{d^2X_j}{dZ^2} \tag{2.2a}$$

$$w_{Yj}(Z) = -GA_{Yj}\frac{d^2Y_j}{dZ^2} \tag{2.2b}$$

$$w_{\theta j}(Z) = -GJ_j\frac{d^2\theta_j}{dZ^2} \tag{2.2c}$$

in which GA_{Xj} and GA_{Yj} are the shear stiffnesses in the X and Y directions respectively, and the other quantities are as defined for equations (2.1).

Let $\bar{X}(Z)$, $\bar{Y}(Z)$, and $\bar{\theta}(Z)$ be the displacements of the centre of mass axis at height Z. Compatibility conditions require that the displacements of any element K located at the coordinate position (x_K, y_K) be given by

$$X_K(Z) = \bar{X}(Z) - y_K\bar{\theta}(Z) \tag{2.3a}$$

$$Y_K(Z) = \bar{Y}(Z) + x_K\bar{\theta}(Z) \tag{2.3b}$$

$$\theta_K(Z) = \bar{\theta}(Z) \tag{2.3c}$$

Let $W_X(Z)$, $W_Y(Z)$ and $W_\theta(Z)$ be the distributed loads applied to the entire structure at the centre of mass axis. Equilibrium conditions require that

$$W_X(Z) = \sum_{i=1}^{m} w_{Xi}(Z) + \sum_{j=1}^{n} w_{Xj}(Z) \tag{2.4a}$$

$$W_Y(Z) = \sum_{i=1}^{m} w_{Yi}(Z) + \sum_{j=1}^{n} w_{Yj}(Z) \tag{2.4b}$$

$$W_\theta(Z) = \sum_{i=1}^{m} w_{\theta i}(Z) + \sum_{j=1}^{n} w_{\theta j}(Z) + \sum_{i=1}^{m} [e_{Xi} w_{Yi}(Z) - e_{Yi} w_{Xi}(Z)] + \sum_{j=1}^{n} [a_{Xj} w_{Yj}(Z) - a_{Yj} w_{Xj}(Z)] \tag{2.4c}$$

in which m and n are the total number of walls and frames respectively. Substituting equations (2.1), (2.2) and (2.3) into equations (2.4) yields

$$W_X(Z) = \overline{EI}_X \frac{d^4\bar{X}}{dZ^4} - \overline{GA}_X \frac{d^2\bar{X}}{dZ^2} - e_Y \overline{EI}_X \frac{d^4\bar{\theta}}{dZ^4} + a_Y \overline{GA}_X \frac{d^2\bar{\theta}}{dZ^2} \tag{2.5a}$$

$$W_Y(Z) = \overline{EI}_Y \frac{d^4\bar{Y}}{dZ^4} - \overline{GA}_Y \frac{d^2\bar{Y}}{dZ^2} + e_X \overline{EI}_Y \frac{d^4\bar{\theta}}{dZ^4} - a_X \overline{GA}_Y \frac{d^2\bar{\theta}}{dZ^2} \tag{2.5b}$$

$$W_\theta(Z) = \overline{EI}_\omega \frac{d^4\bar{\theta}}{dZ^4} - \overline{GJ} \frac{d^2\bar{\theta}}{dZ^2} - e_Y \overline{EI}_X \frac{d^4\bar{X}}{dZ^4} + a_Y \overline{GA}_X \frac{d^2\bar{X}}{dZ^2} + e_X \overline{EI}_Y \frac{d^4\bar{Y}}{dZ^4} - a_X \overline{GA}_Y \frac{d^2\bar{Y}}{dZ^2} \tag{2.5c}$$

in which

$$\overline{EI}_X = \sum_{i=1}^{m} EI_{Xi} \qquad \overline{EI}_Y = \sum_{i=1}^{m} EI_{Yi} \tag{2.6a}$$

$$\overline{GA}_X = \sum_{j=1}^{n} GA_{Xj} \qquad \overline{GA}_Y = \sum_{j=1}^{n} GA_{Yj} \tag{2.6b}$$

$$e_X = \frac{\sum_{i=1}^{m} e_{Xi}\, EI_{Yi}}{\overline{EI}_Y} \qquad e_Y = \frac{\sum_{i=1}^{m} e_{Yi}\, EI_{Xi}}{\overline{EI}_X} \tag{2.6c}$$

$$a_X = \frac{\sum_{j=1}^{n} a_{Xj}\, GA_{Yj}}{\overline{GA}_Y} \qquad a_Y = \frac{\sum_{j=1}^{n} a_{Yj}\, GA_{Xj}}{\overline{GA}_X} \tag{2.6d}$$

$$\overline{EI}_\omega = \sum_{i=1}^{m} [EI_{\omega i} + e_{Xi}^2\, EI_{Yi} + e_{Yi}^2\, EI_{Xi}] \tag{2.6e}$$

$$\overline{GJ} = \sum_{j=1}^{n} [GJ_j + a_{Xj}^2\, GA_{Yj} + a_{Yj}^2\, GA_{Xj}] + \sum_{i=1}^{m} [GJ_i] \tag{2.6f}$$

To formulate the equations of motion of the structure, the dynamic problem is treated as a static problem with the inertial forces added to the elastic forces of the structure. The inertial forces of translation in the X and Y directions and rotation about the centre of mass are given by

$$W_X(Z, t) = -\rho A \frac{\partial^2 \bar{X}}{\partial t^2} \tag{2.7a}$$

$$W_Y(Z, t) = -\rho A \frac{\partial^2 \bar{Y}}{\partial t^2} \tag{2.7b}$$

$$W_\theta(Z, t) = -\rho I_m \frac{\partial^2 \bar{\theta}}{\partial t^2} \tag{2.7c}$$

in which ρA is the mass per unit height, ρI_m is the mass moment of inertia per unit height, and t is the time coordinate. Substituting equations (2.7) into equations (2.5) yields

$$\overline{EI}_X \frac{\partial^4 \bar{X}}{\partial Z^4} - \overline{GA}_X \frac{\partial^2 \bar{X}}{\partial Z^2} - e_Y \overline{EI}_X \frac{\partial^4 \bar{\theta}}{\partial Z^4} + a_Y \overline{GA}_X \frac{\partial^2 \bar{\theta}}{\partial Z^2} = -\rho A \frac{\partial^2 \bar{X}}{\partial t^2} \tag{2.8a}$$

$$\overline{EI}_Y \frac{\partial^4 \bar{Y}}{\partial Z^4} - \overline{GA}_Y \frac{\partial^2 \bar{Y}}{\partial Z^2} + e_X \overline{EI}_Y \frac{\partial^4 \bar{\theta}}{\partial Z^4} - a_X \overline{GA}_Y \frac{\partial^2 \bar{\theta}}{\partial Z^2} = -\rho A \frac{\partial^2 \bar{Y}}{\partial t^2} \tag{2.8b}$$

$$\overline{EI}_{\omega}\frac{\partial^4\bar{\theta}}{\partial Z^4} - \overline{GJ}\frac{\partial^2\bar{\theta}}{\partial Z^2} - e_Y\overline{EI}_X\frac{\partial^4\bar{X}}{\partial Z^4} + a_Y\overline{GA}_X\frac{\partial^2\bar{X}}{\partial Z^2} + e_X\overline{EI}_Y\frac{\partial^4\bar{Y}}{\partial Z^4} - a_X\overline{GA}_Y\frac{\partial^2\bar{Y}}{\partial Z^2} = -\rho I_m\frac{\partial^2\bar{\theta}}{\partial t^2} \tag{2.8c}$$

These equations represent the free vibrations of a three-dimensional wall-frame structure. This set of equations and the boundary conditions of the problem determine the transverse coupled flexural-torsional vibrations of the strucutre. In the particular case with the X-axis as the axis of symmetry, the eccentricities in Y-direction vanish and the problem converts to that of a two-dimensional wall-frame structure.

3. Exact Treatment for Natural Frequencies and Mode Shapes for a 2-Dimensional Wall-Frame Structure

A 2-dimensional analysis is presented for the case of a floor section with the X-axis as the axis of symmetry. This analysis gives a complete understanding of the interaction between various structural elements as well as the effect of coupling between the Y and θ motions. In this particular case the differential equations take the form

$$\overline{EI}_X\frac{\partial^4\bar{X}}{\partial Z^4} - \overline{GA}_X\frac{\partial^2\bar{X}}{\partial Z^2} = -\rho A\frac{\partial^2\bar{X}}{\partial t^2} \tag{2.9a}$$

$$\overline{EI}_Y\frac{\partial^4\bar{Y}}{\partial Z^4} - \overline{GA}_Y\frac{\partial^2\bar{Y}}{\partial Z^2} + e_m\overline{EI}_Y\frac{\partial^4\bar{\theta}}{\partial Z^4} - a_m\overline{GA}_Y\frac{\partial^2\bar{\theta}}{\partial Z^2} = -\rho A\frac{\partial^2\bar{Y}}{\partial t^2} \tag{2.9b}$$

$$\overline{EI}_{\omega}\frac{\partial^4\bar{\theta}}{\partial Z^4} - GJ\frac{\partial^2\bar{\theta}}{\partial Z^2} + e_m\overline{EI}_Y\frac{\partial^4\bar{Y}}{\partial Z^4} - a_m\overline{GA}_Y\frac{\partial^2\bar{Y}}{\partial Z^2} = -\rho I_m\frac{\partial^2\bar{\theta}}{\partial t^2} \tag{2.9c}$$

in which

$$e_Y = 0 \qquad a_Y = 0 \tag{2.10a}$$

$$e_X = e_m \qquad a_X = a_m \tag{2.10b}$$

From the above set of equations, it is obvious that $\bar{X}(Z,t)$ is uncoupled whereas $\bar{Y}(Z,t)$ and $\bar{\theta}(Z,t)$ are coupled. In the present study, only the coupled Y - θ vibrations are investigated since the X-vibration is the case of a shear-flexure member deforming in combined shear or bending configurations; the concept is similar to that used by several previous investigators (22, 25).

Figure 3 shows the coordinate system for a typical cross-section of a 2-dimensional wall-frame structure with point M as centre of mass, point W as centroid of walls and point F as centroid of frames. In this case, the centroid of walls W being located to the right of M gives positive wall eccentricity e_m and the centroid of frames F being located to the left of M gives negative frame eccentricity a_m.

Rearranging the two coupled equations (2.9b) and (2.9c) yields

$$\frac{\partial^4 \bar{Y}}{\partial Z^4} - \alpha^2 \frac{\partial^2 \bar{Y}}{\partial Z^2} + \frac{e_m}{r} \frac{\partial^4 (r\bar{\theta})}{\partial Z^4} - \frac{a_m}{r} \alpha^2 \frac{\partial^2 (r\bar{\theta})}{\partial Z^2} = - \frac{1}{b^2} \frac{\partial^2 \bar{Y}}{\partial t^2} \tag{2.11a}$$

$$\frac{\partial^4 (r\bar{\theta})}{\partial Z^4} - \beta^2 \frac{\partial^2 (r\bar{\theta})}{\partial Z^2} + \frac{e_m}{r} \frac{\partial^4 \bar{Y}}{\partial Z^4} - \frac{a_m}{r} \alpha^2 \frac{\partial^2 \bar{Y}}{\partial Z^2} = - \frac{1}{c^2} \frac{\partial^2 (r\bar{\theta})}{\partial t^2} \tag{2.11b}$$

in which

$$\alpha^2 = \frac{\overline{GA}_Y}{\overline{EI}_Y} \qquad \beta^2 = \frac{\overline{GJ}}{\overline{EI}_\omega} \qquad r^2 = \frac{\overline{EI}_\omega}{\overline{EI}_Y} \tag{2.12a}$$

$$\frac{1}{b^2} = \frac{\rho A}{\overline{EI}_Y} \qquad \frac{1}{c^2} = \frac{\rho I_m}{\overline{EI}_\omega} \tag{2.12b}$$

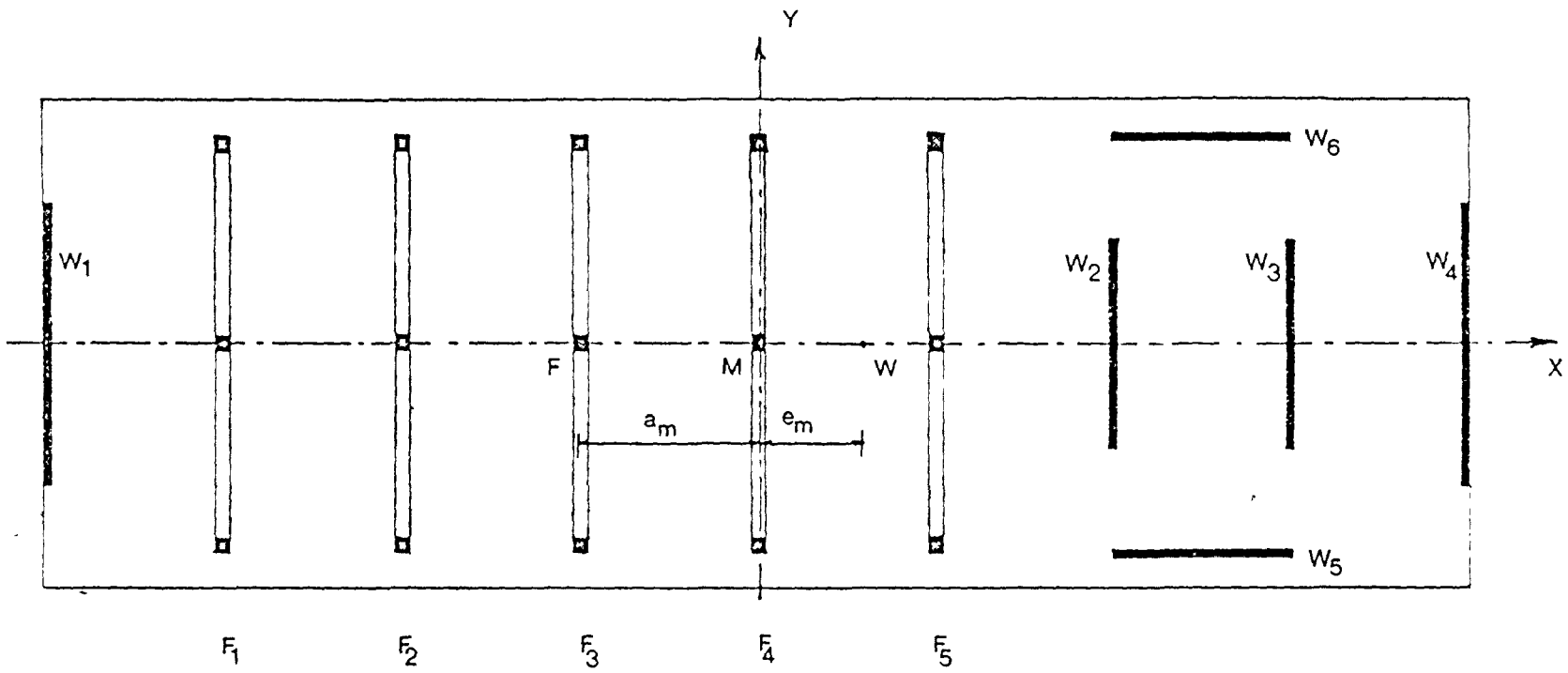

FIGURE 3 COORDINATE SYSTEM FOR A TYPICAL CROSS-SECTION OF A TWO-DIMENSIONAL WALL-FRAME STRUCTURE

Using a matrix form of presentation for equations (2.11), one obtains

$$[K_1] \{U\}^{IV} - [K_2] \{U\}^{II} + [K_3] \{\ddot{U}\} = \{0\} \tag{2.13}$$

in which

$$\{U\}^{IV} = \frac{\partial^4}{\partial Z^4} \begin{Bmatrix} \bar{Y} \\ r\bar{\theta} \end{Bmatrix} , \quad \{U\}^{II} = \frac{\partial^2}{\partial Z^2} \begin{Bmatrix} \bar{Y} \\ r\bar{\theta} \end{Bmatrix} , \quad \{\ddot{U}\} = \frac{\partial^2}{\partial t^2} \begin{Bmatrix} \bar{Y} \\ r\bar{\theta} \end{Bmatrix} \tag{2.14a}$$

$$\left.\begin{aligned} [K_1] &= \begin{bmatrix} 1 & \frac{e_m}{r} \\ \frac{e_m}{r} & 1 \end{bmatrix} \\ [K_2] &= \begin{bmatrix} \alpha^2 & \frac{a_m}{r}\alpha^2 \\ \frac{a_m}{r}\alpha^2 & \beta^2 \end{bmatrix} \\ [K_3] &= \begin{bmatrix} \frac{1}{b^2} & 0 \\ 0 & \frac{1}{c^2} \end{bmatrix} \end{aligned}\right\} \tag{2.14b}$$

The solution to equation (2.13) may conveniently be assumed to be of the form

$$\{U(Z,t)\} = \sum_{n=1}^{\infty} \{\Phi_n(Z)\} \sin \omega_n t \tag{2.15}$$

in which ω_n is the n^{th} frequency of the coupled flexural-torsional modes of deformation and $\Phi_n(Z)$ is the mode shape function for the same mode of vibration. Substituting equation (2.15) into equation

(2.13) yields an ordinary differential equation for the n^{th} mode of vibration

$$[K_1]\{\Phi_n\}^{IV} - [K_2]\{\Phi_n\}^{II} - \omega_n^2 [K_3]\{\Phi_n\} = \{0\} \tag{2.16}$$

The mode shape function $\{\Phi_n\}$ in equation (2.16) is assumed to be

$$\{\Phi_n(Z)\} = \{C_n\} e^{\lambda_n Z} \tag{2.17}$$

in which $\{\Phi_n(Z)\} = \begin{Bmatrix} \Phi_{Yn} \\ \Phi_{\theta n} \end{Bmatrix}$, $\{C_n\} = \begin{Bmatrix} c_{Yn} \\ c_{\theta n} \end{Bmatrix}$ (2.18)

and $\{C_n\}$ is a constant vector. Substituting equation (2.17) into equation (2.16) yields

$$\left[[K_1]\lambda_n^4 - [K_2]\lambda_n^2 - \omega_n^2 [K_3]\right]\{C_n\} = \{0\} \tag{2.19}$$

Substituting equations (2.14b) and (2.18) into equation (2.19) yields

$$\begin{bmatrix} \lambda_n^4 - \alpha^2\lambda_n^2 - \frac{\omega_n^2}{b^2} & \frac{e_m}{r}\lambda_n^4 - \frac{a_m}{r}\alpha^2\lambda_n^2 \\ \frac{e_m}{r}\lambda_n^4 - \frac{a_m}{r}\alpha^2\lambda_n^2 & \lambda_n^4 - \beta^2\lambda_n^2 - \frac{\omega_n^2}{c^2} \end{bmatrix} \begin{Bmatrix} c_{Yn} \\ c_{\theta n} \end{Bmatrix} = \begin{Bmatrix} 0 \\ 0 \end{Bmatrix} \tag{2.20}$$

The characteristic equation governing the non-trivial solution to the above homogeneous set of equations is a fourth order polynomial in λ_n^2 and it is expressed by equating the determinant of the matrix of coefficients of c_{Yn} and $c_{\theta n}$ to zero. The fourth order polynomial equation in λ_n^2 is

$$A_1\lambda_n^8 + A_2\lambda_n^6 + A_3\lambda_n^4 + A_4\lambda_n^2 + A_5 = 0 \tag{2.21}$$

in which

$$A_1 = \left[1 - \left(\frac{e_m}{r}\right)^2 \right] \tag{2.22a}$$

$$A_2 = \alpha^2 \left(2 \frac{e_m a_m}{r^2} - 1\right) - \beta^2 \tag{2.22b}$$

$$A_3 = \alpha^2 \left[\beta^2 - \left(\frac{a_m}{r}\right)^2 \alpha^2 \right] - \omega_n^2 \left[\frac{1}{b^2} + \frac{1}{c^2} \right] \tag{2.22c}$$

$$A_4 = \omega_n^2 \left[\frac{\alpha^2}{c^2} + \frac{\beta^2}{b^2} \right] \tag{2.22d}$$

$$A_5 = \frac{\omega_n^4}{c^2 b^2} \tag{2.22e}$$

It can be shown (10) that two of these roots will be positive and two will be negative. Consequently, the mode shapes of equation (2.17) can be written as a combination of hyperbolic and trigonometric functions of the parameter λ_n. Each shape function requires eight independent constants and equation (2.20) governs the relationship between the mode shapes. These constants are to be determined from the boundary conditions. It can be shown (12, 13) that the boundary conditions governing the behaviour of the structure are given by

(a) at the base of the structure, $Z = 0$

(i) $$\bar{Y}(0,t) = 0 \tag{2.23a}$$

$$r\bar{\theta}(0,t) = 0 \tag{2.23b}$$

(ii) $$\frac{\partial \bar{Y}}{\partial Z}(0,t) = 0 \tag{2.23c}$$

$$\frac{\partial r\bar{\theta}}{\partial Z}(0,t) = 0 \tag{2.23d}$$

(b) at the top of the structure, $Z = H$

(i) $$\frac{\partial^2 \bar{Y}}{\partial Z^2}(H,t) = 0 \tag{2.23e}$$

$$\frac{\partial^2 r\bar{\theta}}{\partial Z^2}(H,t) = 0 \qquad (2.23f)$$

(ii) $$-\frac{\partial^3 \bar{Y}}{\partial Z^3}(H,t) - \frac{e_m}{r}\frac{\partial^3 r\bar{\theta}}{\partial Z^3}(H,t) + \alpha^2 \frac{\partial \bar{Y}}{\partial Z}(H,t) + \frac{a_m}{r}\alpha^2 \frac{\partial r\bar{\theta}}{\partial Z}(H,t) = 0 \qquad (2.23g)$$

$$-\frac{\partial^3 r\bar{\theta}}{\partial Z^3}(H,t) - \frac{e_m}{r}\frac{\partial^3 \bar{Y}}{\partial Z^3}(H,t) + \beta^2 \frac{\partial r\bar{\theta}}{\partial Z}(H,t) + \frac{a_m}{r}\alpha^2 \frac{\partial \bar{Y}}{\partial Z}(H,t) = 0 \qquad (2.23h)$$

Referring to equations (2.14), (2.15) and (2.18) the above boundary conditions may be written for the n^{th} mode of vibration as,

(a) at $Z = 0$

$$\phi_{Yn}(0) = 0 \qquad (2.24a)$$

$$\phi_{\theta n}(0) = 0 \qquad (2.24b)$$

$$\frac{d\phi_{Yn}}{dZ}(0) = 0 \qquad (2.24c)$$

$$\frac{d\phi_{\theta n}}{dZ}(0) = 0 \qquad (2.24d)$$

(b) at $Z = H$

$$\frac{d^2\phi_{Yn}}{dZ^2}(H) = 0 \qquad (2.24e)$$

$$\frac{d^2\phi_{\theta n}}{dZ^2}(H) = 0 \qquad (2.24f)$$

$$-\frac{d^3\phi_{Yn}}{dZ^3}(H) - \frac{e_m}{r}\frac{d^3\phi_{\theta n}}{dZ^3}(H) + \alpha^2 \frac{d\phi_{Yn}}{dZ}(H) + \frac{a_m}{r}\alpha^2 \frac{d\phi_{\theta n}}{dZ}(H) = 0 \qquad (2.24g)$$

$$-\frac{d^3\phi_{\theta n}}{dZ^3}(H) - \frac{e_m}{r}\frac{d^3\phi_{Yn}}{dZ^3}(H) + \beta^2 \frac{d\phi_{\theta n}}{dZ}(H) + \frac{a_m}{r}\alpha^2 \frac{d\phi_{Yn}}{dZ}(H) = 0 \qquad (2.24h)$$

It should be noted that the mode shapes are for one particular frequency ω_n corresponding to one particular mode n.

Assume λ_{ni} $(i = 1,2,\ldots,8)$ are the roots of the fourth order polynomial equation in λ_n^2 for a known value ω_n, then equation (2.17) can be replaced by

$$\{\Phi_n\} = \sum_{i=1}^{8} \{C_{ni}\} \; e^{\lambda_{ni} Z} \tag{2.25a}$$

or

$$\begin{Bmatrix} \phi_{Yn} \\ \phi_{\theta n} \end{Bmatrix} = \sum_{i=1}^{8} \begin{Bmatrix} c_{Yni} \\ c_{\theta ni} \end{Bmatrix} e^{\lambda_{ni} Z} \tag{2.25b}$$

The sixteen unknowns, c_{Yni}, $c_{\theta ni}$ $(i = 1,2,\ldots,8)$ in equation (2.25b) can be reduced to eight unknowns by considering the relationship between c_{Yni} and $c_{\theta ni}$ in equation (2.20)

$$\frac{c_{\theta ni}}{c_{Yni}} = - \frac{\lambda_{ni}^4 - \alpha^2 \lambda_{ni}^2 - \omega_n^2/b^2}{\frac{e_m}{r} \lambda_{ni}^4 - \frac{a_m}{r} \alpha^2 \lambda_{ni}^2}$$

$$= - \frac{\frac{e_m}{r} \lambda_{ni}^4 - \frac{a_m}{r} \alpha^2 \lambda_{ni}^2}{\lambda_{ni}^4 - \beta^2 \lambda_{ni}^2 - \omega_n^2/c^2} = R_{ni} \tag{2.26}$$

Substituting equation (2.25b) into equations (2.24) yields

$$\sum_{i=1}^{8} c_{Yni} = 0 \tag{2.27a}$$

$$\sum_{i=1}^{8} c_{\theta ni} = 0 \tag{2.27b}$$

$$\sum_{i=1}^{8} c_{Yni} \cdot \lambda_{ni} = 0 \tag{2.27c}$$

$$\sum_{i=1}^{8} c_{\theta ni} \cdot \lambda_{ni} = 0 \qquad (2.27d)$$

$$\sum_{i=1}^{8} c_{Yni} \cdot \lambda_{ni}^2 \cdot e^{\lambda_{ni} H} = 0 \qquad (2.27e)$$

$$\sum_{i=1}^{8} c_{\theta ni} \cdot \lambda_{ni}^2 \cdot e^{\lambda_{ni} H} = 0 \qquad (2.27f)$$

$$\sum_{i=1}^{8} \left[- c_{Yni} \lambda_{ni}^3 - \frac{e_m}{r} c_{\theta ni} \lambda_{ni}^3 + \alpha^2 c_{Yni} \lambda_{ni} + \frac{a_m}{r} \alpha^2 c_{\theta ni} \lambda_{ni} \right] e^{\lambda_{ni} H} = 0 \qquad (2.27g)$$

$$\sum_{i=1}^{8} \left[- c_{\theta ni} \lambda_{ni}^3 - \frac{e_m}{r} c_{Yni} \lambda_{ni}^3 + \beta^2 c_{\theta ni} \lambda_{ni} + \frac{a_m}{r} \alpha^2 c_{Yni} \lambda_{ni} \right] e^{\lambda_{ni} H} = 0 \qquad (2.27h)$$

Substituting equation (2.26) into equations (2.27) and using a matrix form of presentation yields equation (2.28) (See next page).

Equation (2.28) is more general than that derived by Heidebrecht and Raina (10) to develop the frequency analysis of shear walls, using a continuous thin-walled beam model. The above equation represents a set of eight linear homogeneous equations which may also be written in brief as

$$\left[D_n [\omega_n^2 , \lambda_{ni} \ (i = 1,2,\ldots,8)] \right] \{c_{Yn}\} = \{0\} \qquad (2.29)$$

where $\{c_{Yn}\}$ is the column vector containing the unknown coefficients c_{Yni} $(i = 1,2,\ldots,8)$, n is the frequency number and $[D]$ is the matrix of equation (2.28). A nontrivial solution for equation (2.29) can only be obtained if the determinant of the matrix $[D]$ is zero. Thus

$$| D_n [\omega_n^2 , \lambda_{ni} \ (i = 1,2,\ldots,8)] | = 0 \qquad (2.30)$$

$$
\begin{bmatrix}
1 & 1 & 1 & 1 & 1 & 1 & 1 & 1 \\
R_{n1} & R_{n2} & R_{n3} & R_{n4} & R_{n5} & R_{n6} & R_{n7} & R_{n8} \\
\lambda_{n1} & \lambda_{n2} & \lambda_{n3} & \lambda_{n4} & \lambda_{n5} & \lambda_{n6} & \lambda_{n7} & \lambda_{n8} \\
R_{n1}\lambda_{n1} & R_{n2}\lambda_{n2} & R_{n3}\lambda_{n3} & R_{n4}\lambda_{n4} & R_{n5}\lambda_{n5} & R_{n6}\lambda_{n6} & R_{n7}\lambda_{n7} & R_{n8}\lambda_{n8} \\
\lambda_{n1}^2 e^{\lambda_{n1}H} & \lambda_{n2}^2 e^{\lambda_{n2}H} & \lambda_{n3}^2 e^{\lambda_{n3}H} & \lambda_{n4}^2 e^{\lambda_{n4}H} & \lambda_{n5}^2 e^{\lambda_{n5}H} & \lambda_{n6}^2 e^{\lambda_{n6}H} & \lambda_{n7}^2 e^{\lambda_{n7}H} & \lambda_{n8}^2 e^{\lambda_{n8}H} \\
R_{n1}\lambda_{n}^2 e^{\lambda_{n1}H} & R_{n2}\lambda_{n2}^2 e^{\lambda_{n2}H} & R_{n3}\lambda_{n3}^2 e^{\lambda_{n3}H} & R_{n4}\lambda_{n4}^2 e^{\lambda_{n4}H} & R_{n5}\lambda_{n5}^2 e^{\lambda_{n5}H} & R_{n6}\lambda_{n6}^2 e^{\lambda_{n6}H} & R_{n7}\lambda_{n7}^2 e^{\lambda_{n7}H} & R_{n8}\lambda_{n8}^2 e^{\lambda_{n8}H} \\
U_{n1} e^{\lambda_{n1}H} & U_{n2} e^{\lambda_{n2}H} & U_{n3} e^{\lambda_{n3}H} & U_{n4} e^{\lambda_{n4}H} & U_{n5} e^{\lambda_{n5}H} & U_{n6} e^{\lambda_{n6}H} & U_{n7} e^{\lambda_{n7}H} & U_{n8} e^{\lambda_{n8}H} \\
V_{n1} e^{\lambda_{n1}H} & V_{n2} e^{\lambda_{n2}H} & V_{n3} e^{\lambda_{n3}H} & V_{n4} e^{\lambda_{n4}H} & V_{n5} e^{\lambda_{n5}H} & V_{n6} e^{\lambda_{n6}H} & V_{n7} e^{\lambda_{n7}H} & V_{n8} e^{\lambda_{n8}H}
\end{bmatrix}
\begin{bmatrix} c_{Yn1} \\ c_{Yn2} \\ c_{Yn3} \\ c_{Yn4} \\ c_{Yn5} \\ c_{Yn6} \\ c_{Yn7} \\ c_{Yn8} \end{bmatrix}
=
\begin{bmatrix} 0 \\ 0 \\ 0 \\ 0 \\ 0 \\ 0 \\ 0 \\ 0 \end{bmatrix}
\tag{2.28}
$$

$$
U_{ni} = \lambda_{ni} \left(\alpha^2 + \alpha^2 \frac{a_m}{r} R_{ni}\right) - \lambda_{ni}^3 \left(1 + \frac{e_m}{r} R_{ni}\right) \tag{2.28a}
$$

$$
V_{ni} = \lambda_{ni} \left(\beta^2 R_{ni} + \alpha^2 \frac{a_m}{r}\right) - \lambda_{ni}^3 \left(R_{ni} + \frac{e_m}{r}\right) \tag{2.28b}
$$

The determination of the exact natural frequency and mode shape for each individual mode requires a complex trial and error procedure. The first step is to assume a frequency ω_a. Using equations (2.22) for the known properties of the structure and the assumed frequency, the five coefficients of the fourth order polynomial equation in λ_a^2 are calculated

The corresponding λ_{ai} $(i = 1,2,\ldots,8)$ being obtained from equation (2.21), the second step is to calculate the elements of the matrix $[D_a]$. If $|D_a| = 0$, the assumed frequency ω_a is a natural frequency for the structure. If $|D_a| \gtrless 0$, the direct search method is used to determine the natural frequency with a permissible error of 0.001 rad./sec. For a particular natural frequency ω_n and the corresponding parameters λ_{ni} $(i = 1,2,\ldots,8)$, the coefficients c_{Yni} $(i = 1,2,\ldots,8)$ are determined from equation (2.28). The flexural and torsional components $\phi_{Yn}(Z)$ and $\phi_{\theta n}(Z)$ of the corresponding mode shape are calculated from equations (2.25) and (2.26). A computer program based on the previously described procedure of analysis is developed. This program can treat any 2-dimensional building made up of frames and walls. Application of the mathematical model is shown in the following example structures.

Example Structure I

The floor plan given in Figure 4 is that for a sixteen storey building first analysed by Mendelson (18). The storey height is 3 m (9.84 ft.) the geometrical properties of the members are given

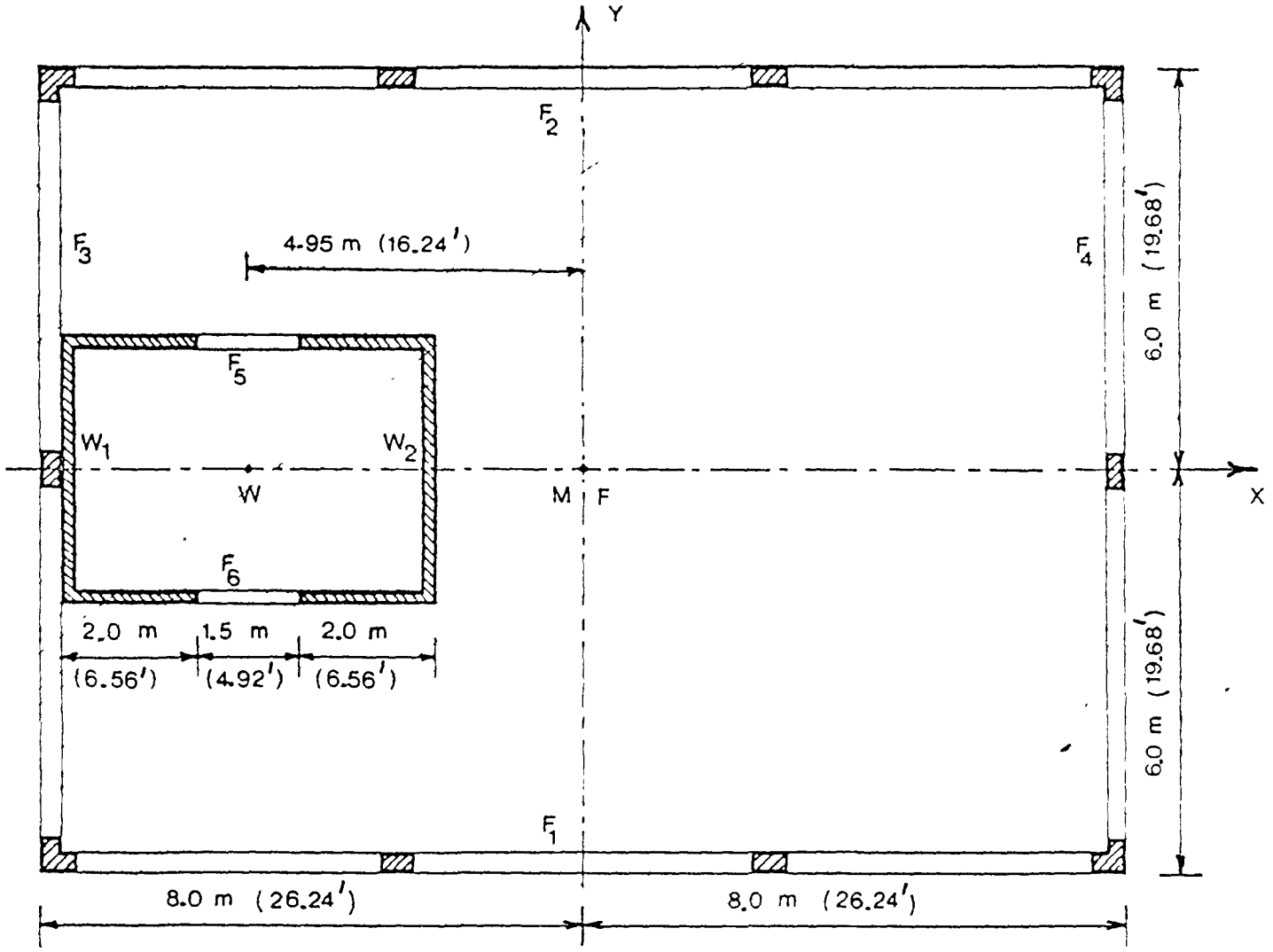

FIGURE 4 FLOOR PLAN FOR EXAMPLE STRUCTURE I

	EI_{Yi}		EI_{Xi}		$EI_{\omega i}$		GJ_i		e_{Xi}		e_{Yi}	
Units / Wall	$t.m^2$	$K.ft^2$	$t.m^2$	$K.ft^2$	$t.m^4$	$K.ft^4$	$t.m^2$	$K.ft^2$	m	ft	m	ft
	10^6	10^6	10^6	10^6	10^6	10^9	10^3	10^6	1	1	1	1
W_1	7.34	173.68	1.15	27.27	4.50	1.146	19.73	0.467	-8.31	-27.27	0.00	0.00
W_2	7.34	173.68	1.15	27.27	4.50	1.146	19.73	0.467	-1.59	-5.21	0.00	0.00

Table 1.a - Physical and Geometrical Properties of Walls - Example Structure I

	GA_{Yj}		GA_{Xj}		GJ_j		a_{Xj}		a_{Yj}	
Units / Frame	t	K	t	K	$t.m^2$	$K.ft^2$	m	ft	m	ft
	10^3	10^3	10^3	10^3	10^6	10^6	1	1	1	1
F_1	0.00	0.00	4.36	9.59	0.00	0.00	0.00	0.00	-5.85	-19.19
F_2	0.00	0.00	4.36	9.59	0.00	0.00	0.00	0.00	+5.85	+19.19
F_3	5.09	11.20	0.00	0.00	0.00	0.00	-7.85	-25.75	0.00	0.00
F_4	5.09	11.20	0.00	0.00	0.00	0.00	+7.85	+25.75	0.00	0.00
F_5	0.00	0.00	395.00	869.00	2.40	56.80	-4.95	-16.24	+1.90	+6.23
F_6	0.00	0.00	395.00	869.00	2.40	56.80	+4.95	+16.24	-1.90	-6.23

Table 1.b - Physical and Geometrical Properties of Frames - Example Structure I

in Tables 1.a and 1.b.

Taking the Z-axis at centre of mass gives e_m = -4.95 m (16.24 ft) and a_m = 0.0. The basic parameters associated with the dynamic properties of the structure are

$\overline{EI}_Y$ = 14.68×10^6 $t.m^2$ (347.45×10^6 $K.ft^2$)

$\overline{EI}_\omega$ = 534.60×10^6 $t.m^4$ (136.13×10^9 $K.ft^4$)

$\overline{GA}_Y$ = 10.18×10^3 $t.$ (22.40×10^3 $K.$)

$\overline{GJ}$ = 8633.00×10^3 $t.m^2$ (204.33×10^6 $K.ft^2$)

ρA = 6.26 $t.sec^2/m^2$ (1.28 $K.sec^2/ft^2$)

ρI_m = 208.70 $t.sec^2$ (459.14 $K.sec^2$)

Table 2 shows the coupled natural periods computed by the proposed trial and error procedure presented in this section, using a digital computer. This table shows also the results given in reference (18). By comparing these results it can be seen that this proposed method yields results which compare very well with those obtained by Mendelson.

Figure 5 shows the coupled flexural-torsional mode shapes for the first six normal modes. Denoting the top displacement of the edge of the structure due to the Y motion by δ_Y, that due to the θ motion by δ_θ and computing the ratio δ_θ/δ_Y one can obtain the predominant motion for each mode of vibration and at which degree that one is predominant. Table 3 shows the ratio δ_θ/δ_Y for the first six normal modes and the predominant motion for each one. From this table one can conclude that the first mode is approximately pure bending

	Natural Periods (Seconds)					
Mode	1	2	3	4	5	6
Author's Results	2.219	0.828	0.465	0.245	0.200	0.132
Mendelson's Results(18)	2.220	0.827	0.465	0.245	0.200	——

Table 2 - Natural Periods of Vibration in Example Structure I
Comparison of Results

Mode	1	2	3	4	5	6
δ_θ / δ_Y	0.110	2.886	0.763	0.537	4.593	0.797
Predominant in	Bending	Torsion	Bending	Bending	Torsion	Bending

Table 3 - The Predominant Motion for each Mode of Vibration - Example Structure I

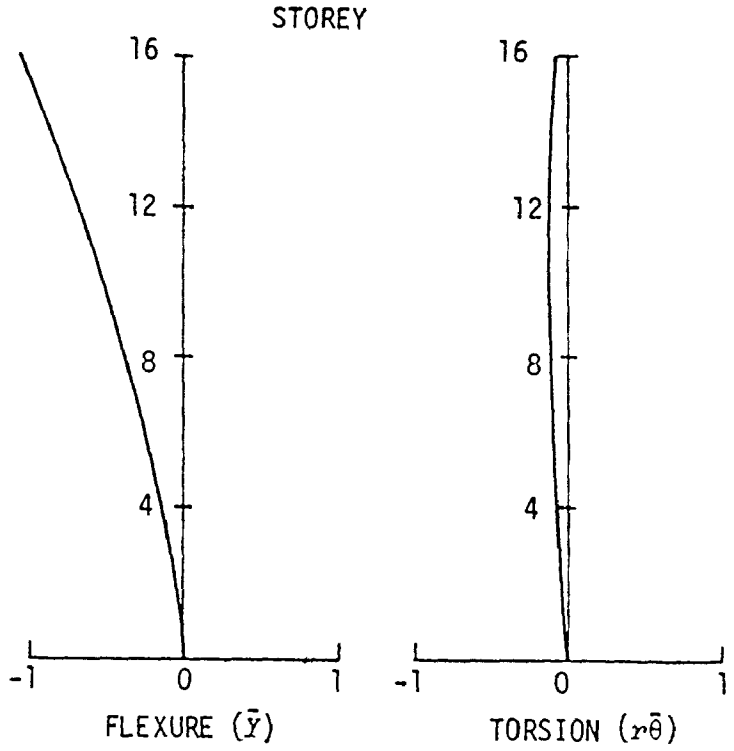

FIRST MODE
T = 2.219 SEC.

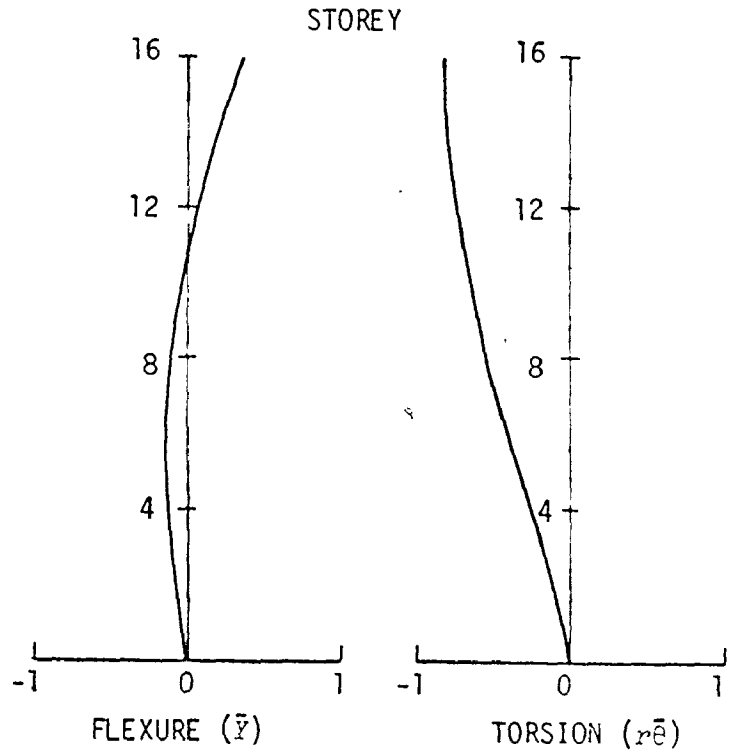

SECOND MODE
T = 0.828 SEC.

FIGURE 5(i) - THE COUPLED FLEXURAL-TORSIONAL MODE SHAPES - EXAMPLE STRUCTURE I

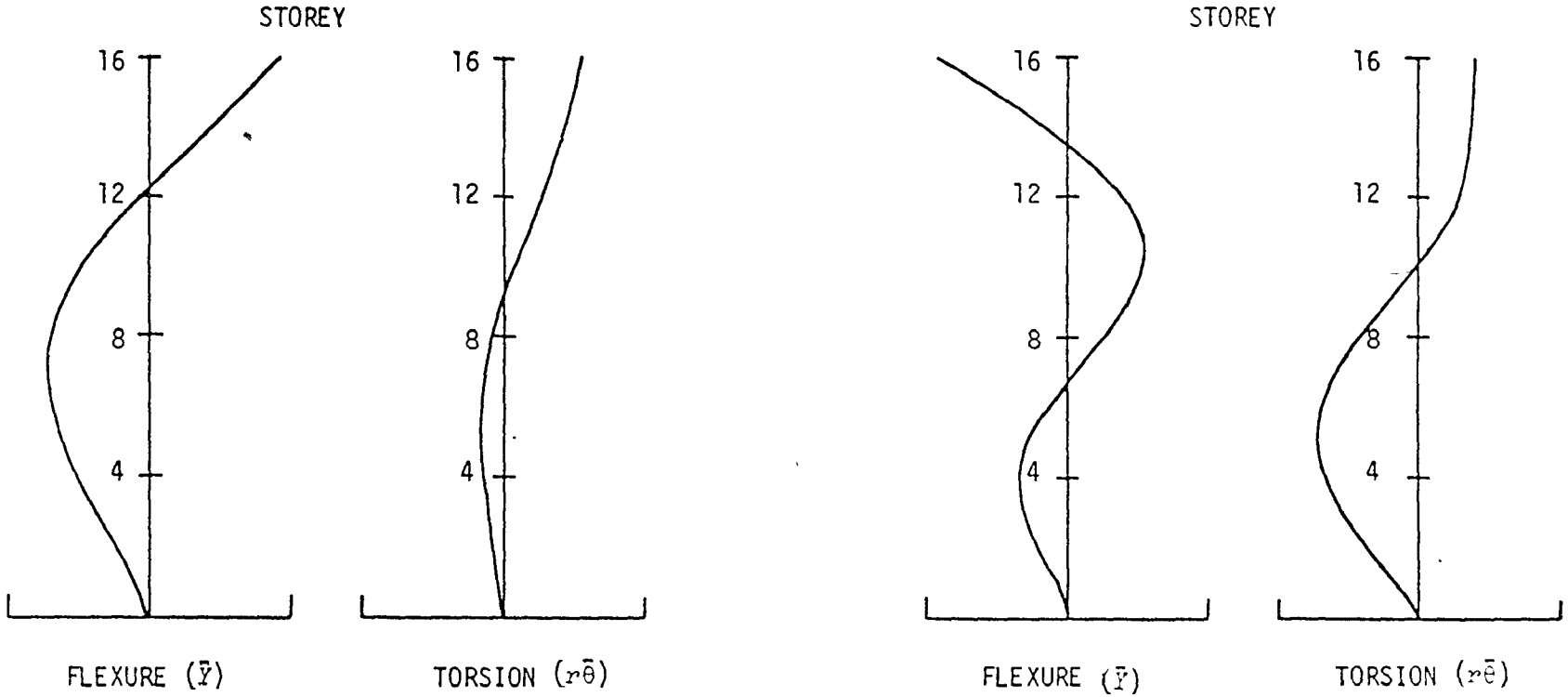

FIGURE 5(ii) - THE COUPLED FLEXURAL-TORSIONAL MODE SHAPES - EXAMPLE STRUCTURE I

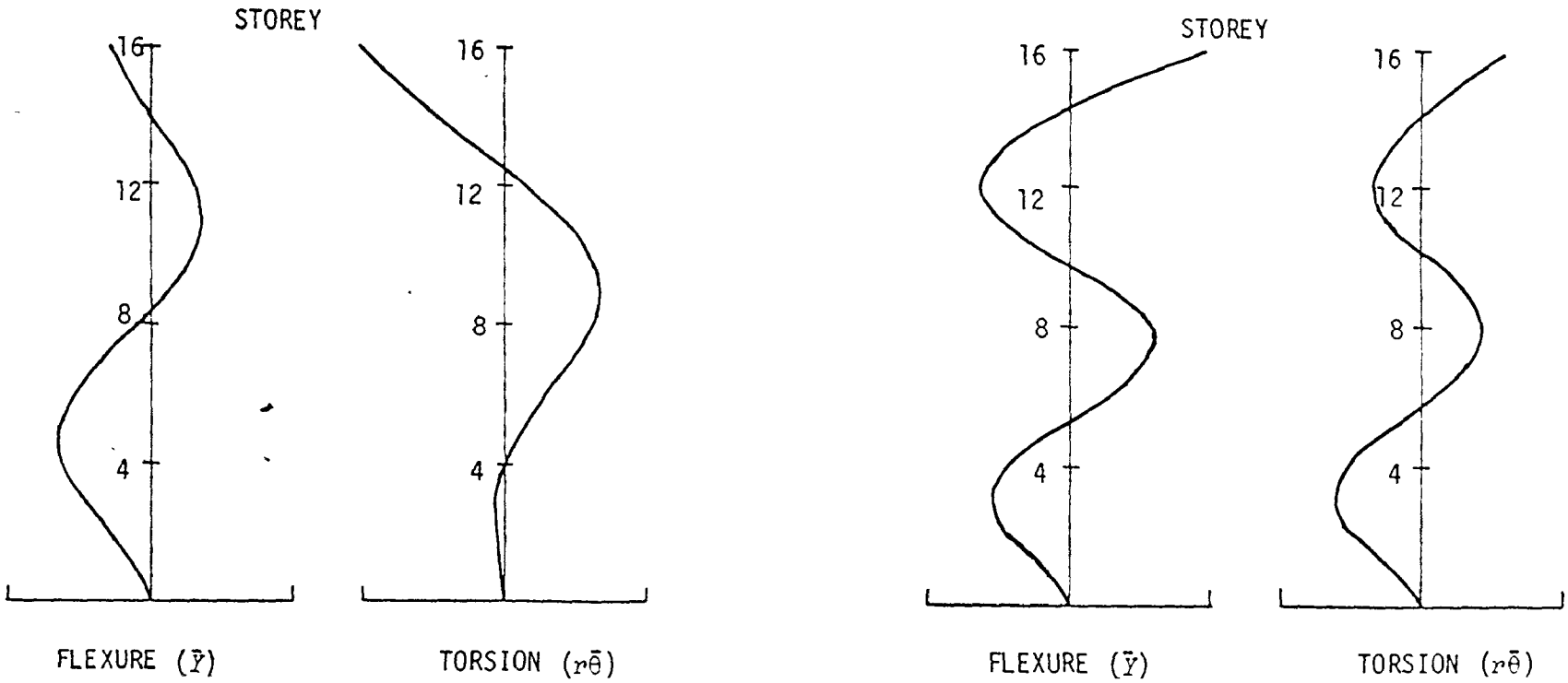

FIFTH MODE
T = 0.200 SEC.

SIXTH MODE
T = 0.132 SEC.

FIGURE 5(iii) - THE COUPLED FLEXURAL-TORSIONAL MODE SHAPES - EXAMPLE STRUCTURE I

(difference of 11%) and the fifth mode is approximately pure torsion (difference of 22%).

Example Structure II

The building whose floor plan is given in Figure 6 [$\bar{x}_c^*$ = -15.24 m(-50.0ft)] as well as three buildings in which the core is located at $\bar{x}_c$ = 0.0, -7.62 m(-25.0ft), -22.86 m(-75.0 ft); was first analysed by Rutenberg, Tso and Heidebrecht (25). This building is 25 storeys high with storey height of 3.66 m(12 ft), unit mass of 28.4 $t.sec^2/m^2$ (5.8 $K.sec^2/ft^2$) and unit mass moment of inertia of 6562.5 $t.sec^2$ (14418.8 $K.sec^2$). The structural stiffness properties for the core are given in Table 4.a, the shear stiffnesses of the frames are given in Table 4.b in which the frame designated F_5 pertains to the case $\bar{x}_c$ = -22.86 m(-75ft), the relevant column data are given in Table 4.c and the basic parameters associated with the dynamic properties of the four buildings are given in Table 4.d. The different location of the core enables one to consider the effect of core eccentricity on the behavior of the building.

Tables 5.a, 5.b, 5.c and 5.d show the coupled natural periods obtained by the author's analysis. These tables show also the results given in reference (25) for a lumped mass solution, those obtained by the approximate hand method proposed in reference (25) and those obtained from the uncoupled approximate method. The uncoupled flexural and torsional natural periods given in these tables are determined by

---

* $(\bar{x}_c, 0)$ are the coordinate position of the core

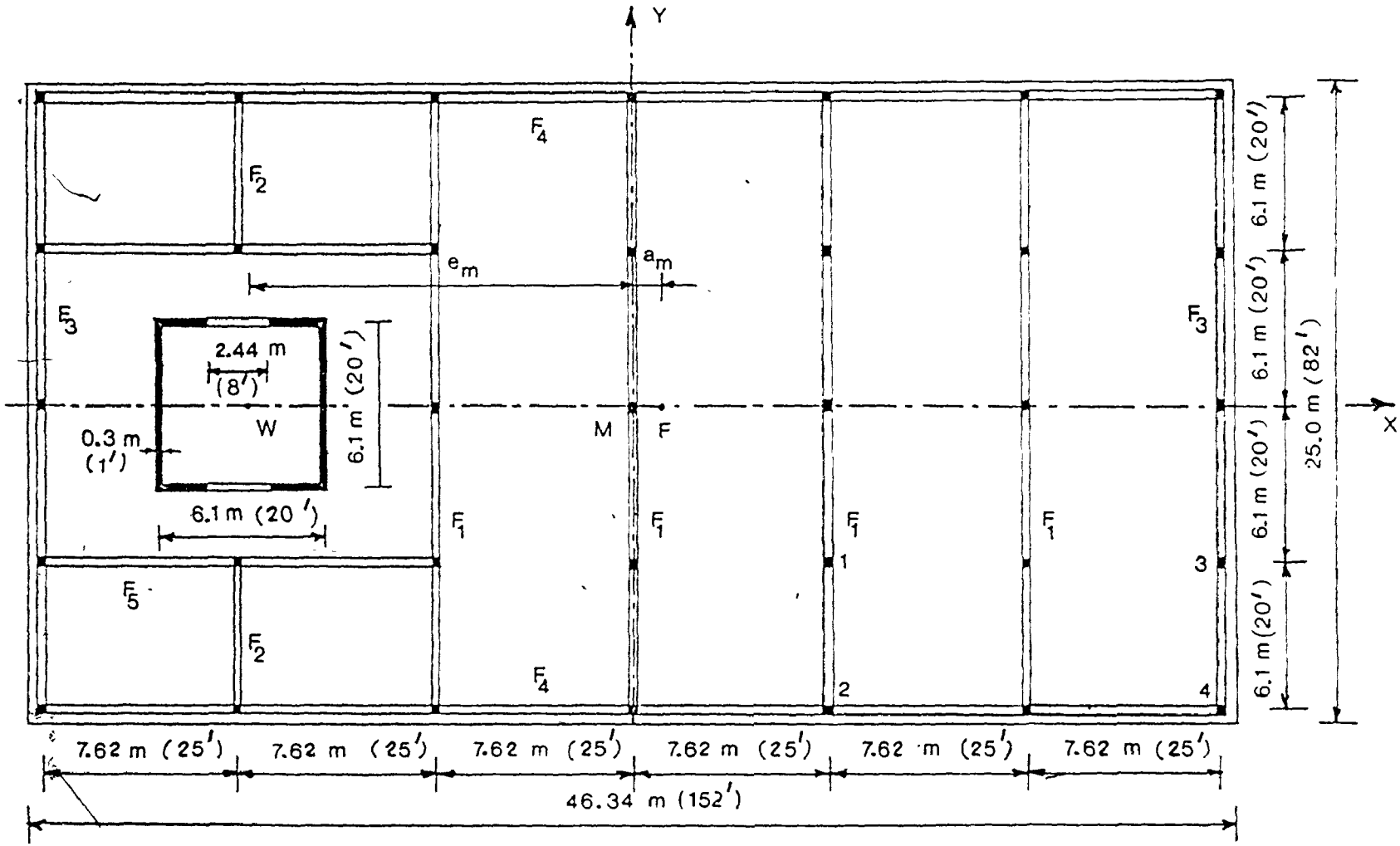

FIGURE 6 FLOOR PLAN FOR EXAMPLE STRUCTURE II

	EI_{Yc}		GJ_c		$EI_{\omega c}$	
Units	$t.m^2$	$K.ft^2$	$t.m^2$	$K.ft^2$	$t.m^4$	$K.ft^4$
	10^6	10^9	10^6	10^9	10^9	10^{12}
Core	89.57	2.12	14.69	0.35	1.11	0.28

Table 4.a - Stiffness Properties of the Core - Example Structure II

	GA_{Yj}		GA_{Xj}	
Units	t	K	t	K
Frame	10^3	10^3	10^3	10^3
F_1	104.32	229.50	0.00	0.00
F_2	27.82	61.20	0.00	0.00
F_3	69.54	153.00	0.00	0.00
F_4	0.00	0.00	125.18	275.40
F_5	0.00	0.00	41.73	91.80
F_5'	20.86	45.90	0.00	0.00

Table 4.b - Shear Stiffnesses of the Frames - Example Structure II

	I_Y		I_X	
Units / Column	m^4	ft^4	m^4	ft^4
	10^{-3}	10^{-1}	10^{-3}	10^{-1}
1	28.12	32.55	28.12	32.55
2	15.84	18.34	23.41	27.10
3	18.75	21.70	8.34	9.65
4	10.54	12.20	6.95	8.04

Table 4.c - Geometrical Properties of the Columns - Example Structure II

	$\bar{x}_c$		$\overline{EI}_Y$		$\overline{EI}_\omega$		$\overline{GA}_Y$		$\overline{GJ}$		e_m		a_m	
Units \ Bld.	m	ft	$t.m^2$	$K.ft^2$	$t.m^4$	$K.ft^4$	t	K	$t.m^2$	$K.ft^2$	m	ft	m	ft
	1	1	10^6	10^9	10^9	10^{12}	10^6	10^6	10^8	10^9	1	1	1	1
1	0.00	0.0	91.94	2.18	1.70	0.43	0.61	1.34	1.88	4.45	0.00	0.0	0.00	0.0
2	-7.62	-25.0	91.94	2.18	6.91	1.76	0.61	1.34	1.85	4.38	-7.44	-24.4	+0.61	+2.0
3	-15.24	-50.0	91.94	2.18	22.56	5.74	0.61	1.34	1.76	4.17	-14.87	-48.8	+1.22	+4.0
4	-22.86	-75.0	91.94	2.18	48.62	12.38	0.63	1.39	1.74	4.11	-22.32	-73.2	+1.01	+3.3

Table 4.d - The Basic Parameters associated with the Dynamic Properties of the four Buildings - Example Structure II

	Natural Periods (Seconds) Predominant in					
	Bending	Torsion	Torsion	Bending	Torsion	Bending
Mode	1	2	3	4	5	6
Lumped Mass	2.166	2.135	0.709	0.658	0.423	0.339
Uncoupled exact method	2.133	2.088	0.689	0.642	0.405	0.327

Table 5.a - Natural Periods of Vibration in Building 1 ($\bar{x}_c = 0$)

Example Structure II - Comparison of Results

Mode	Natural Periods (Seconds)					
	1	2	3	4	5	6
Author's Results	2.193	2.015	0.712	0.609	0.417	0.306
Lumped Mass	2.238	2.048	0.733	0.624	0.436	0.319
Approximate hand method(25)	2.265	1.960	0.713	0.608	0.417	0.313
Uncoupled Approximate method	2.133	2.025	0.651	0.642	0.366	0.327

Table 5.b - Natural Periods of Vibration in Building 2 [$\bar{x}_o$ = -7.62 m (-25.0ft)]

Example Structure II - Comparison of Results

Mode	Natural Periods (Seconds)					
	1	2	3	4	5	6
Author's Results	2.252	1.93	0.737	0.559	0.434	0.304
Lumped Mass	2.298	1.958	0.758	0.572	0.453	0.324
Approximate hand method (25)	2.308	1.848	0.744	0.544	0.436	0.304
Uncoupled Approximate method	2.133	1.936	0.642	0.589	0.304	0.327

Table 5.c - Natural Periods of Vibration in Building 3 [$\bar{x}_c$ = - 15.24 m(-50.0ft)]

Example Structure II - Comparison of Results

Mode	Natural Periods (Seconds)					
	1	2	3	4	5	6
Author's Results	2.278	1.796	0.751	0.497	0.444	0.312
Lumped Mass	2.330	1.823	0.774	0.509	0.463	0.333
Approximate hand method (25)	2.280	1.795	0.752	0.495	0.446	0.312
Uncoupled Approximate method	2.101	1.810	0.635	0.520	0.247	0.324

Table 5.d - Natural Periods of Vibration in Building 4 [$\bar{x}_c$ = -22.86 m(-75.0ft)]

Example Structure II - Comparison of Results

assuming that the centroids of walls and frames coincide with the centre of mass, i.e., $e_m = 0$ and $a_m = 0$. For this special case, the motion is uncoupled and the values given in Table 5.a are in fact the exact uncoupled natural periods.

Combining the natural periods of the four buildings obtained by the author's analysis in one table, a complete understanding of the effect of the core eccentricity on the dynamic behaviour of the structure can be achieved. From Table 6.a one can conclude that the increase in the core eccentricity increases the natural period of the odd modes and decreases that of the even modes while Table 6.b shows that the ratio δ_θ/δ_Y varies in an opposite manner, for this type of structures.

Figures 7-a, 7-b and 7-c show the coupled flexural-torsional mode shapes for the first six normal modes of buildings 2, 3 and 4 respectively.

4. Special Case of a Single Wall-Frame System

The above section represents the dynamic analysis of a 2-dimensional wall-frame structure. The two coupled equations of motion and the eight boundary conditions of the problem determine the transverse coupled flexural-torsional vibrations of the structure. In the particular case with one planar wall, the problem converts to a special problem of a single wall-frame system.

Figure 8 shows the coordinate system for a typical cross-section of the system with one planar wall at point W. For this case

$$\overline{EI}_\omega = e_m^2 \cdot \overline{EI}_Y = r^2 \cdot \overline{EI}_Y \qquad (2.31)$$

Bld. \ Mode	Natural Periods (Seconds)					
	1	2	3	4	5	6
1	2.133	2.088	0.689	0.642	0.405	0.327
2	2.193	2.015	0.712	0.609	0.417	0.306
3	2.252	1.930	0.737	0.559	0.434	0.304
4	2.278	1.796	0.751	0.497	0.444	0.312

Table 6.a - Effect of Core Eccentricity on the Natural Periods - Example Structure II

	The ratio δ_θ / δ_Y					
Bld. \ Mode	1	2	3	4	5	6
2	0.781 (Bending)	2.431 (Torsion)	1.611 (Torsion)	1.075 (Torsion)	2.441 (Torsion)	0.560 (Bending)
3	0.652 (Bending)	2.700 (Torsion)	1.051 (Torsion)	1.657 (Torsion)	1.495 (Torsion)	1.071 (Torsion)
4	0.605 (Bending)	3.057 (Torsion)	0.826 (Bending)	1.963 (Torsion)	1.345 (Torsion)	0.874 (Bending)

Table 6.b - Effect of Core Eccentricity on the ratio δ_θ / δ_Y
Example Structure II

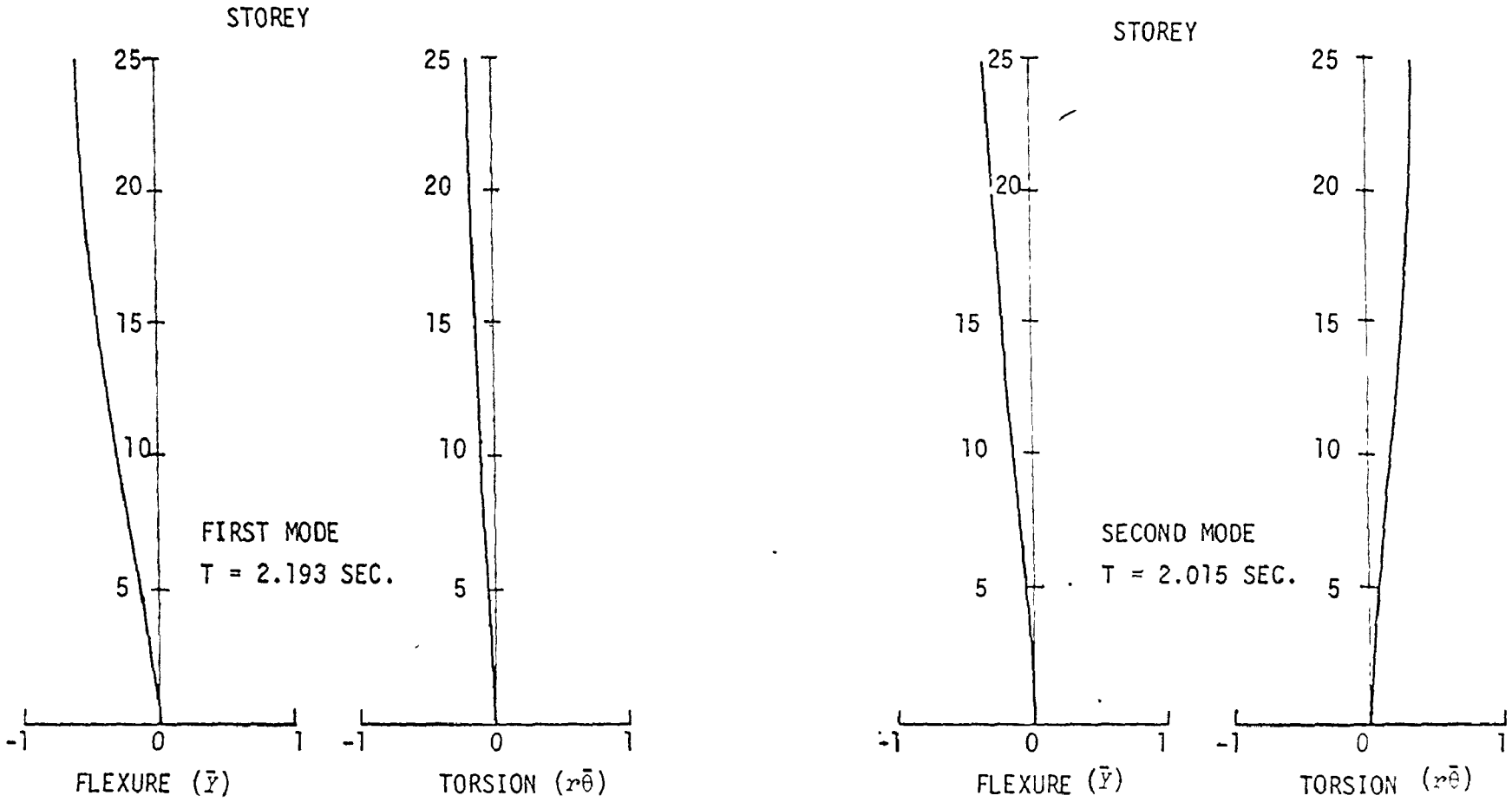

CORE ECCENTRICITY = -7.62 m (-25.0ft)

FIGURE 7-a(i) - THE COUPLED FLEXURAL-TORSIONAL MODE SHAPES - BUILDING 2 of EXAMPLE STRUCTURE II

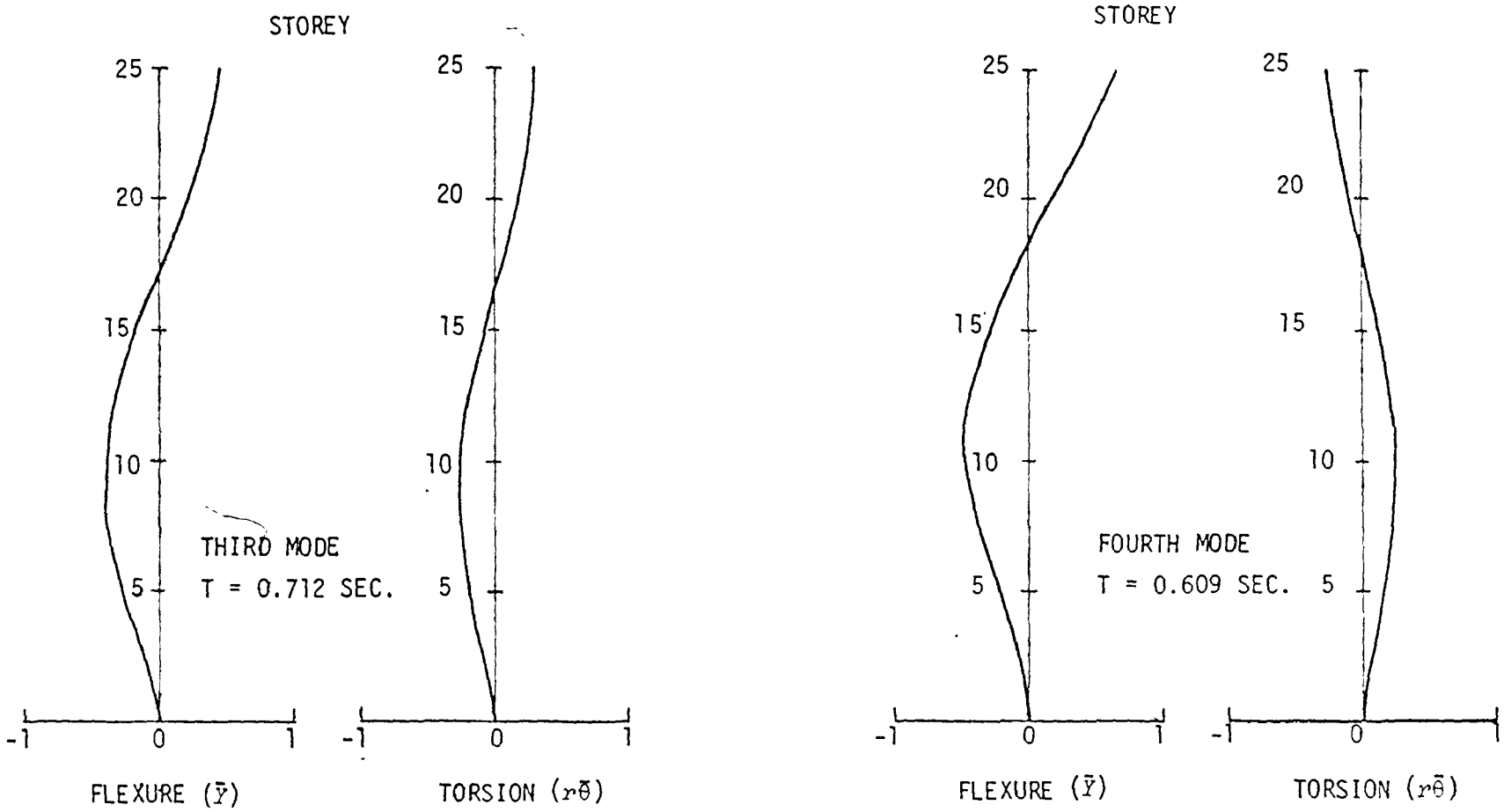

CORE ECCENTRICITY = -7.62 m (-25.0ft)

FIGURE 7-a(ii) - THE COUPLED FLEXURAL-TORSIONAL MODE SHAPES - BUILDING 2 of EXAMPLE STRUCTURE II

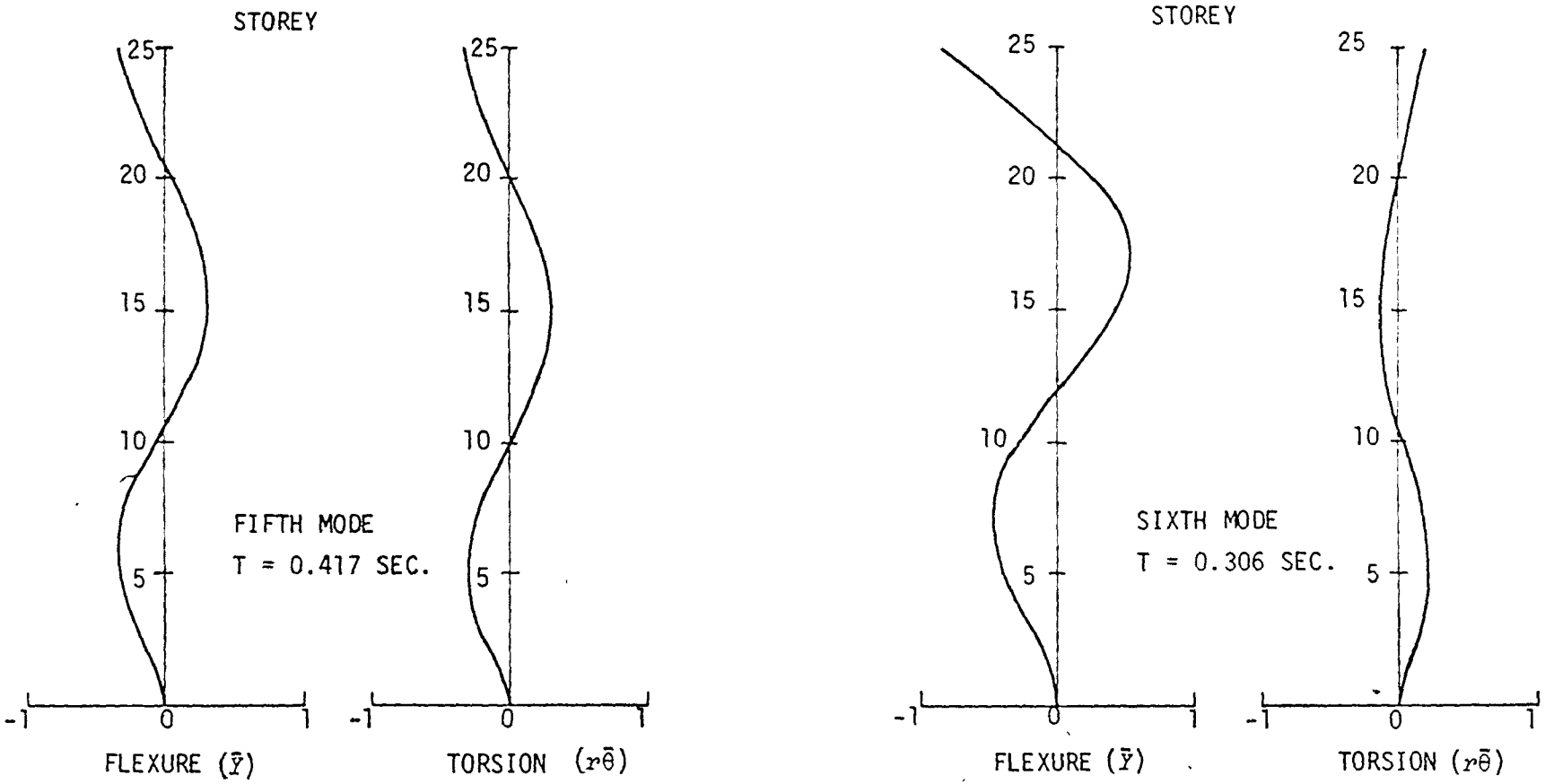

CORE ECCENTRICITY = -7.62 m (-25.0ft)

FIGURE 7-a(iii) - THE COUPLED FLEXURAL-TORSIONAL MODE SHAPES - BUILDING 2 of EXAMPLE STRUCTURE II

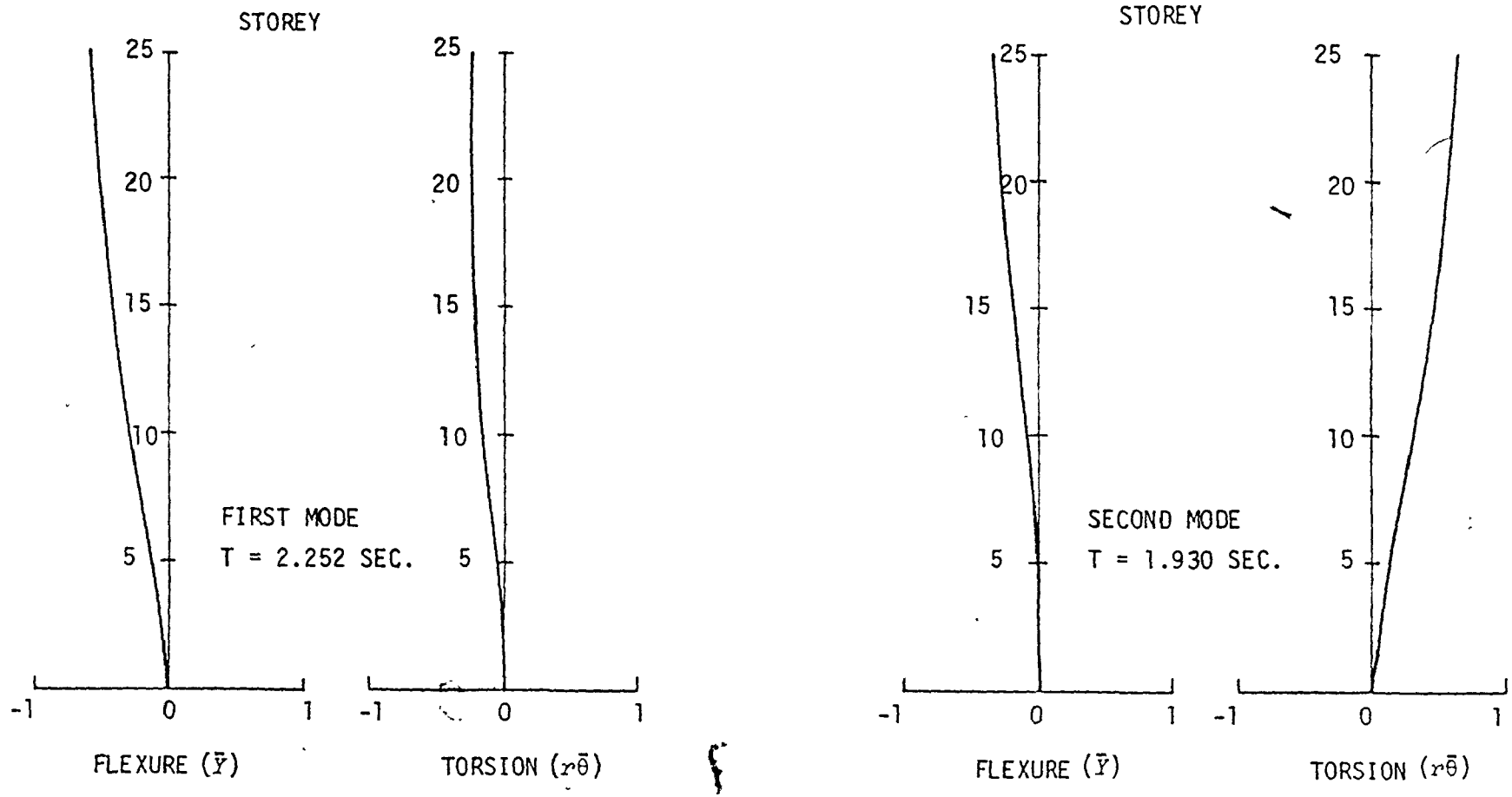

CORE ECCENTRICITY = -15.24 m (-50.0ft)

FIGURE 7-b(i) - THE COUPLED FLEXURAL-TORSIONAL MODE SHAPES - BUILDING 3 of EXAMPLE STRUCTURE II

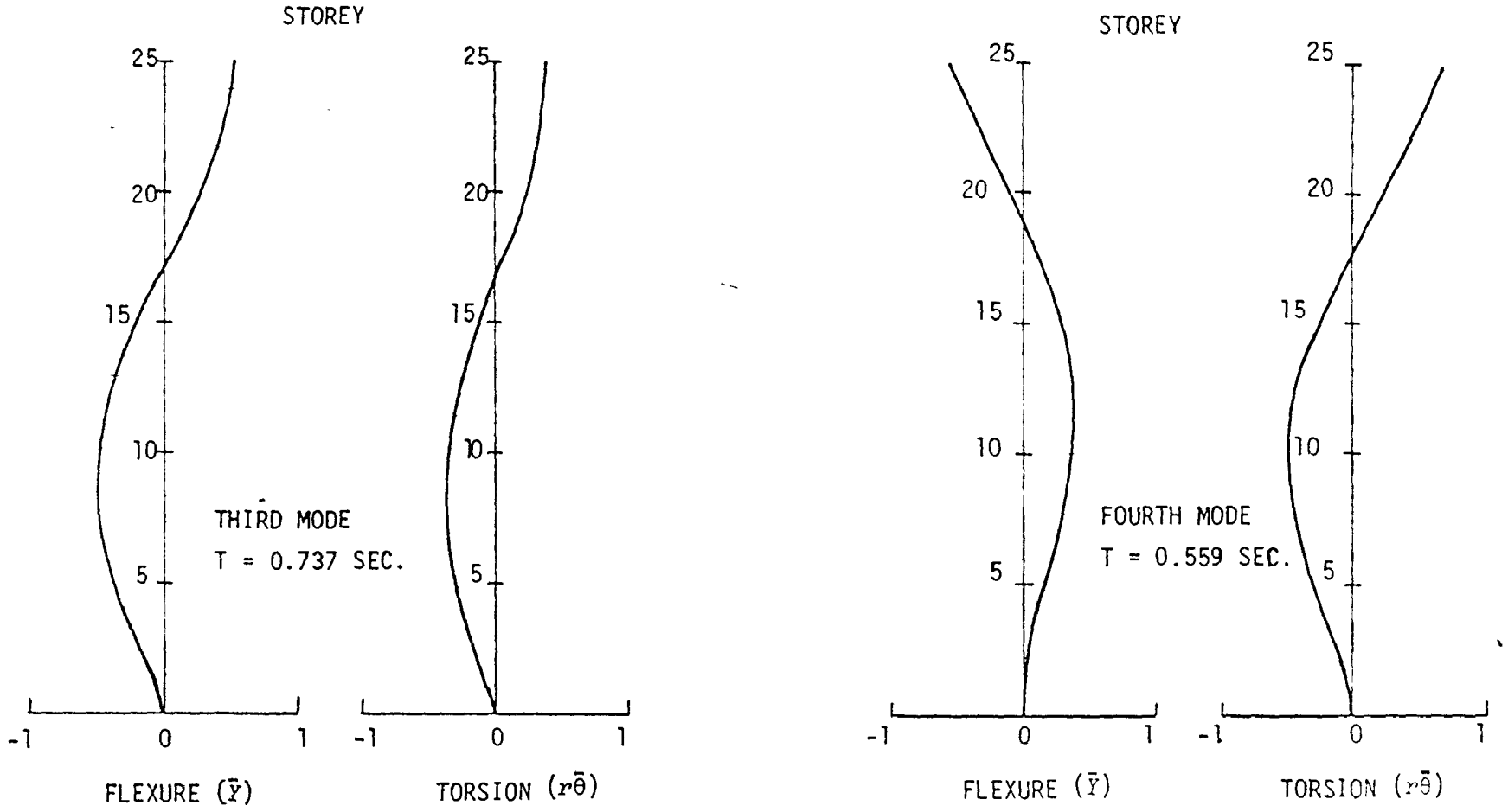

CORE ECCENTRICITY = -15.24 m (-50.0ft)

FIGURE 7-b(ii) - THE COUPLED FLEXURAL-TORSIONAL MODE SHAPES-
BUILDING 3 of EXAMPLE STRUCTURE II

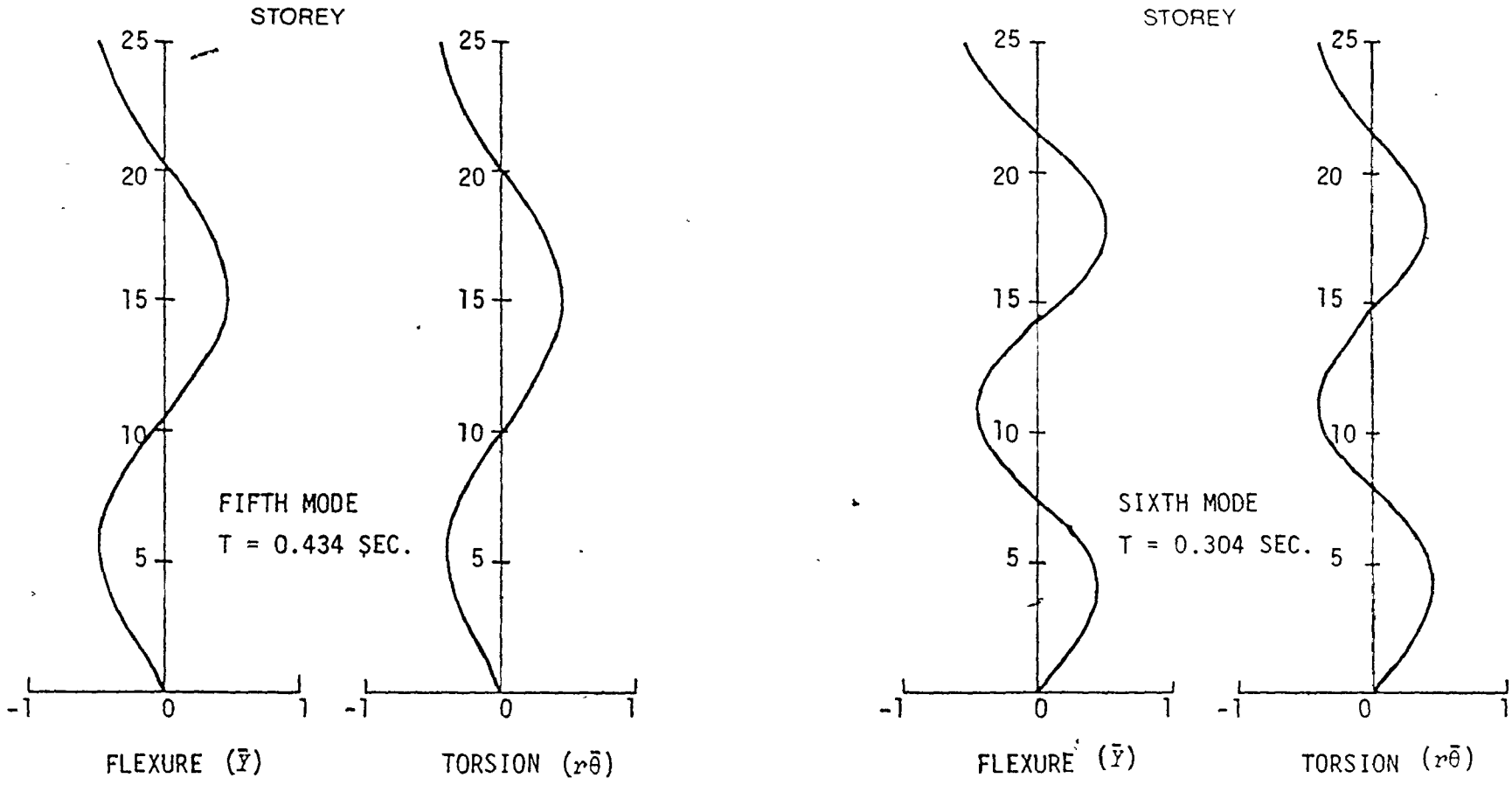

CORE ECCENTRICITY = -15.24 m (-50.0ft)

FIGURE 7-b(iii) - THE COUPLED FLEXURAL-TORSIONAL MODE SHAPES - BUILDING 3 of EXAMPLE STRUCTURE II

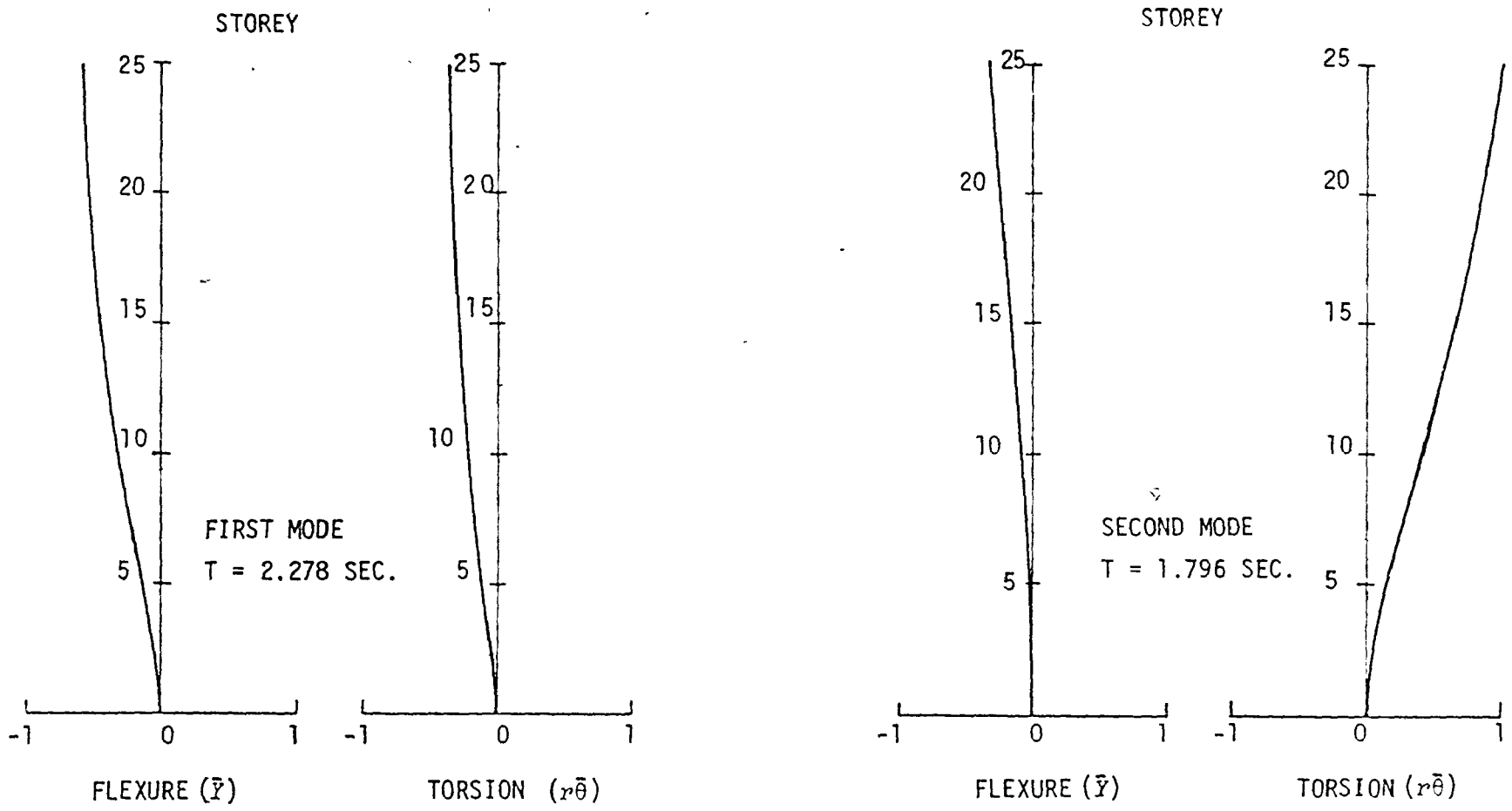

CORE ECCENTRICITY = -22.86 m (-75.0ft)

FIGURE 7-c(i) - THE COUPLED FLEXURAL-TORSIONAL MODE SHAPES-
BUILDING 4 of EXAMPLE STRUCTURE II

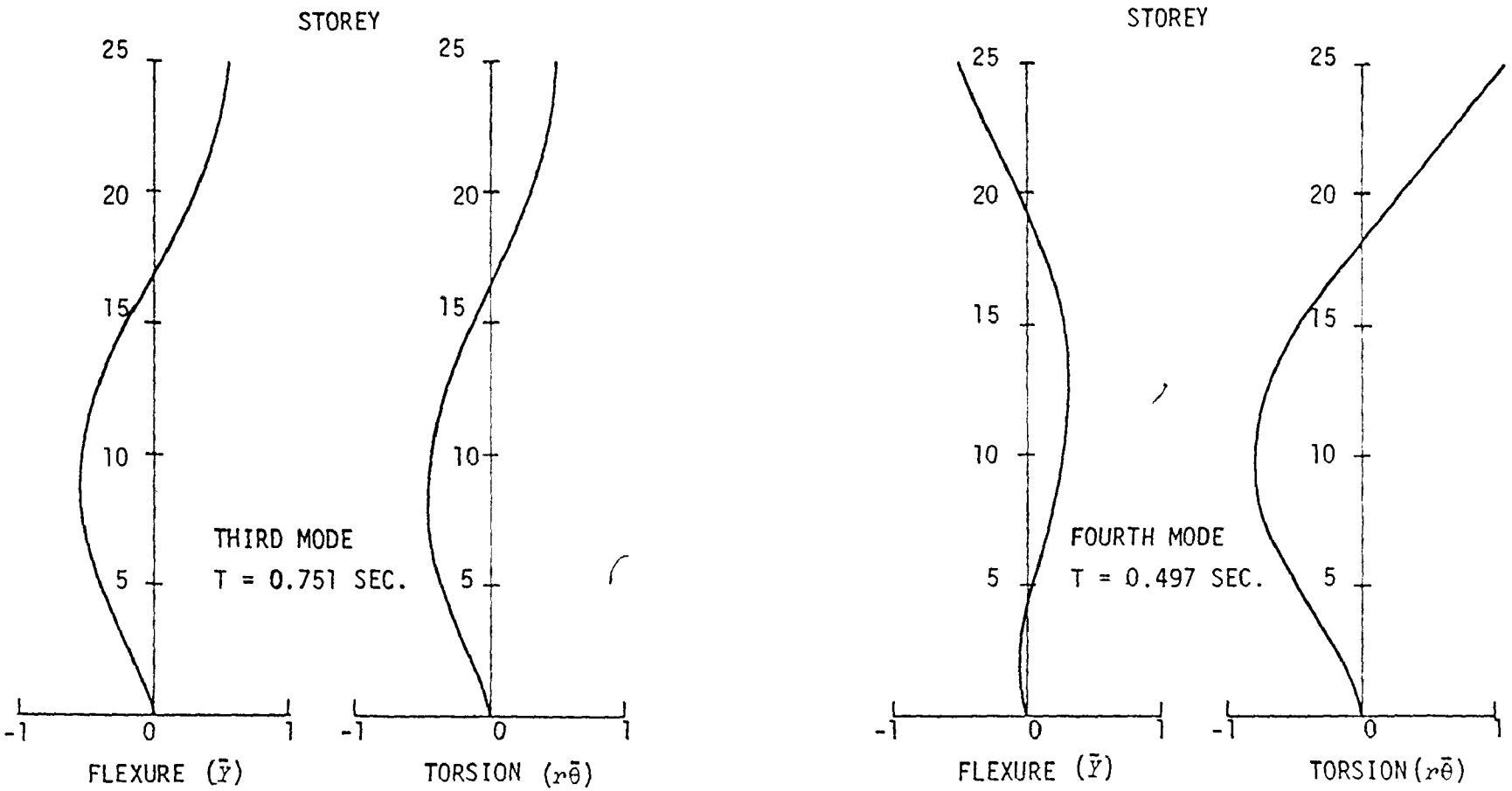

CORE ECCENTRICITY = -22.86 m (-75.0ft)

FIGURE 7-c(ii) - THE COUPLED FLEXURAL-TORSIONAL MODE SHAPES-
BUILDING 4 of EXAMPLE STRUCTURE II

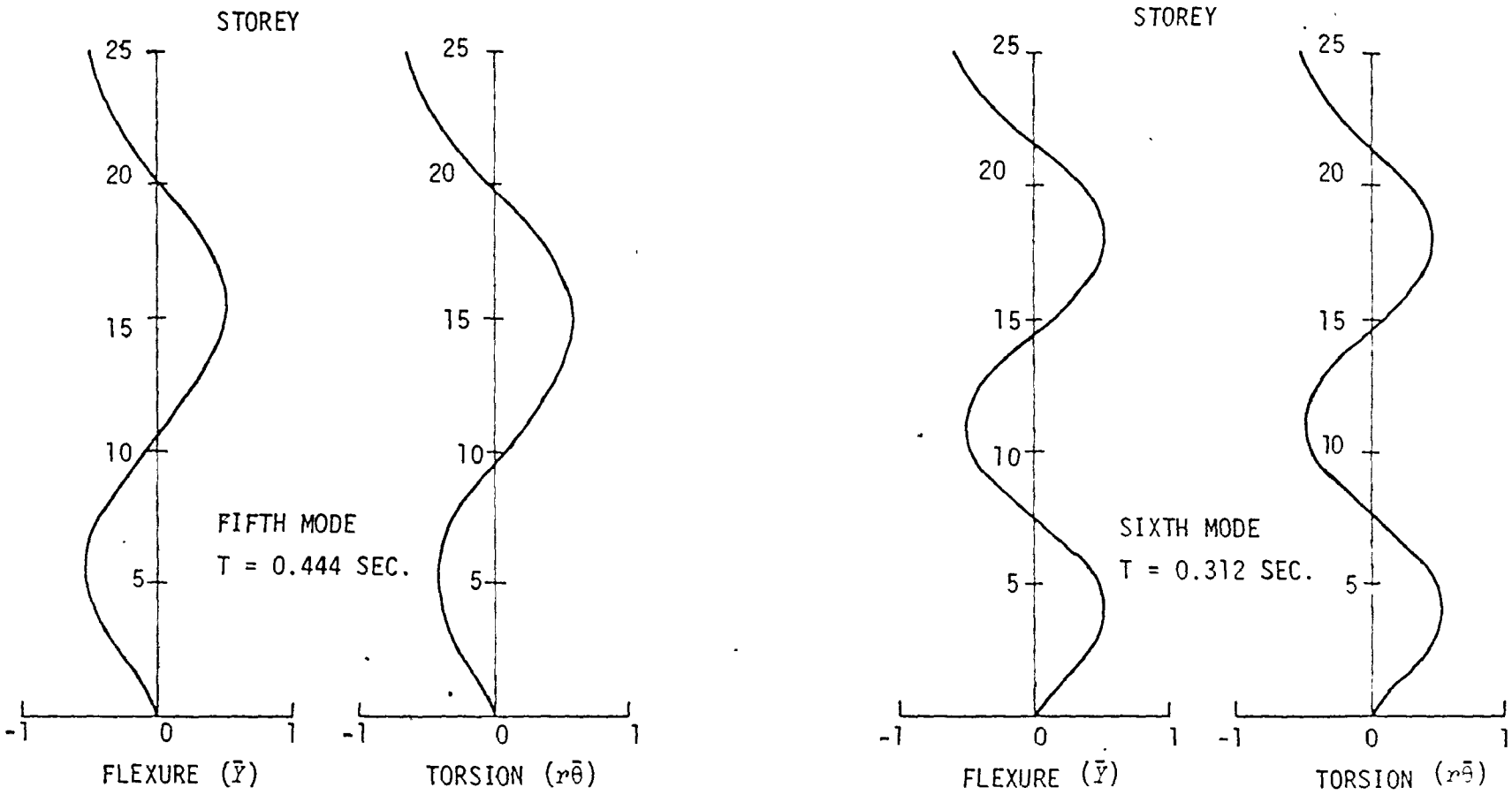

CORE ECCENTRICITY = -22.86 m (-75.0ft)

FIGURE 7-c(iii) - THE COUPLE FLEXURAL-TORSIONAL MODE SHAPES - BUILDING 4 of EXAMPLE STRUCTURE II

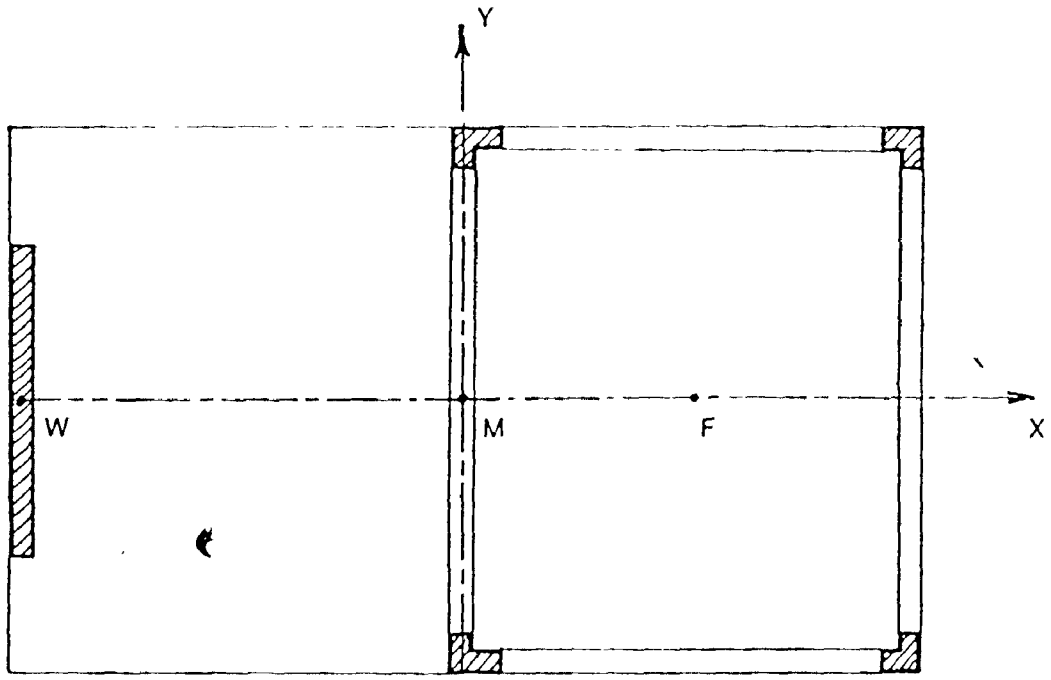

FIGURE 8 COORDINATE SYSTEM FOR A TYPICAL CROSS-SECTION OF A SINGLE WALL-FRAME SYSTEM

The two coupled equations of motion are

$$\frac{\partial^4 \bar{Y}}{\partial Z^4} - \alpha^2 \frac{\partial^2 \bar{Y}}{\partial Z^2} + \frac{\partial^4 (r\bar{\theta})}{\partial Z^4} - \frac{a_m}{r} \alpha^2 \frac{\partial^2 (r\bar{\theta})}{\partial Z^2} = - \frac{1}{b^2} \frac{\partial^2 \bar{Y}}{\partial t^2} \qquad (2.32a)$$

$$\frac{\partial^4 (r\bar{\theta})}{\partial Z^4} - \beta^2 \frac{\partial^2 (r\bar{\theta})}{\partial Z^2} + \frac{\partial^4 \bar{Y}}{\partial Z^4} - \frac{a_m}{r} \alpha^2 \frac{\partial^2 \bar{Y}}{\partial Z^2} = - \frac{1}{c^2} \frac{\partial^2 (r\bar{\theta})}{\partial t^2} \qquad (2.32b)$$

Solving by the same procedure of the previous section, the homogeneous matrix equation governing the constants c_{Yn} and $c_{\theta n}$ is arranged as follows

$$\begin{bmatrix} \lambda_n^4 - \alpha^2 \lambda_n^2 - \frac{\omega_n^2}{b^2} & \lambda_n^4 - \frac{a_m}{r} \alpha^2 \lambda_n^2 \\ \lambda_n^4 - \frac{a_m}{r} \alpha^2 \lambda_n^2 & \lambda_n^4 - \beta^2 \lambda_n^2 - \frac{\omega_n^2}{c^2} \end{bmatrix} \begin{Bmatrix} c_{Yn} \\ c_{\theta n} \end{Bmatrix} = \begin{Bmatrix} 0 \\ 0 \end{Bmatrix} \qquad (2.33)$$

The characteristic equation governing the non-trivial solution to the above homogeneous set of equations is a third order polynomial in λ_n^2 and it is written in the form

$$A_2^1 \lambda_n^6 + A_3 \lambda_n^4 + A_4 \lambda_n^2 + A_5 = 0 \qquad (2.34)$$

in which

$$A_2^1 = \alpha^2 (2 \frac{a_m}{r} - 1) - \beta^2 \qquad (2.35)$$

and the other coefficients are as given in equations (2.22). In this case each shape function requires six independent constants. These constants are to be determined from six boundary conditions. The only departure from the normal boundary conditions are the longitudinal displacement and the longitudinal strain at the base and at the top of the wall respectively, because of the effect of the wall sectorial coordinate.

The equation governing the longitudinal displacement of the wall is given by

$$\Delta_W (Z,t) = Z_W (Z,t) - \frac{\partial X_W}{\partial Z} (Z,t)\, x_W - \frac{\partial Y_W}{\partial Z} (Z,t)\, y_W - \frac{\partial \theta_W}{\partial Z} (Z,t)\, \omega_W \tag{2.36}$$

in which Δ_W is the longitudinal displacement in wall W, X_W, Y_W and Z_W are the displacements of the wall in the X, Y and Z directions respectively, θ_W is the rotational deformation, ω_W is the sectorial coordinate, (x_W , y_W) are the coordinate position and Z is the height above the foundation. In the present case since $Z_W(Z)$, $X_W(Z)$ and ω_W equal zero, equation (2.36) reduces to

$$\Delta_W (Z,t) = - \frac{\partial Y_W}{\partial Z} (Z,t)\, y_W \tag{2.37}$$

At the base of the structure, longitudinal displacement in wall W equals zero, yielding

$$\frac{\partial Y_W}{\partial Z} (0,t) = 0 \tag{2.38}$$

Substituting equation (2.3b) into the above equation yields

$$\frac{\partial \bar{Y}}{\partial Z} (0,t) + \frac{\partial (r\bar{\theta})}{\partial Z} (0,t) = 0 \tag{2.39}$$

The equation governing the longitudinal strain in the wall is given by

$$\varepsilon_W (Z,t) = \frac{\partial Z_W}{\partial Z} (Z,t) - \frac{\partial^2 X_W}{\partial Z^2} (Z,t)\, x_W - \frac{\partial^2 Y_W}{\partial Z^2} (Z,t)\, y_W - \frac{\partial^2 \theta_W}{\partial Z^2} (Z,t)\, \omega_W \tag{2.40}$$

in which ε_W is the longitudinal strain in wall W and the other quantities are as defined for equation (2.36). In this case equation (2.40) reduces to

$$\varepsilon_W (Z,t) = - \frac{\partial^2 Y_W}{\partial Z^2} (Z,t)\, y_W \tag{2.41}$$

At the top of the structure, longitudinal strain in wall W equals zero, yields

$$\frac{\partial^2 Y_W}{\partial Z}(H,t) = 0 \tag{2.42}$$

Substituting equation (2.3b) into the above equation, yields

$$\frac{\partial^2 \bar{Y}}{\partial Z^2}(H,t) + \frac{\partial^2 (r\bar{\theta})}{\partial Z^2}(H,t) = 0 \tag{2.43}$$

Equations (2.39) and (2.43) are the two combined boundary conditions instead of four boundary conditions in the general case studied in Section 3. For the particular case it can be shown that the boundary conditions governing the mode shapes are given by

(a) at the base of the structure, $Z = 0$

(i) $$\bar{Y}(0,t) = 0 \tag{2.44a}$$

$$r\bar{\theta}(0,t) = 0 \tag{2.44b}$$

(ii) $$\frac{\partial \bar{Y}}{\partial Z}(0,t) + \frac{\partial r\bar{\theta}}{\partial Z}(0,t) = 0 \tag{2.44c}$$

(b) at the top of the structure, $Z = H$

(i) $$\frac{\partial^2 \bar{Y}}{\partial Z^2}(H,t) + \frac{\partial^2 r\bar{\theta}}{\partial Z^2}(H,t) = 0 \tag{2.44d}$$

(ii) $$-\frac{\partial^3 \bar{Y}}{\partial Z^3}(H,t) - \frac{\partial^3 r\bar{\theta}}{\partial Z^3}(H,t) + \alpha^2 \frac{\partial \bar{Y}}{\partial Z}(H,t) + \frac{a_m}{r}\ \alpha^2 \frac{\partial r\bar{\theta}}{\partial Z}(H,t) = 0 \tag{2.44e}$$

$$-\frac{\partial^3 r\bar{\theta}}{\partial Z^3}(H,t) - \frac{\partial^3 \bar{Y}}{\partial Z^3}(H,t) + \beta^2 \frac{\partial r\bar{\theta}}{\partial Z}(H,t) + \frac{a_m}{r}\ \alpha^2 \frac{\partial \bar{Y}}{\partial Z}(H,t) = 0 \tag{2.44f}$$

Referring to equations (2.14), (2.15) and (2.18) the above boundary conditions may be written for the n^{th} mode of vibration as,

(a) at $Z = 0$

$$\phi_{Yn}(0) = 0 \tag{2.45a}$$

$$\phi_{\theta n}(0) = 0 \tag{2.45b}$$

$$\frac{d\phi_{Yn}}{dZ}(0) + \frac{d\phi_{\theta n}}{dZ}(0) = 0 \tag{2.45c}$$

(b) at $Z = H$

$$\frac{d^2\phi_{Yn}}{dZ^2}(H) + \frac{d^2\phi_{\theta n}}{dZ^2}(H) = 0 \tag{2.45d}$$

$$-\frac{d^3\phi_{Yn}}{dZ^3}(H) - \frac{d^3\phi_{\theta n}}{dZ^3}(H) + \alpha^2 \frac{d\phi_{Yn}}{dZ}(H) + \frac{a_m}{r}\alpha^2 \frac{d\phi_{\theta n}}{dZ}(H) = 0 \tag{2.45e}$$

$$-\frac{d^3\phi_{\theta n}}{dZ^3}(H) - \frac{d^3\phi_{Yn}}{dZ^3}(H) + \beta^2 \frac{d\phi_{\theta n}}{dZ}(H) + \frac{a_m}{r}\alpha^2 \frac{d\phi_{Yn}}{dZ}(H) = 0 \tag{2.45f}$$

Putting the six boundary conditions in a matrix form similar to equation (2.28), this equation (2.46) represents a set of six linear homogeneous equations which may also be written in brief as

$$\left[F_n[\omega_n^2 , \lambda_{ni} \ (i = 1,2,\ldots,6)]\right] \ \{c_{Yn}\} = \{0\} \tag{2.47}$$

where $\{c_{Yn}\}$ is the column vector containing the unknown coefficients c_{Yni} $(i = 1,2,\ldots,6)$, n is the frequency number and $[F]$ is the matrix of equation (2.46). A nontrivial solution for equation (2.47) can only be obtained if the determinant of the matrix $[F]$ is zero. Thus

$$| F_n [\omega_n^2 , \lambda_{ni} \ (i = 1,2,\ldots,6)] | = 0 \tag{2.48}$$

The procedure for determining the natural frequencies and the coupled flexural-torsional modes of vibration is similar to that of the general case.

$$
\begin{bmatrix}
1 & 1 & 1 & 1 & 1 & 1 \\
R_{n1} & R_{n2} & R_{n3} & R_{n4} & R_{n5} & R_{n6} \\
\lambda_{n1}(1+R_{n1}) & \lambda_{n2}(1+R_{n2}) & \lambda_{n3}(1+R_{n3}) & \lambda_{n4}(1+R_{n4}) & \lambda_{n5}(1+R_{n5}) & \lambda_{n6}(1+R_{n6}) \\
\lambda_{n1}^2(1+R_{n1})e^{\lambda_{n1}H} & \lambda_{n2}^2(1+R_{n2})e^{\lambda_{n2}H} & \lambda_{n3}^2(1+R_{n3})e^{\lambda_{n3}H} & \lambda_{n4}^2(1+R_{n4})e^{\lambda_{n4}H} & \lambda_{n5}^2(1+R_{n5})e^{\lambda_{n5}H} & \lambda_{n6}^2(1+R_{n6})e^{\lambda_{n6}H} \\
U_{n1}e^{\lambda_{n1}H} & U_{n2}e^{\lambda_{n2}H} & U_{n3}e^{\lambda_{n3}H} & U_{n4}e^{\lambda_{n4}H} & U_{n5}e^{\lambda_{n5}H} & U_{n6}e^{\lambda_{n6}H} \\
V_{n1}e^{\lambda_{n1}H} & V_{n2}e^{\lambda_{n2}H} & V_{n3}e^{\lambda_{n3}H} & V_{n4}e^{\lambda_{n4}H} & V_{n5}e^{\lambda_{n5}H} & V_{n6}e^{\lambda_{n6}H}
\end{bmatrix}
\begin{bmatrix} c_{Yn1} \\ c_{Yn2} \\ c_{Yn3} \\ c_{Yn4} \\ c_{Yn5} \\ c_{Yn6} \end{bmatrix}
=
\begin{bmatrix} 0 \\ 0 \\ 0 \\ 0 \\ 0 \\ 0 \end{bmatrix}
\tag{2.46}
$$

$$
U_{ni} = \lambda_{ni}\left(\alpha^2 + \alpha^2 \frac{a_m}{r} R_{ni}\right) - \lambda_{ni}^3 (1 + R_{ni}) \tag{2.46a}
$$

$$
V_{ni} = \lambda_{ni}\left(\beta^2 R_{ni} + \alpha^2 \frac{a_m}{r}\right) - \lambda_{ni}^3 (R_{ni} + 1) \tag{2.46b}
$$

The above particular case is applicable for a general asymmetric wall-frame structure in which the core is located at large eccentricity from the centre of mass.

Building 4 [$\bar{x}_c$ = -22.86 m(-75.0ft)] of Example Structure II whose floor plan is given in Figure 6 is solved by the particular method and the coupled natural periods computed are given in Table 7. In addition to these approximate natural periods, Table 7 shows the exact results already given in Table 5.d. By comparing these results it can be seen that this particular analysis yields results which compare very well with those obtained from the general analysis for this kind of buildings with large core eccentricity. This agreement is due to the negligible warping torsional stiffness of the core $EI_{\omega c}$ with respect to the total warping torsional stiffness of the structure $\overline{EI}_{\omega}$. For this case the flexural radius of gyration r is approximately equal to the wall eccentricity e_m.

Mode	Natural Periods (Seconds)					
	1	2	3	4	5	6
Exact Method (8 boundary Conditions)	2.278	1.796	0.751	0.497	0.444	0.312
Approximate Method (6 boundary Conditions)	2.336	1.796	0.774	0.497	0.462	0.331
Difference	+2.5%	0.0%	+3.0%	0.0%	+4.0%	+6.0%

$$\text{Difference} = \frac{\text{Approximate Period - Exact Period}}{\text{Exact Period}} \times 100\%$$

Table 7 - Comparison of Exact and Approximate Natural Periods for Building 4[$\bar{x}_c$ = -22.86 m(-75.0ft)] - Example Structure II

CHAPTER III

RESPONSE ANALYSIS

1. Introduction

It was shown in Section 3 of Chapter II that for a 2-dimensional wall-frame structure with X-axis as the axis of symmetry, the displacements $\bar{Y}(Z,t)$ and $\bar{\theta}(Z,t)$ are coupled with each other whereas the displacement $\bar{X}(Z,t)$ is uncoupled; where $\bar{X}(Z,t)$ and $\bar{Y}(Z,t)$ are the translational displacements of the centre of mass in X and Y directions and $\bar{\theta}(Z,t)$ is the rotation of the structure about the centre of mass. In this chapter, the flexural and torsional components $\phi_{Yn}(Z)$ and $\phi_{\theta n}(Z)$ of the corresponding mode shape being calculated, the two coupled displacements $\bar{Y}(Z,t)$ and $\bar{\theta}(Z,t)$ can be found for any ground motion excitation applied to the structure. When finding the response of the structure under the influence of such base motion, orthogonality of modes of vibration is used in the analysis. This orthogonality normality relationship as derived by Raina (22) for coupled n - θ modes in the thin-walled model is derived in the more general case of wall-frame structure for coupled Y - θ modes. The centre of mass response due to a sinusoidal base motion is studied and generalized to that due to seismic ground motion.

2. Treatment for Normalized Mode Shapes

The coupled linear, homogeneous differential equations governing the entire structure can be written in the form

$$[K_3]\begin{Bmatrix}\ddot{\bar{Y}}\\ r\ddot{\bar{\theta}}\end{Bmatrix} + [K]\begin{Bmatrix}\bar{Y}\\ r\bar{\theta}\end{Bmatrix} = \begin{Bmatrix}0\\0\end{Bmatrix} \tag{3.1}$$

in which

$$[K] = \begin{bmatrix} \frac{\partial^4}{\partial Z^4} - \alpha^2 \frac{\partial^2}{\partial Z^2} & \frac{e_m}{r}\frac{\partial^4}{\partial Z^4} - \frac{a_m}{r}\alpha^2\frac{\partial^2}{\partial Z^2} \\ \frac{e_m}{r}\frac{\partial^4}{\partial Z^4} - \frac{a_m}{r}\alpha^2\frac{\partial^2}{\partial Z^2} & \frac{\partial^4}{\partial Z^4} - \beta^2\frac{\partial^2}{\partial Z^2} \end{bmatrix} \tag{3.2}$$

and $[K_3]$ is as defined in equation (2.14b); $\ddot{\bar{Y}} = \partial^2\bar{Y}/\partial t^2$ and $r\ddot{\bar{\theta}} = \partial^2 r\bar{\theta}/\partial t^2$

Rewriting equation (2.15) in a convenient form gives

$$\begin{Bmatrix}\bar{Y}(Z,t)\\ r\bar{\theta}(Z,t)\end{Bmatrix} = \sum_{n=1}^{\infty}\begin{Bmatrix}\phi_{Yn}(Z)\\ \phi_{\theta n}(Z)\end{Bmatrix}\sin\omega_n t \tag{3.3}$$

Substitution of equation (3.3) into equation (3.1) yields for the n^{th} mode of vibration

$$-\omega_n^2[K_3]\begin{Bmatrix}\phi_{Yn}\\ \phi_{\theta n}\end{Bmatrix} + [K]\begin{Bmatrix}\phi_{Yn}\\ \phi_{\theta n}\end{Bmatrix} = \begin{Bmatrix}0\\0\end{Bmatrix} \tag{3.4}$$

Premultiplication of equation (3.4) by $\begin{Bmatrix}\phi_{Ym}\\ \phi_{\theta m}\end{Bmatrix}^T$, the transpose of $\begin{Bmatrix}\phi_{Ym}\\ \phi_{\theta m}\end{Bmatrix}$, and subsequent integration along the structure from $Z = 0$ to H yields

$$\int_0^H \begin{Bmatrix}\phi_{Ym}\\ \phi_{\theta m}\end{Bmatrix}^T [K]\begin{Bmatrix}\phi_{Yn}\\ \phi_{\theta n}\end{Bmatrix} dZ = \omega_n^2 \int_0^H \begin{Bmatrix}\phi_{Ym}\\ \phi_{\theta m}\end{Bmatrix}^T [K_3]\begin{Bmatrix}\phi_{Yn}\\ \phi_{\theta n}\end{Bmatrix} dZ \tag{3.5}$$

Interchanging the indices m and n in equation (3.5) gives

$$\int_0^H \begin{Bmatrix}\phi_{Yn}\\ \phi_{\theta n}\end{Bmatrix}^T [K]\begin{Bmatrix}\phi_{Ym}\\ \phi_{\theta m}\end{Bmatrix} dZ = \omega_m^2 \int_0^H \begin{Bmatrix}\phi_{Yn}\\ \phi_{\theta n}\end{Bmatrix}^T [K_3]\begin{Bmatrix}\phi_{Ym}\\ \phi_{\theta m}\end{Bmatrix} dZ \tag{3.6}$$

Denoting the left hand side integrals of equations (3.5) and (3.6) by I_1 and I_2 respectively, and subtracting equation (3.6) from equation (3.5) yields

$$(\omega_n^2 - \omega_m^2) \int_0^H \begin{Bmatrix} \phi_{Yn} \\ \phi_{\theta n} \end{Bmatrix}^T [K_3] \begin{Bmatrix} \phi_{Ym} \\ \phi_{\theta m} \end{Bmatrix} dZ = I_1 - I_2 \tag{3.7}$$

Substitution of equation (3.2) and simplification of I_1 and I_2 yields

$$I_1 = \int_0^H \left[\phi_{Ym} \left(\frac{d^4\phi_{Yn}}{dZ^4} - \alpha^2 \frac{d^2\phi_{Yn}}{dZ^2} + \frac{e_m}{r} \frac{d^4\phi_{\theta n}}{dZ^4} - \frac{a_m}{r} \alpha^2 \frac{d^2\phi_{\theta n}}{dZ^2} \right) + \phi_{\theta m} \left(\frac{e_m}{r} \frac{d^4\phi_{Yn}}{dZ^4} - \frac{a_m}{r} \alpha^2 \frac{d^2\phi_{Yn}}{dZ^2} + \frac{d^4\phi_{\theta n}}{dZ^4} - \beta^2 \frac{d^2\phi_{\theta n}}{dZ^2} \right) \right] dZ \tag{3.8}$$

$$I_2 = \int_0^H \left[\phi_{Yn} \left(\frac{d^4\phi_{Ym}}{dZ^4} - \alpha^2 \frac{d^2\phi_{Ym}}{dZ^2} + \frac{e_m}{r} \frac{d^4\phi_{\theta m}}{dZ^4} - \frac{a_m}{r} \alpha^2 \frac{d^2\phi_{\theta m}}{dZ^2} \right) + \phi_{\theta n} \left(\frac{e_m}{r} \frac{d^4\phi_{Ym}}{dZ^4} - \frac{a_m}{r} \alpha^2 \frac{d^2\phi_{Ym}}{dZ^2} + \frac{d^4\phi_{\theta m}}{dZ^4} - \beta^2 \frac{d^2\phi_{\theta m}}{dZ^2} \right) \right] dZ \tag{3.9}$$

Successive integration by parts of I_1 and application of the homogeneous boundary conditions given by the equations (2.23) yields

$$I_1 = \int_0^H \left[\phi_{Yn} \left(\frac{d^4\phi_{Ym}}{dZ^4} - \alpha^2 \frac{d^2\phi_{Ym}}{dZ^2} + \frac{e_m}{r} \frac{d^4\phi_{\theta m}}{dZ^4} - \frac{a_m}{r} \alpha^2 \frac{d^2\phi_{\theta m}}{dZ^2} \right) + \phi_{\theta n} \left(\frac{e_m}{r} \frac{d^4\phi_{Ym}}{dZ^4} - \frac{a_m}{r} \alpha^2 \frac{d^2\phi_{Ym}}{dZ^2} + \frac{d^4\phi_{\theta m}}{dZ^4} - \beta^2 \frac{d^2\phi_{\theta m}}{dZ^2} \right) \right] dZ \tag{3.10}$$

Subtracting equation (3.9) from equation (3.10) it is seen that

$$I_1 - I_2 = 0 \tag{3.11}$$

Substituting equation (3.11) into equation (3.7) gives

$$(\omega_n^2 - \omega_m^2) \int_0^H \begin{Bmatrix} \phi_{Yn} \\ \phi_{\theta n} \end{Bmatrix}^T [K_3] \begin{Bmatrix} \phi_{Ym} \\ \phi_{\theta m} \end{Bmatrix} dZ = 0 \tag{3.12}$$

Since $\omega_n^2 \neq \omega_m^2$ for $m \neq n$, so

$$\int_0^H \begin{Bmatrix} \phi_{Yn} \\ \phi_{\theta n} \end{Bmatrix} [K_3] \begin{Bmatrix} \phi_{Ym} \\ \phi_{\theta m} \end{Bmatrix} dZ = 0 \quad ; \quad m \neq n \tag{3.13}$$

The above equation is the orthogonality condition for the non-degenerate modes of vibration.

Multiplying the vector of shape functions ϕ_{Yn} and $\phi_{\theta n}$ by a constant Q_n yields another vector function given by

$$\begin{Bmatrix} {}^N\phi_{Yn} \\ {}^N\phi_{\theta n} \end{Bmatrix} = Q_n \begin{Bmatrix} \phi_{Yn} \\ \phi_{\theta n} \end{Bmatrix} \tag{3.14}$$

where the constant Q_n is chosen such that

$$\int_0^H \begin{Bmatrix} {}^N\phi_{Yn} \\ {}^N\phi_{\theta n} \end{Bmatrix}^T [K_3] \begin{Bmatrix} {}^N\phi_{Yn} \\ {}^N\phi_{\theta n} \end{Bmatrix} dZ = 1 \tag{3.15}$$

Substituting equation (3.14) into equation (3.15) gives

$$Q_n = \frac{1}{\sqrt{\int_0^H \begin{Bmatrix} \phi_{Yn} \\ \phi_{\theta n} \end{Bmatrix}^T [K_3] \begin{Bmatrix} \phi_{Yn} \\ \phi_{\theta n} \end{Bmatrix} dZ}} \tag{3.16}$$

The vector function $\begin{Bmatrix} {}^N\phi_{Yn} \\ {}^N\phi_{\theta n} \end{Bmatrix}$ is the orthonormal eigen-vector for the n^{th} mode of vibration. Equation (3.15) gives the normality condition

for the n^{th} mode. Substitution of equation (2.14b) and simplification of equation (3.15) gives the normality condition in the form

$$\int_0^H \left[\frac{\left(\phi_{Yn}^N\right)^2}{b^2} + \frac{\left(\phi_{\theta n}^N\right)^2}{c^2} \right] dZ = 1 \qquad (3.17)$$

Similarly, the normalization factor Q_n, may be given as

$$Q_n = \frac{1}{\sqrt{\int_0^H \left(\frac{\phi_{Yn}^2}{b^2} + \frac{\phi_{\theta n}^2}{c^2} \right) dZ}} \qquad (3.18)$$

Substituting equation (3.18) into equation (3.14) gives the normalized flexural-torsional mode shape for the n^{th} mode of vibration.

3. Centre of Mass Response due to a Sinusoidal Base Motion

Equation (3.1) represents the case of free vibration of the structure. This equation is similar in shape with that of the two degree of freedom system, in which $[K_3]$ represents the lumped mass matrix and $[K]$ represents the stiffness matrix.

Assuming the lateral displacement applied to the base of the structure to be given by

$$Y = Y_0 \sin \Omega t \qquad (3.19)$$

where Y_0 is the amplitude of the motion and Ω is the excitation frequency in radians / second. It can be shown (22) that the global displacements of the centre of mass at any time are given by

$$\begin{Bmatrix} \bar{Y}(Z,t) \\ r\bar{\theta}(Z,t) \end{Bmatrix}_n^G = \begin{Bmatrix} \bar{Y}(Z,t) \\ r\bar{\theta}(Z,t) \end{Bmatrix}_n^L + \begin{Bmatrix} Y_0 \sin \Omega t \\ 0 \end{Bmatrix} \qquad (3.20)$$

in which $\begin{Bmatrix} \bar{Y} \\ r\bar{\theta} \end{Bmatrix}_n^G$ are the global displacements of the centre of mass at any time and $\begin{Bmatrix} \bar{Y} \\ r\bar{\theta} \end{Bmatrix}_n^L$ are the local displacements of the centre of mass with reference to the OXZ plane passing through the X-axis of the base of the structure at any time.

As the strains are caused only by the local displacements it is of major interest to investigate $\begin{Bmatrix} \bar{Y} \\ r\bar{\theta} \end{Bmatrix}_n^L$.

Substitution of equation (3.20) into equation (3.1) yields

$$[K_3] \begin{Bmatrix} \ddot{\bar{Y}} \\ r\ddot{\bar{\theta}} \end{Bmatrix}_n^L + [K] \begin{Bmatrix} \bar{Y} \\ r\bar{\theta} \end{Bmatrix}_n^L = [K_3] \begin{Bmatrix} \Omega^2 Y_0 \sin \Omega t \\ 0 \end{Bmatrix} \quad (3.21)$$

in which $[K_3]$ and $[K]$ are as defined in equations (2.14b) and (3.2), respectively. This is the non-homogeneous differential equation of motion governing the case of a sinusoidal base motion applied to the base of the structure, for mode n.

The initial conditions of the motion are given by

$$\begin{Bmatrix} \bar{Y}(Z,0) \\ r\bar{\theta}(Z,0) \end{Bmatrix}_n^G = \begin{Bmatrix} 0 \\ 0 \end{Bmatrix} , \begin{Bmatrix} \dot{\bar{Y}}(Z,0) \\ r\dot{\bar{\theta}}(Z,0) \end{Bmatrix}_n^G = \begin{Bmatrix} Y_0 \ \Omega \\ 0 \end{Bmatrix} \quad (3.22)$$

Therefore, the initial conditons for the local displacements $\begin{Bmatrix} \bar{Y} \\ r\bar{\theta} \end{Bmatrix}_n^L$ are obtained by substituting equation (3.22) into equation (3.20) which gives

$$\begin{Bmatrix} \bar{Y}(Z,0) \\ r\bar{\theta}(Z,0) \end{Bmatrix}_n^L = \begin{Bmatrix} 0 \\ 0 \end{Bmatrix} , \begin{Bmatrix} \dot{\bar{Y}}(Z,0) \\ r\dot{\bar{\theta}}(Z,0) \end{Bmatrix}_n^L = \begin{Bmatrix} 0 \\ 0 \end{Bmatrix} \quad (3.23)$$

For the sake of convenience the superscript L, refering to the local axis, is dropped in the following analysis.

The solution to equation (3.21) may conveniently be assumed to be of the form

$$\begin{Bmatrix} \bar{Y}(Z,t) \\ r\bar{\theta}(Z,t) \end{Bmatrix} = \sum_{n=1}^{\infty} T_n(t) \begin{Bmatrix} \phi^N_{Yn}(Z) \\ \phi^N_{\theta n}(Z) \end{Bmatrix} \tag{3.24}$$

in which $T_n(t)$ determines the variation with time (t) for the n^{th} mode of vibration satisfying the initial conditions given in equation (3.23), $\begin{Bmatrix} \phi^N_{Yn}(Z) \\ \phi^N_{\theta n}(Z) \end{Bmatrix}$ determines the variation with height (Z) for this mode of vibration satisfying the boundary conditions given in equations (2.23). Rearranging the right hand side of equation (3.21) by inserting equation (2.14b) in it, substituting equation (3.24) into equation (3.21) and writing the resulting equation for the m^{th} mode of vibration gives

$$[K_3] \begin{Bmatrix} \phi^N_{Ym}(Z) \\ \phi^N_{\theta m}(Z) \end{Bmatrix} \ddot{T}_m(t) + [K] \begin{Bmatrix} \phi^N_{Ym}(Z) \\ \phi_{\theta m}(Z) \end{Bmatrix} T_m(t) = Y_0 \Omega^2 \sin \Omega t \begin{Bmatrix} \frac{1}{b^2} \\ 0 \end{Bmatrix} \tag{3.25}$$

Inserting equation (3.4) into equation (3.25), yields

$$[K_3] \begin{Bmatrix} \phi^N_{Ym} \\ \phi^N_{\theta m} \end{Bmatrix} \ddot{T}_m(t) + \omega_m^2 [K_3] \begin{Bmatrix} \phi^N_{Ym} \\ \phi^N_{\theta m} \end{Bmatrix} T_m(t) = Y_0 \Omega^2 \sin \Omega t \begin{Bmatrix} \frac{1}{b^2} \\ 0 \end{Bmatrix} \tag{3.26}$$

Premultiplying equation (3.26) by $\begin{Bmatrix} \phi^N_{Ym} \\ \phi^N_{\theta m} \end{Bmatrix}^T$, integrating along the building height from 0 to H and using the orthogonality-normality relationship given by equation (3.15) yields

$$\ddot{T}_m(t) + \omega_m^2 T_m(t) = Y_0 \Omega^2 \sin \Omega t \int_0^H \begin{Bmatrix} \phi^N_{Ym} \\ \phi^N_{\theta m} \end{Bmatrix}^T \begin{Bmatrix} \frac{1}{b^2} \\ 0 \end{Bmatrix} dZ \quad (3.27)$$

Rewriting the above equation in a convenient form gives

$$\ddot{T}_m(t) + \omega_m^2 T_m(t) = F_{om} \sin \Omega t \quad (3.28)$$

in which the modal participation factor is given by

$$F_{om} = Y_0 \Omega^2 \int_0^H \left[\phi^N_{Ym} / b^2 \right] dZ \quad (3.29)$$

Equation (3.28) is of exactly the same form as that governing a single degree of freedom system without damping. Introducing the viscous damping, this equation is written as

$$\ddot{T}_m(t) + 2\zeta\omega_m \dot{T}_m(t) + \omega_m^2 T_m(t) = F_{om} \sin \Omega t \quad (3.30)$$

in which ζ is the damping factor.

Solution of equation (3.30) is given by the following equation

$$T_m(t) = e^{-\zeta\omega_m t} (A_m \cos \omega_{dm} t + B_m \sin \omega_{dm} t) + C_m \sin (\Omega t - \psi_m) \quad (3.31)$$

in which

$$\omega_{dm} = \omega_m \sqrt{1 - \zeta^2} \quad (3.32)$$

$$\psi_m = \tan^{-1} \frac{2\zeta\omega_m\Omega}{\omega_m^2 - \Omega^2} \quad (3.33)$$

$$G_m = \frac{F_{om}}{\sqrt{(\omega_m^2 - \Omega^2)^2 + (2\zeta\omega_m\Omega)^2}} \qquad (3.34)$$

A_m and B_m are constants to be determined from the initial conditions of the motion given in equation (3.23).

Neglecting the transient component of equation (3.31) and substituting into equation (3.24), the response corresponding to the m^{th} mode of steady forced vibrations can be written in the form

$$\begin{Bmatrix} \bar{y} \\ r\bar{\theta} \end{Bmatrix}_m = G_m \sin(\Omega t - \psi_m') \begin{Bmatrix} N \\ \phi_{Ym} \\ N \\ \phi_{\theta m} \end{Bmatrix} \qquad (3.35)$$

The above equation is more general than that derived by Raina (22) to determine the shear centre response of a thin walled shear wall model.

It was mentioned in Section 3 of Chapter II that the natural frequencies and the corresponding coupled flexural- torsional mode shapes can be determined by a trial and error procedure using a digital computer. Once these dynamic properties are computed for the structure, the normalized coupled flexural-torsional mode shapes can be calculated and the modal participation factor for a given sinusoidal base motion can be obtained. The response is determined for each mode individually using equation (3.35). The total response is calculated using equation (3.24).

4. Centre of Mass Response due to Seismic Ground Motion

In the previous section, the response was determined for a special case of base motion in which the structure was subjected to a

lateral displacement pulse of sinusoidal character. In the general case, presented in this section, the base acceleration is an arbitrary function of time. For the m^{th} mode of vibration, the equation of motion governing this case of seismic ground motion applied to the entire structure can be written in the form

$$\begin{bmatrix} \frac{1}{b^2} & 0 \\ 0 & \frac{1}{c^2} \end{bmatrix} \begin{Bmatrix} \ddot{\bar{y}} \\ r\ddot{\bar{\theta}} \end{Bmatrix}_m + \begin{bmatrix} \frac{\partial^4}{\partial Z^4} - \alpha^2 \frac{\partial^2}{\partial Z^2} & \frac{e_m}{r}\frac{\partial^4}{\partial Z^4} - \frac{a_m}{r}\alpha^2 \frac{\partial^2}{\partial Z^2} \\ \frac{e_m}{r}\frac{\partial^4}{\partial Z^4} - \frac{a_m}{r}\alpha^2 \frac{\partial^2}{\partial Z^2} & \frac{\partial^4}{\partial Z^4} - \beta^2 \frac{\partial^2}{\partial Z^2} \end{bmatrix} \begin{Bmatrix} \bar{y} \\ r\bar{\theta} \end{Bmatrix}_m$$

$$= -\text{Acc}\ (t) \begin{Bmatrix} \frac{1}{b^2} \\ 0 \end{Bmatrix} \quad (3.36)$$

in which Acc (t) is the applied base acceleration.

The above equation is a generalization of equation (3.21). Assuming the solution to equation (3.36) is the same as to equation (3.21) and following the same procedure given in the previous section, the modal participation factor for this general case can be obtained and the generalization of equation (3.28) can be written in the form

$$\ddot{T}_m\ (t) + 2\zeta\omega_m\ \dot{T}_m\ (t) + \omega_m^2\ T_m\ (t) = -P_{om}\ \text{Acc}\ (t) \quad (3.37)$$

in which P_{om} is the modal participation factor and is given by

$$P_{om} = \int_0^H [\phi_{Ym}^N / b^2]\, dZ \quad (3.38)$$

Equation (3.28), in which the loading function is expressed in relatively simple mathematical term (sinusoidal function), is solved by rigorous solution. As the type of loading being a general function, equation (3.37), a numerical integration approach is needed. As the

name implies a numerical integration procedure is one in which the differential equations of motion of the system are integrated over finite time steps. By a suitable choice of the integration procedure and length of the time steps, good accuracy can be obtained.

Equation (3.37), which is treated as a single degree of freedom equation of motion, is solved step by step, starting at zero time, where the displacement and velocity are known from the initial conditions given in equation (3.23). The time scale is divided into discrete intervals Δt in which the variations of acceleration and velocity are assumed to be linear (7). This time interval should not be greater than one-tenth of the natural period of the last mode taken into consideration in the modal analysis of the structure. The equations governing the numerical integration procedure as shown in reference (7), are given by

$$\dot{T}_{i+1} = \frac{2}{\Delta t} (T_{i+1} - T_i) - \dot{T}_i \tag{3.39a}$$

$$\ddot{T}_{i+1} = \frac{2}{\Delta t} (\dot{T}_{i+1} - \dot{T}_i) - \ddot{T}_i \tag{3.39b}$$

$$\left[\frac{4}{(\Delta t)^2} + \frac{4}{\Delta t}\omega\zeta + \omega^2\right] T_{i+1} = \left[\frac{4}{(\Delta t)^2} + \frac{4}{\Delta t}\omega\zeta\right] T_i + \left[\frac{4}{\Delta t} + 2\omega\zeta\right] \dot{T}_i + \ddot{T}_i - \mathrm{Acc}_{i+1} \tag{3.39c}$$

in which T, $\dot{T}$ and $\ddot{T}$ are the displacement, velocity and acceleration, respectively, for a single degree of freedom system, ω is the natural frequency of the system, ζ is the fraction of critical damping and Acc (t) is the applied acceleration function to the system.

Knowing the displacement, velocity and acceleration at any time t as well as the applied acceleration function at the next time $(t + \Delta t)$ enable one to compute displacement at the time $(t + \Delta t)$. As T_o and $\dot{T}_o$ are known from the initial conditions, $\ddot{T}_o$ can be determined from equation (3.37). Then, the procedure is to determine T_1 from equation (3.39c), $\dot{T}_1$ from equation (3.39a) and $\ddot{T}_1$ from equation (3.39b) and the calculations then continue in identical manner.

The temporal variation function $T_m(t)$, of the coupled displacements, being determined by the previous numerical integration procedure, the response corresponding to the m^{th} mode due to a given seismic ground motion can be written in the form

$$\begin{Bmatrix} \bar{Y} \\ \bar{\theta} \end{Bmatrix}_m = T_m(t) \begin{Bmatrix} N \\ \phi_{Ym} \\ N \\ \phi_{\theta m} \end{Bmatrix} \tag{3.40}$$

and the total response can be obtained using equation (3.24).

From the above procedure, it can be seen that the total response is a function of two parameters (Z,t); in equation (3.24), the separation of variables gives a complete understanding of the response variation individually with each parameter. Also, the variation of the modal participation factor enables one to determine the number of modes which must be taken into consideration in the response analysis.

Thus, it is of major interest to study the variation of the modal participation factor with the modes of vibration for different building structures. For Example Structure I, shown in Figure 4,

in which the non-dimensional parameters $\alpha H = 1.264$ and $\beta H = 6.099$, the modal participation factor *MPF* is obtained and given in Table 8. This table shows also the natural periods *NP* of the structure, the ratio between each natural period and the previous one and finally the ratio δ_θ / δ_Y for each mode of vibration. For Example Structure II, shown in Figure 6, the modal participation factor *MPF* is given in Tables 9 (i),(ii) and (iii) for the different core location which gives different values of the non-dimensional parameter βH and as a result different dynamic properties of the structure. From these tables one can conclude that the modal participation factor is function of the ratio between two successive natural periods and of the non-dimensional parameters αH and βH which express the ratio of the frames to the walls in the building. It is clear also that the ratio δ_θ / δ_Y which express the degree of coupling between the two motions is a function also of the ratio between two successive natural periods. It should be pointed out that the torsional to bending natural period ratio is an important parameter to determine the degree of coupling as well as the variation of the modal participation factor.

Mode	1	2	3	4	5	6
MPF	100	2.93	50.43	3.76	30.21	12.35
$\delta_{\theta} / \delta_{Y}$	0.110	2.886	0.763	0.537	4.593	0.797
NP (Sec.)	2.219	0.828	0.465	0.245	0.200	0.132
NP_{i+1} / NP_{i}	0.373	0.562	0.527	0.816	0.660	

Table 8 - Variation of the MPF with the Modes of Vibration - Example Structure I

$\alpha H = 1.264$ $\beta H = 6.099$

Mode	1	2	3	4	5	6
MPF	100	53.41	27.29	32.47	14.68	21.98
δ_θ / δ_Y	0.781	2.431	1.611	1.075	2.441	0.560
NP (Sec.)	2.193	2.015	0.712	0.609	0.417	0.306
NP_{i+1} / NP_i	0.919	0.354	0.855	0.686	0.733	

Table 9 (i) - Variation of the MPF with the Modes of Vibration - Building 2 of Example Structure II

αH = 7.45 βH = 14.96

Mode	1	2	3	4	5	6
MPF	100	45.17	31.92	24.22	19.47	10.79
δ_θ / δ_Y	0.652	2.700	1.051	1.657	1.495	1.071
NP (Sec.)	2.252	1.93	0.737	0.559	0.434	0.304
NP_{i+1} / NP_i	0.857	0.382	0.759	0.776	0.701	

Table 9(ii)- Variation of the MPF with the Modes of Vibration - Building 3 of Example Structure II

αH = 7.45 βH = 8.08

Mode	1	2	3	4	5	6
MPF	100	39.68	33.46	18.28	22.17	13.36
δ_θ / δ_Y	0.605	3.057	0.826	1.963	1.345	0.874
NP (Sec.)	2.278	1.795	0.751	0.497	0.444	0.312
NP_{i+1} / NP_i	0.788	0.418	0.661	0.893	0.704	

Table 9 (iii) - Variation of the MPF with the Modes of Vibration - Building 4 of Example Structure II

αH = 7.58 βH = 5.46

CHAPTER IV

RESPONSE PARAMETERS FOR ASYMMETRIC WALL-FRAME STRUCTURES SUBJECTED TO SEISMIC GROUND MOTIONS

1. Introduction

In Section 4 of Chapter III, the two coupled displacements $\bar{Y}(Z,t)$ and $\bar{\theta}(Z,t)$ were determined due to seismic ground motion. These coupled displacements are for a 2-dimensional wall-frame structure with the X-axis as the axis of symmetry.

In this Chapter, using these parameters for deflection in Y-direction and rotation about Z-direction, the other response parameters for asymmetric wall-frame structures can be determined. These response parameters are the bending moment, shearing force, bimoment and torsion in the wall system, shearing force and torsion in the frame system, obtained at the centroids of shear walls, and frames, respectively. An example wall-frame structure is solved for different earthquake records using the numerical integration procedure discussed previously and a complete time history response for the various parameters at the top and the bottom of the structure is shown. Whenever possible, the calculated values of the response parameters are compared with the 1975 National Building Code of Canada (21) requirements to evaluate the adequacy of such static loading provisions and to develop guide lines to define situations for which a detailed dynamic response computation is required.

2. Response Parameters

The response parameters associated with the dynamic analysis of the wall-frame structures are divided in two groups. The first, applicable to the system of walls, is obtained at their centroid and the parameters are the bending moment, shearing force, bimoment and torsion. The second, applicable to the system of frames, is obtained at their centroid and the parameters are the shearing force and torsion.

The differential equations for the stress resultants applicable to the system of walls are given by

$$M_W = \overline{EI}_Y \frac{d^2 Y_W}{dZ^2} \tag{4.1a}$$

$$S_W = -\overline{EI}_Y \frac{d^3 Y_W}{dZ^3} \tag{4.1b}$$

$$B_W = -\overline{EI}_\omega \frac{d^2 \theta_W}{dZ^2} \tag{4.1c}$$

$$T_W = -\overline{EI}_\omega \frac{d^3 \theta_W}{dZ^3} + \sum_{i=1}^{m} GJ_i \frac{d\theta_W}{dZ} \tag{4.1d}$$

in which Y_W and θ_W are the two coupled displacements of the centroid of the walls, M is the bending moment, S is the shearing force, B is the bimoment, T is the torsional moment and the subscript W refers to the flexural type resisting elements.

The two coupled displacements Y_W and θ_W can be determined from equations (2.3b) and (2.3c). Thus

$$Y_W = \bar{Y} + e_m \bar{\theta} \tag{4.2a}$$

$$\theta_W = \bar{\theta} \tag{4.2b}$$

Substituting equations (4.2) into equations (4.1) yields

$$M_W = \overline{EI}_Y \frac{d^2\bar{Y}}{dZ^2} + e_m \overline{EI}_Y \frac{d^2\bar{\theta}}{dZ^2} \tag{4.3a}$$

$$S_W = -\overline{EI}_Y \frac{d^3\bar{Y}}{dZ^3} - e_m \overline{EI}_Y \frac{d^3\bar{\theta}}{dZ^3} \tag{4.3b}$$

$$B_W = -\overline{EI}_\omega \frac{d^2\bar{\theta}}{dZ^2} \tag{4.3c}$$

$$T_W = -\overline{EI}_\omega \frac{d^3\bar{\theta}}{dZ^3} + \overline{GJ}_W \frac{d\bar{\theta}}{dZ} \tag{4.3d}$$

in which

$$\overline{GJ}_W = \sum_{i=1}^{m} [GJ_i] \tag{4.4}$$

The differential equations for the stress resultants applicable to the system of frames are given by

$$S_F = \overline{GA}_Y \frac{dY_F}{dZ} \tag{4.5a}$$

$$T_F = \sum_{j=1}^{n} (GJ_j + a_{Xj}^2 GA_{Yj} + a_{Yj}^2 GA_{Xj}) \frac{d\theta_F}{dZ} \tag{4.5b}$$

in which Y_F and θ_F are the two coupled displacements of the centroid of the frames and the subscript F refers to the shear type resisting elements. The two coupled displacements Y_F and θ_F can be determined from equations (2.3b) and 2.3c). Thus

$$Y_F = \bar{Y} + a_m \bar{\theta} \tag{4.6a}$$

$$\theta_F = \bar{\theta} \tag{4.6b}$$

Substituting equations (4.6) into equations (4.5) yields

$$S_F = \overline{GA}_Y \frac{d\bar{Y}}{dZ} + a_m \overline{GA}_Y \frac{d\bar{\theta}}{dZ} \tag{4.7a}$$

$$T_F = \overline{GJ}_F \frac{d\bar{\theta}}{dZ} \tag{4.7b}$$

in which

$$\overline{GJ}_F = \sum_{j=1}^{n} (GJ_j + a_{Xj}^2 GA_{Yj} + a_{Yj}^2 GA_{Xj}) \tag{4.8a}$$

and

$$\overline{GJ} = \overline{GJ}_W + \overline{GJ}_F \tag{4.8b}$$

The two groups of equations (4.3) and (4.7) represent the response parameters applicable to the wall-frame structure in addition to the two coupled displacements $(\bar{Y} - \bar{\theta})$ determined by equation (3.23) in the previous Chapter. These are the representative parameters needed for a complete understanding of the coupled response of a 2-dimensional wall-frame structure.

Due to a sinusoidal base motion, the stress resultants applicable to the wall-frame system can be determined by substituting equation (3.35) into equations (4.3) and (4.7). The resulting equations are

$$[M_W(Z,t)]_m = [\overline{EI}_Y \frac{d^2}{dZ^2} (\phi_{Ym}^N) + \frac{e_m}{r} \overline{EI}_Y \frac{d^2}{dZ^2} (\phi_{\theta m}^N)] \cdot [G_m \sin(\Omega t - \psi_m)] \tag{4.9}$$

$$[S_W(Z,t)]_m = [-\overline{EI}_Y \frac{d^3}{dZ^3} (\phi_{Ym}^N) - \frac{e_m}{r} \overline{EI}_Y \frac{d^3}{dZ^3} (\phi_{\theta m}^N)] \cdot [G_m \sin(\Omega t - \psi_m)] \tag{4.10}$$

$$[B_W(Z,t)]_m = [-\frac{1}{r}\overline{EI}_\omega \frac{d^2}{dZ^2}(\overset{N}{\phi}_{\theta m})] \cdot [G_m \sin(\Omega t - \psi_m)] \quad (4.11)$$

$$[T_W(Z,t)]_m = [-\frac{1}{r}\overline{EI}_\omega \frac{d^3}{dZ^3}(\overset{N}{\phi}_{\theta m}) + \frac{1}{r}\overline{GJ}_W \frac{d}{dZ}(\overset{N}{\phi}_{\theta m})] \cdot [G_m \sin(\Omega t - \psi_m)] \quad (4.12)$$

$$[S_F(Z,t)]_m = [\overline{GA}_Y \frac{d}{dZ}(\overset{N}{\phi}_{Ym}) + \frac{a_m}{r}\overline{GA}_Y \frac{d}{dZ}(\overset{N}{\phi}_{\theta m})] \cdot [G_m \sin(\Omega t - \psi_m)] \quad (4.13)$$

$$[T_F(Z,t)]_m = [\frac{1}{r}\overline{GJ}_F \frac{d}{dZ}(\overset{N}{\phi}_{\theta m})] \cdot [G_m \sin(\Omega t - \psi_m)] \quad (4.14)$$

in which the subscript m refers to the m^{th} mode of vibration.

The generalization of the above equations gives the stress resultants due to a seismic ground motion. The resulting equations are

$$[M_W(Z,t)]_m = [\overline{EI}_Y \frac{d^2}{dZ^2}(\overset{N}{\phi}_{Ym}) + \frac{e_m}{r}\overline{EI}_Y \frac{d^2}{dZ^2}(\overset{N}{\phi}_{\theta m})] \cdot [T_m(t)] \quad (4.15)$$

$$[S_W(Z,t)]_m = [-\overline{EI}_Y \frac{d^3}{dZ^3}(\overset{N}{\phi}_{Ym}) - \frac{e_m}{r}\overline{EI}_Y \frac{d^3}{dZ^3}(\overset{N}{\phi}_{\theta m})] \cdot [T_m(t)] \quad (4.16)$$

$$[B_W(Z,t)]_m = [-\frac{1}{r}\overline{EI}_\omega \frac{d^2}{dZ^2}(\overset{N}{\phi}_{\theta m})] \cdot [T_m(t)] \quad (4.17)$$

$$[T_W(Z,t)]_m = [-\frac{1}{r}\overline{EI}_\omega \frac{d^3}{dZ^3}(\overset{N}{\phi}_{\theta m}) + \frac{1}{r}\overline{GJ}_W \frac{d}{dZ}(\overset{N}{\phi}_{\theta m})] \cdot [T_m(t)] \quad (4.18)$$

$$[S_F(Z,t)]_m = [\overline{GA}_Y \frac{d}{dZ}(\overset{N}{\phi}_{Ym}) + \frac{a_m}{r}\overline{GA}_Y \frac{d}{dZ}(\overset{N}{\phi}_{\theta m})] \cdot [T_m(t)] \quad (4.19)$$

$$[T_F(Z,t)]_m = [\frac{1}{r}\overline{GJ}_F \frac{d}{dZ}(\overset{N}{\phi}_{\theta m})] \cdot [T_m(t)] \quad (4.20)$$

in which $T_m(t)$ is the temporal variation function of the displacements for the m^{th} mode of vibration already determined using the numerical

integration procedure discussed in Section 4 of Chapter III.

The stress resultants obtained from the above equations are for the m^{th} mode vibration. The total stress resultants can be determined by

$$M_W(Z,t) = \sum_{m=1,2,\ldots} [M_W(Z,t)]_m \tag{4.21}$$

$$S_W(Z,t) = \sum_{m=1,2,\ldots} [S_W(Z,t)]_m \tag{4.22}$$

$$B_W(Z,t) = \sum_{m=1,2,\ldots} [B_W(Z,t)]_m \tag{4.23}$$

$$T_W(Z,t) = \sum_{m=1,2,\ldots} [T_W(Z,t)]_m \tag{4.24}$$

$$S_F(Z,t) = \sum_{m=1,2,\ldots} [S_F(Z,t)]_m \tag{4.25}$$

$$T_F(Z,t) = \sum_{m=1,2,\ldots} [T_F(Z,t)]_m \tag{4.26}$$

For the walls, the critical response parameters are the top displacements and the base stress resultants. For the frames, the top displacements are critical and the maximum stress resultants occur at certain height Z which can be determined by a trial and error procedure. From equations (4.19) and (4.20) and the boundary conditions given by equations (2.23) and (2.24), one can conclude that the base stress resultants of the frames vanish for any type of loading and at any time t.

Thus, it is of major interest to determine the top displacement $\bar{Y}(H,t)$, the top rotation $\bar{\theta}(H,t)$, the base moment $M_W(0,t)$, the base shear $S_W(0,t)$, the base bimoment $B_W(0,t)$, the base torsion $T_W(0,t)$, their variation with time, their maxima, and the corresponding time t for each maximum parameter.

Analysing the response results, one can conclude that the eccentricity causes coupling of the forces and displacements; when the acceleration had only a Y-component, substantial forces and displacements were obtained in other directions as well. The degree of coupling, between the rotation and the displacement, between the torque and the shear and between the bimoment and the bending moment, give a complete understanding of the influence of the eccentricities on the dynamic behaviour of the structure and the dynamic amplification of the various response parameters.

3. Example Wall-Frame Structure Subjected to Different Earthquake Records

The floor plan given in Figure 4, first analysed in Section 3 of Chapter II is that for a typical 2-dimensional wall-frame building structure. The response to the W-E component of the EL CENTRO earthquake of May 18, 1940, Figure 9, acting along the Y-axis of this example structure is calculated incorporating the first six normal modes. The earthquake record is normalized to give a maximum acceleration of 0.1 g. The damping is assumed to be equivalent to 5% of critical viscous damping. The representative parameters determined are the top displacement $\bar{Y}(H,t)$, the top rotation $\bar{\theta}(H,t)$, the base

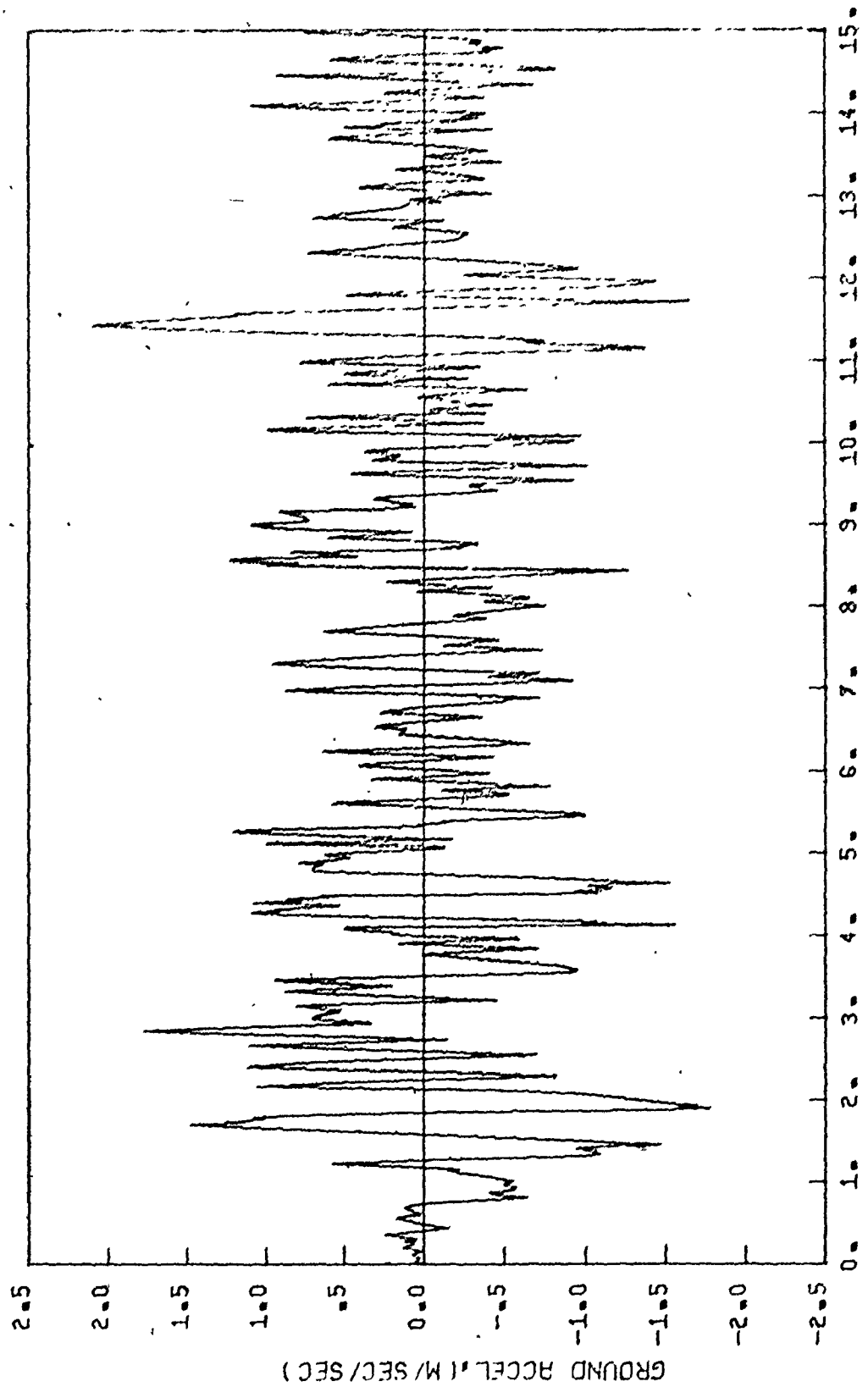

FIGURE 9 EARTHQUAKE RECORD OF ELCENTRO W-E MAY 18,1940

moment $M_W(0,t)$, the base shear $S_W(0,t)$, the base bimoment $B_W(0,t)$ and the base torsion $T_W(0,t)$. These response diagrams, for the first 15 seconds, are shown in Figures 10-a, 10-b, 10-c, 10-d, 10-e and 10-f, respectively. From these diagrams one can obtain the maximum response parameters and the corresponding time t for each one. These values are given in Table 10.

In order to check on the validity of the computer programme, comparisons were made with maximum response parameters computed by the root sum square technique; these comparisons are shown in Appendix 3. Similarly, the basic example wall-frame structure is subjected to three different earthquake records. These earthquakes are:

(i) EL CENTRO, Component *N-S*, May 18, 1940 (Figure 11)

(ii) TAFT, Component *N21E*, July 21, 1952 (Figure 12)

(iii) SAN FRANCISCO, Component *N10E*, March 22, 1957 (Figure 13)

Normalizing the earthquake records with a maximum acceleration of 0.1 g and assuming a constant damping factor of 0.05, the response is computed incorporating the first six normal modes. The response diagrams of the design seismic parameters are shown in Figures 14, 15 and 16 for the first 15 seconds of each earthquake record, respectively; a comparison between their maxima due to each ground motion is given in Table 11.

4. Amplification Parameters

The maximum stress resultants associated with the equivalent static analysis suggested by the 1975 National Building Code of Canada (21), are the base shear, the base overturning moment and the base torsion. For the Example Structure I, shown in Figure 4, these parameters are computed assuming the structure is located in zone 3

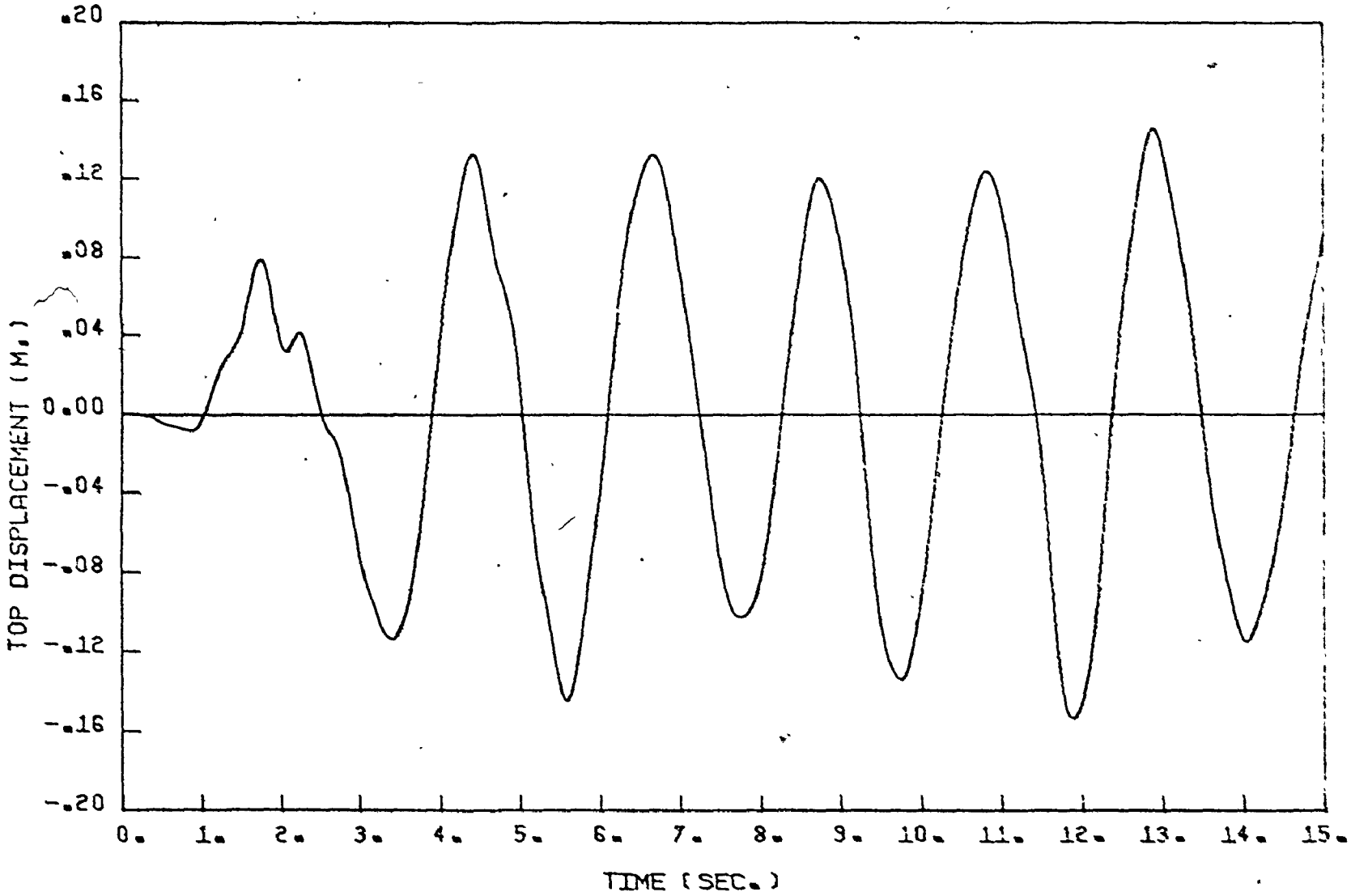

FIGURE 10-a VARIATION OF TOP DISPLACEMENT $\bar{Y}$ WITH TIME

ELCENTRO W-E EXAMPLE STRUCTURE I

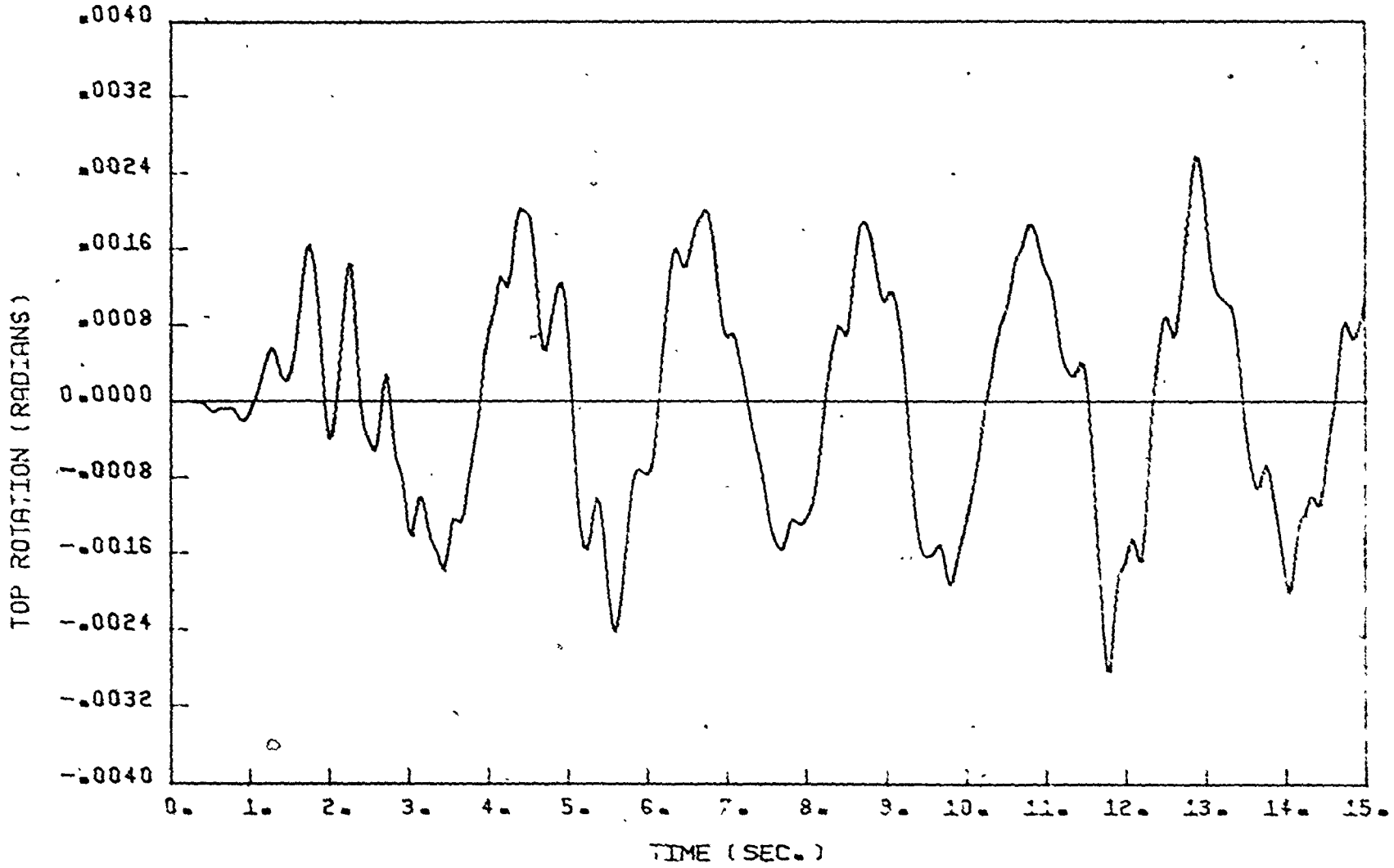

FIGURE 10-b VARIATION OF TOP ROTATION $\bar{\theta}$ WITH TIME

ELCENTRO W-E : EXAMPLE STRUCTURE I

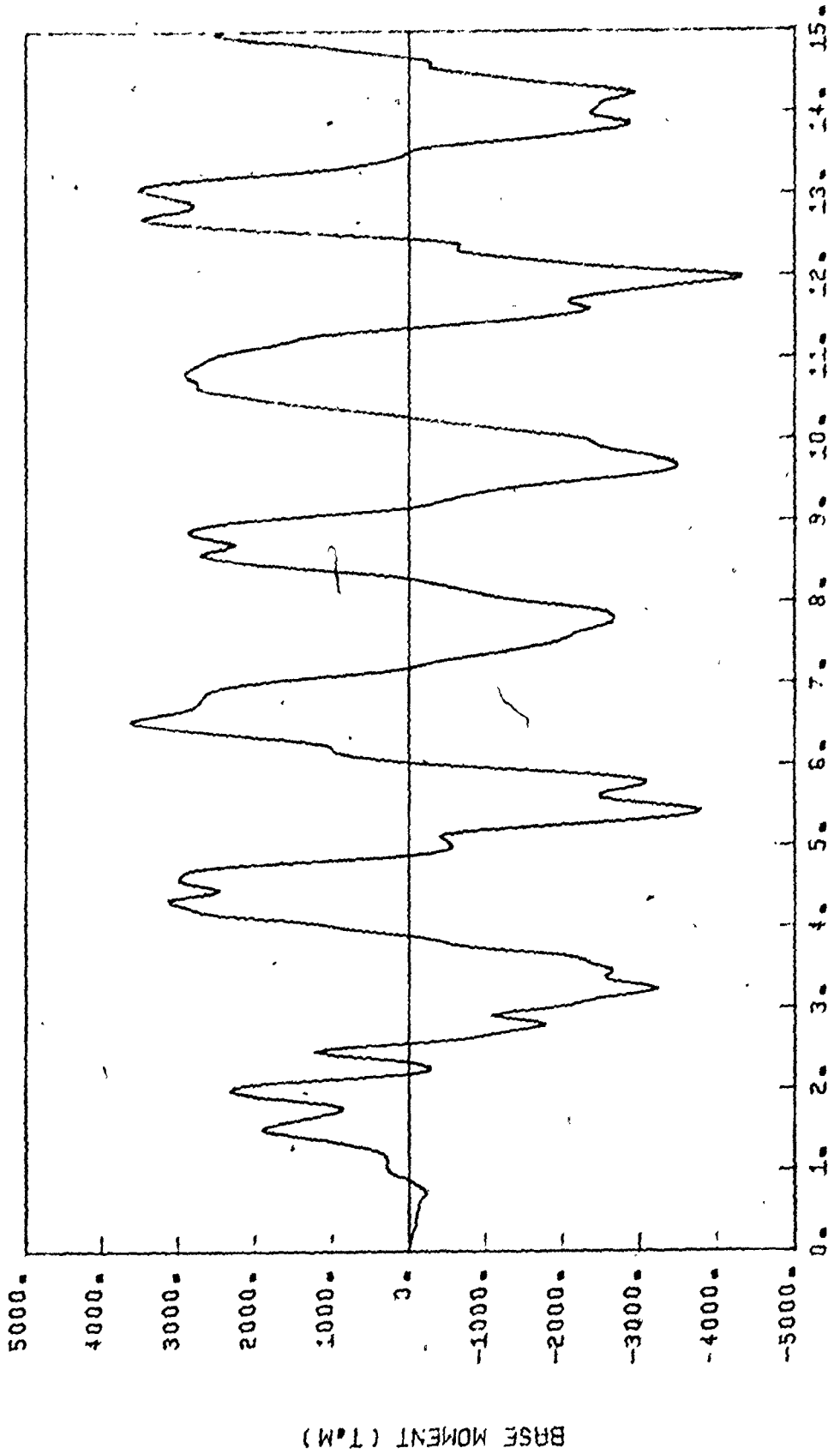

FIGURE 10-c VARIATION OF BASE MOMENT M_w WITH TIME
ELCENTRO W-E EXAMPLE STRUCTURE I

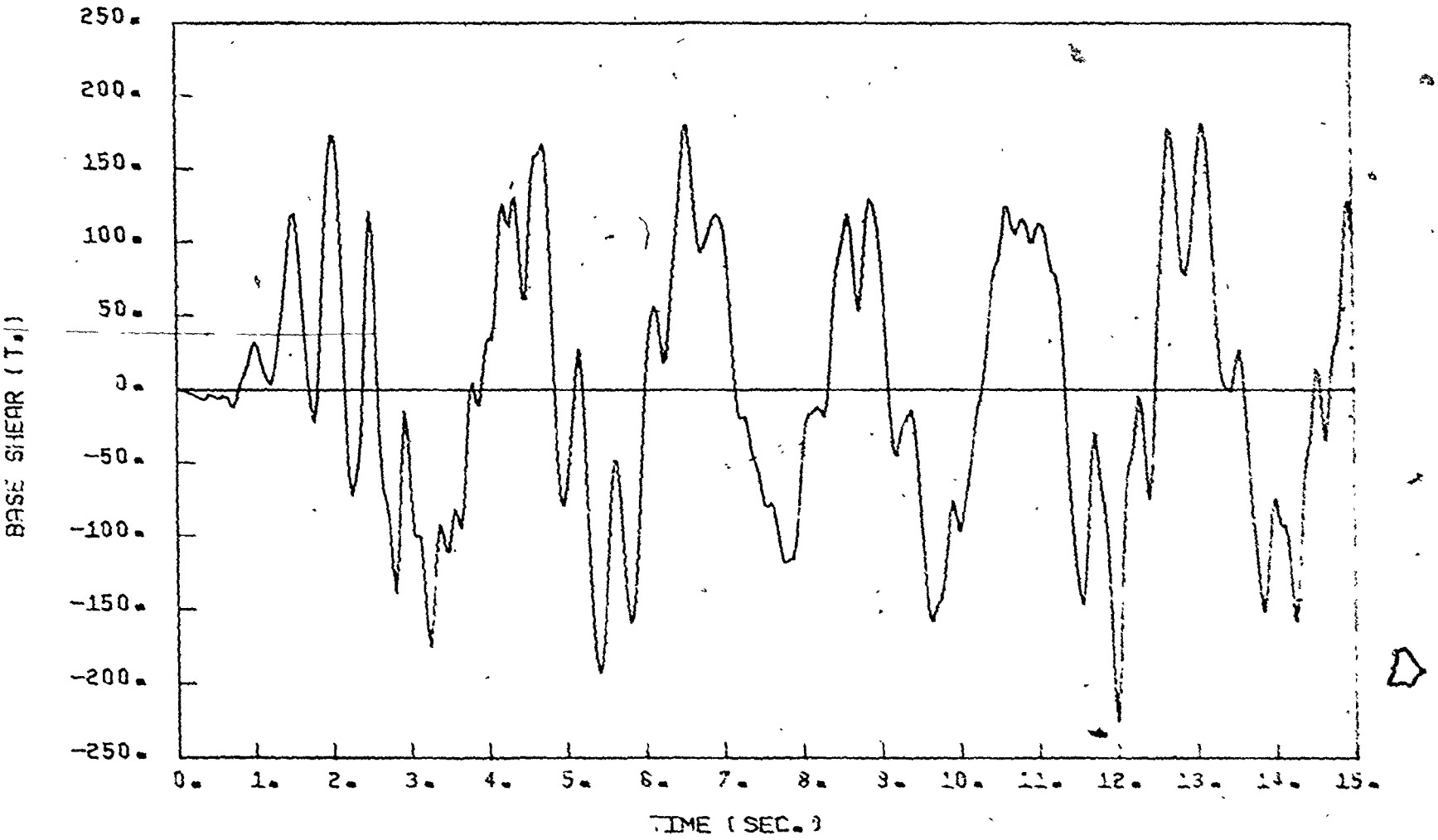

FIGURE 10-d VARIATION OF BASE SHEAR S_{1V} WITH TIME

ELCENTRO W-E EXAMPLE STRUCTURE I.

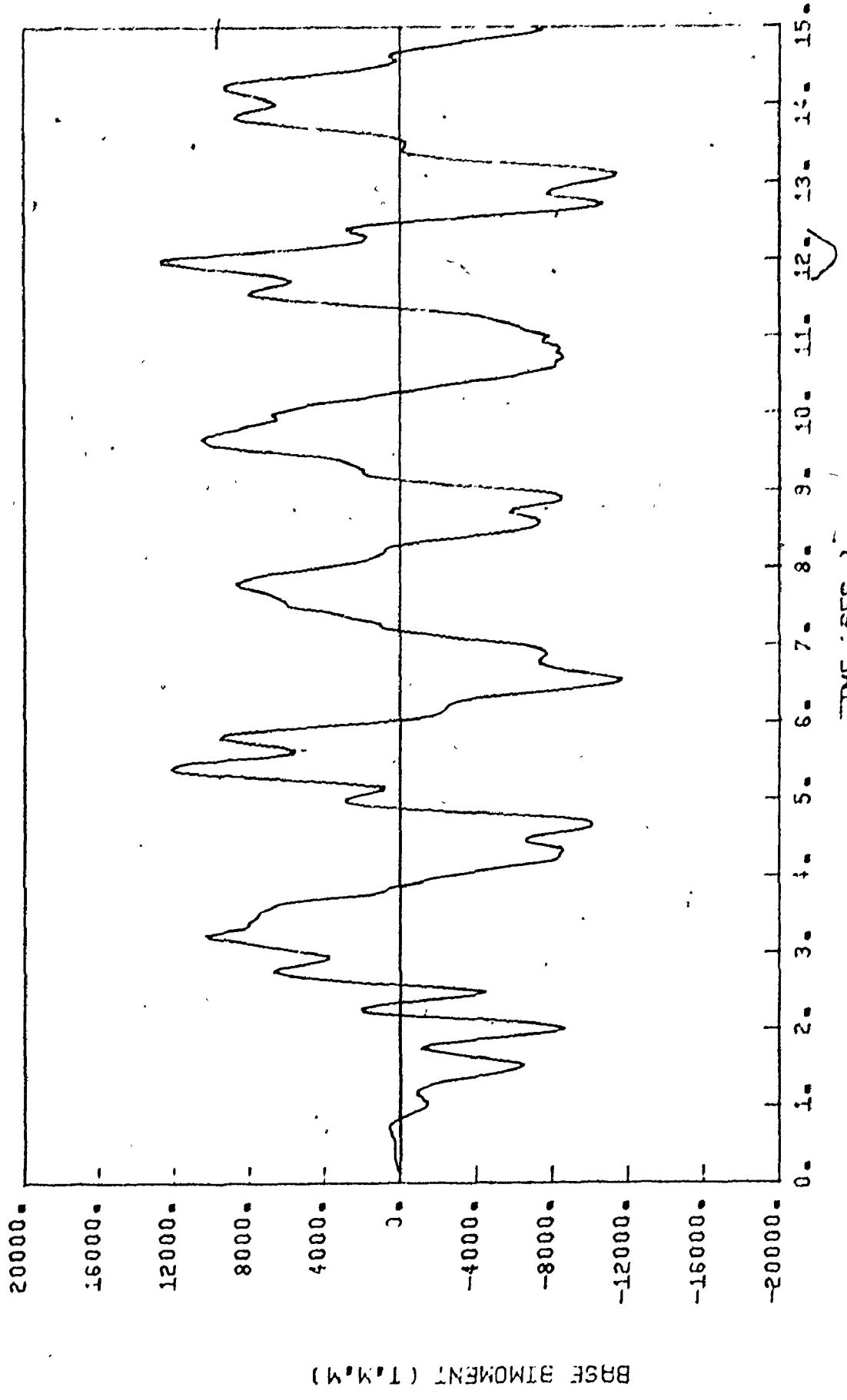

FIGURE 10-e VARIATION OF BASE MOMENT B_W WITH TIME

ELCENTRO N-E EXAMPLE STRUCTURE I

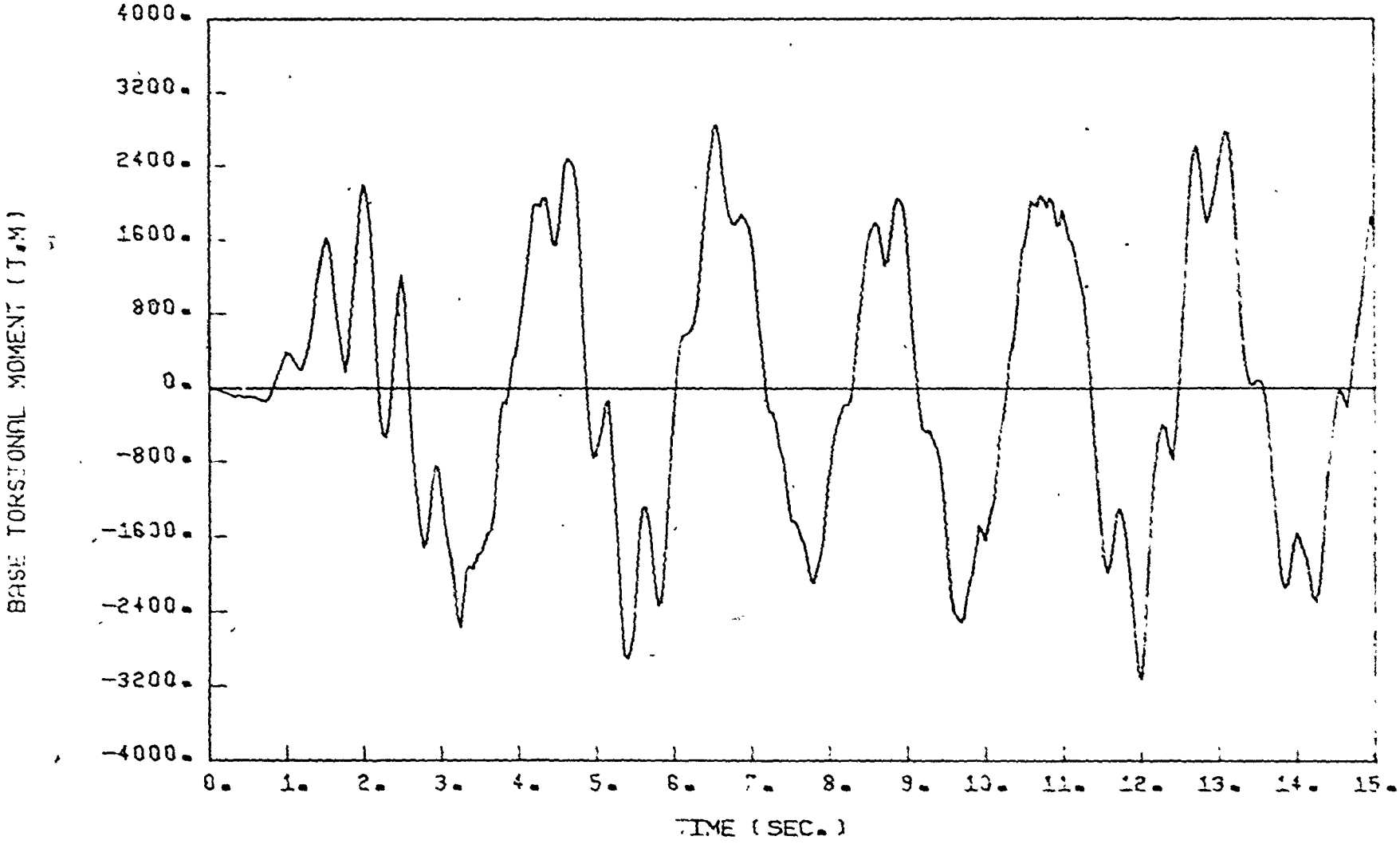

FIGURE 10-1 VARIATION OF BASE TORSION T_w WITH TIME
ELCENTRO N-E EXAMPLE STRUCTURE I

Response Parameter	Maximum Value	Time (Sec.)
Base Moment [$t.m$ ($K.$ ft)]	4326 / (31218)	12.00
Base Shear [t (K)]	226 / (497)	12.00
Base Bimoment [$t.m^2$ ($K.$ ft^2)]	12690 / (300355)	12.00
Base Torsion [$t.m$ ($K.$ ft)]	3135 / (22625)	12.00
Top Displacement [m (ft)]	0.1539 / (0.5048)	11.88
Top Rotation [radians]	0.002836	11.80

Table 10 - Maximum Response Parameters due to the *W-E* Component of EL CENTRO Earthquake - Example Structure I

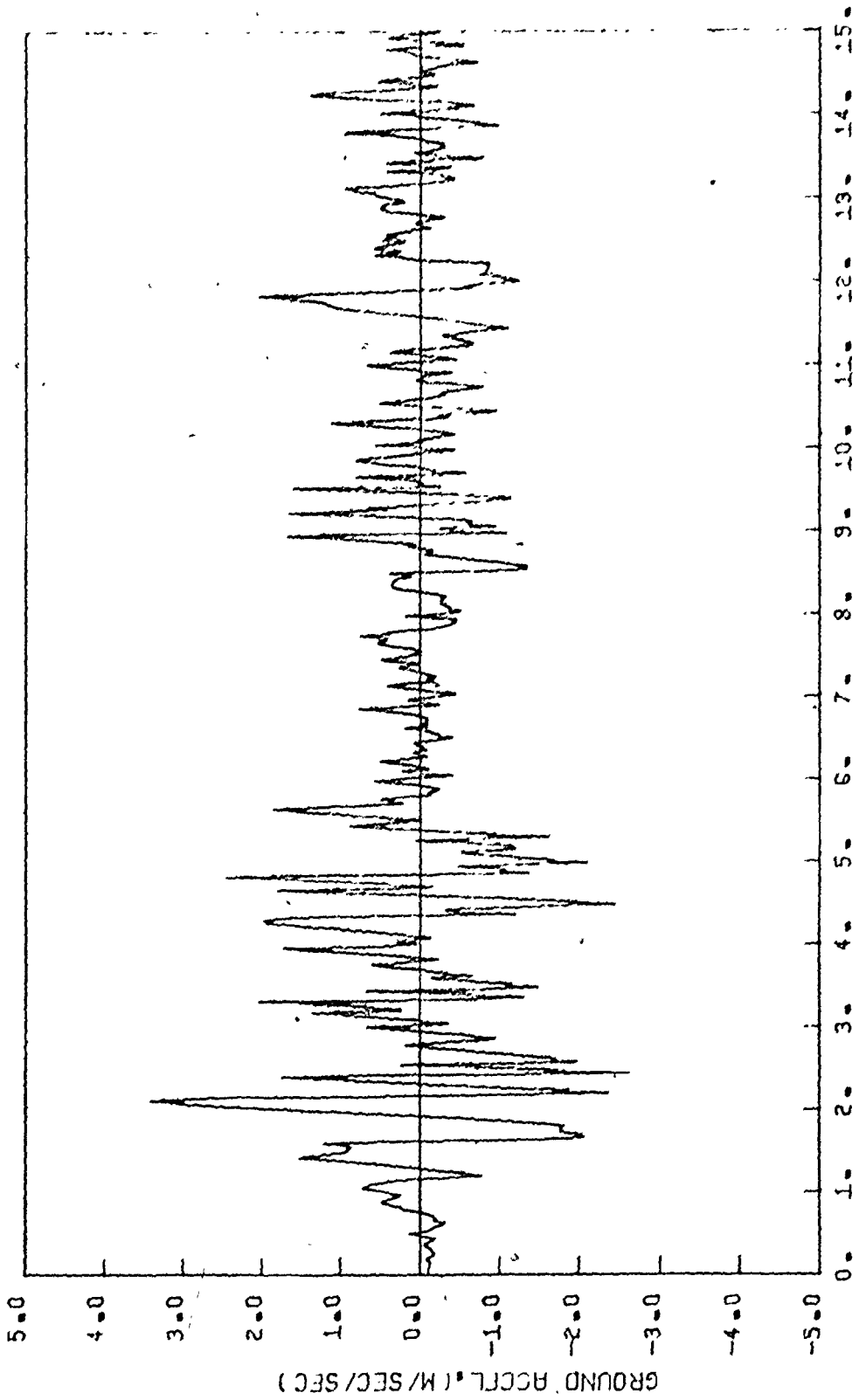

FIGURE 11 EARTHQUAKE RECORD OF ELCENTRO N-S MAY 18, 1940

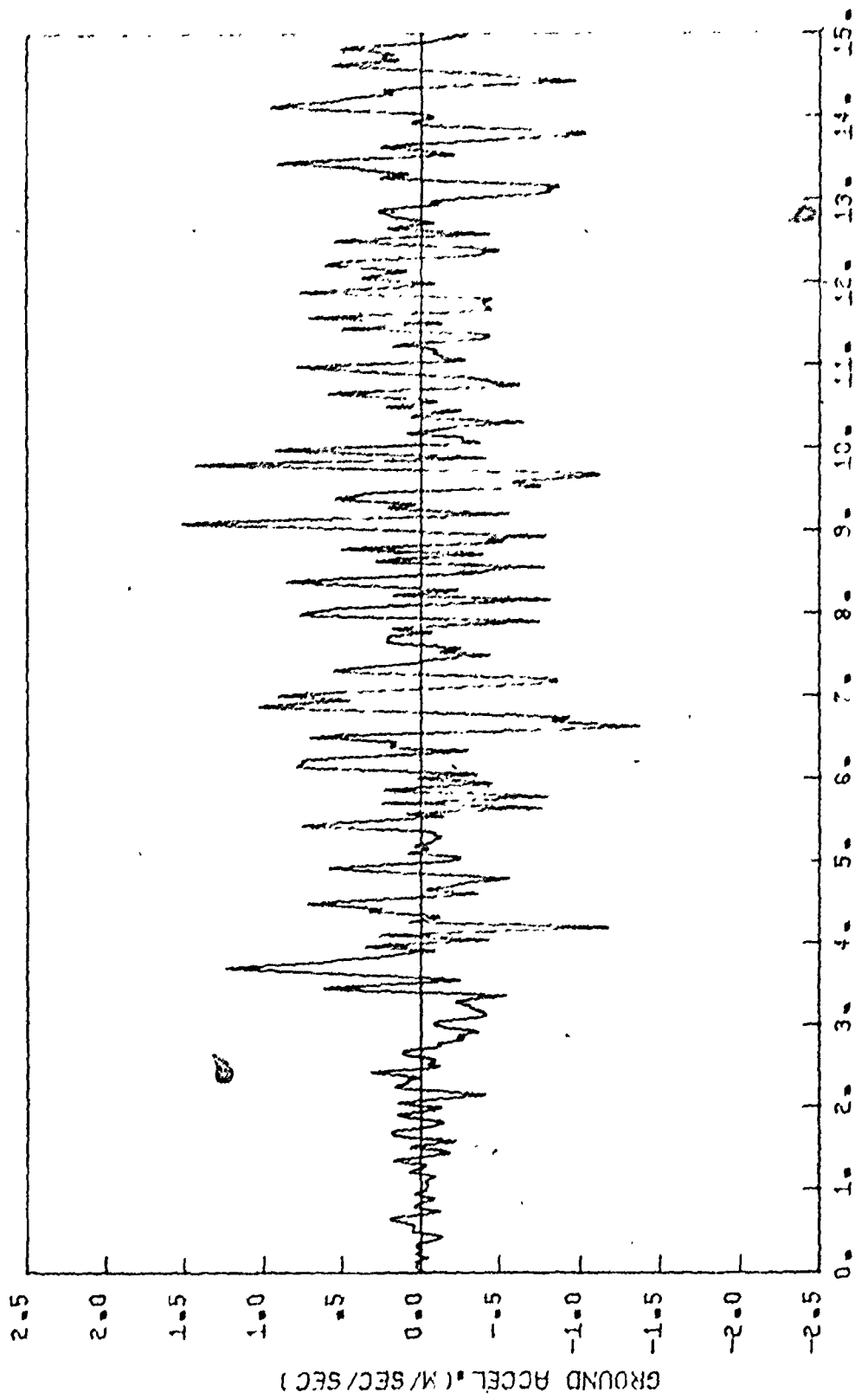

FIGURE 12 EARTHQUAKE RECORD OF TAFT N21E JULY 21,1952

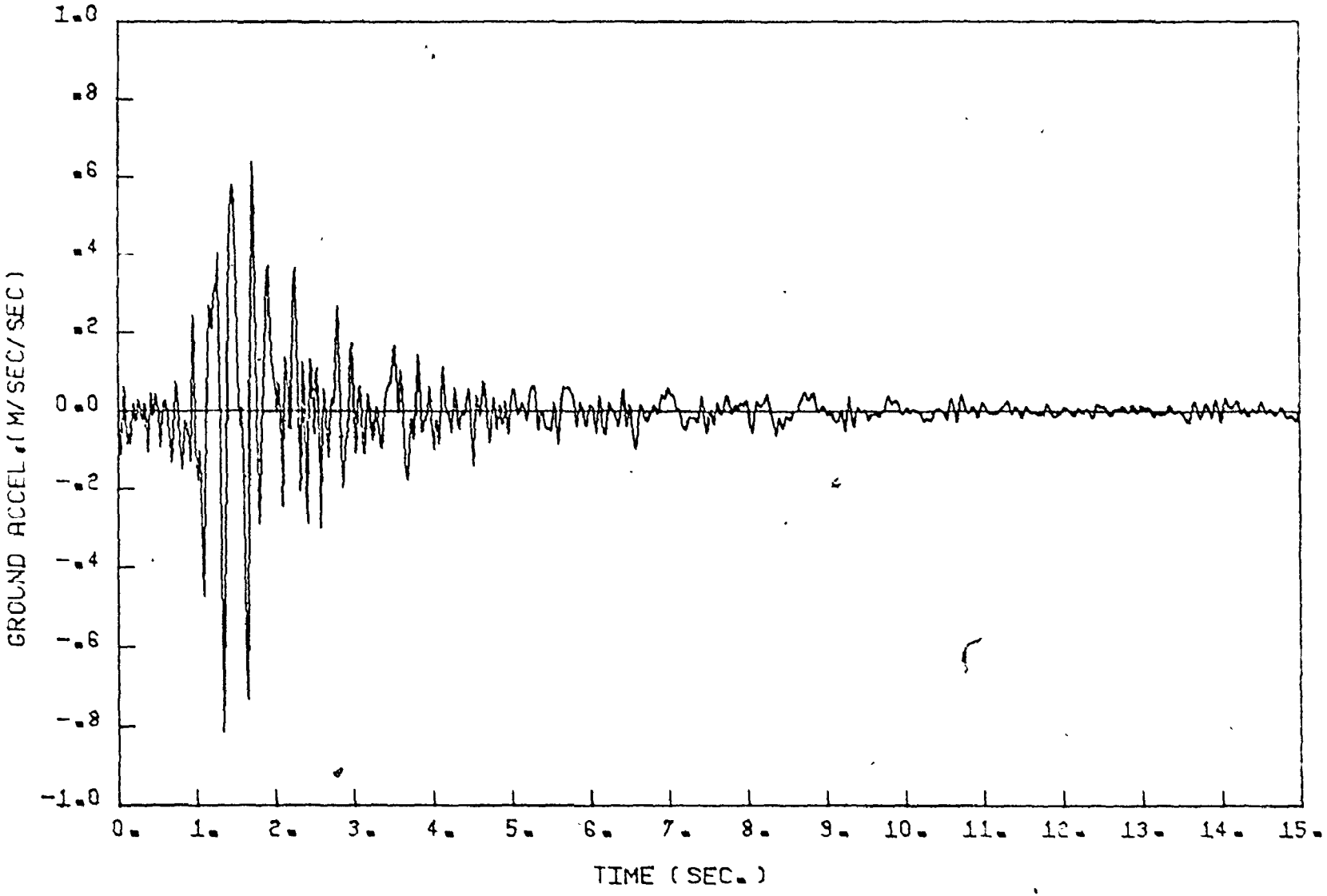

FIGURE 13 EARTHQUAKE RECORD OF SAN FRANCISCO N10E MARCH 22,1957

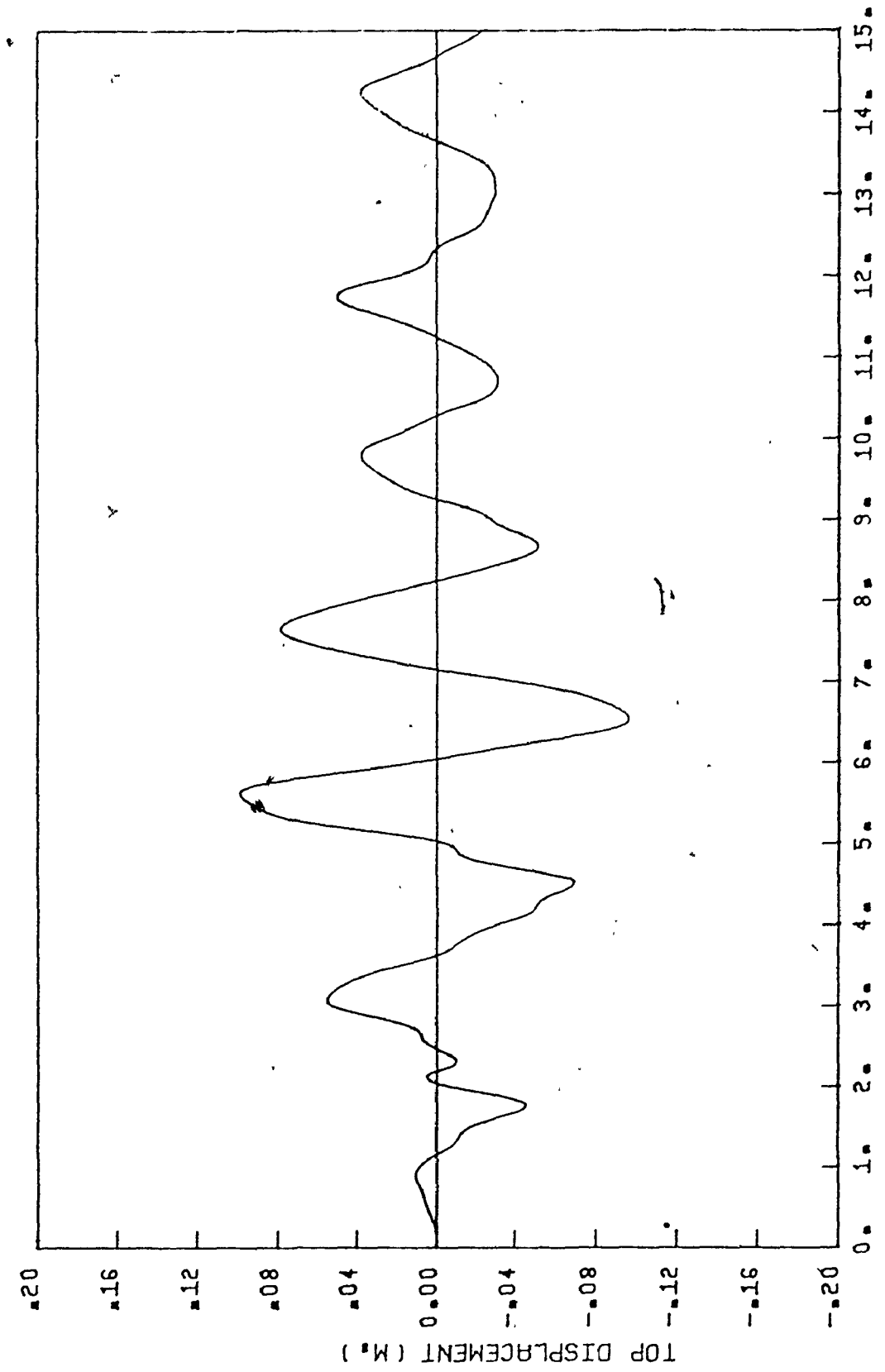

FIGURE 14-a VARIATION OF TOP DISPLACEMENT $\bar{Y}$ WITH TIME

ELCENTRO N-S EXAMPLE STRUCTURE I

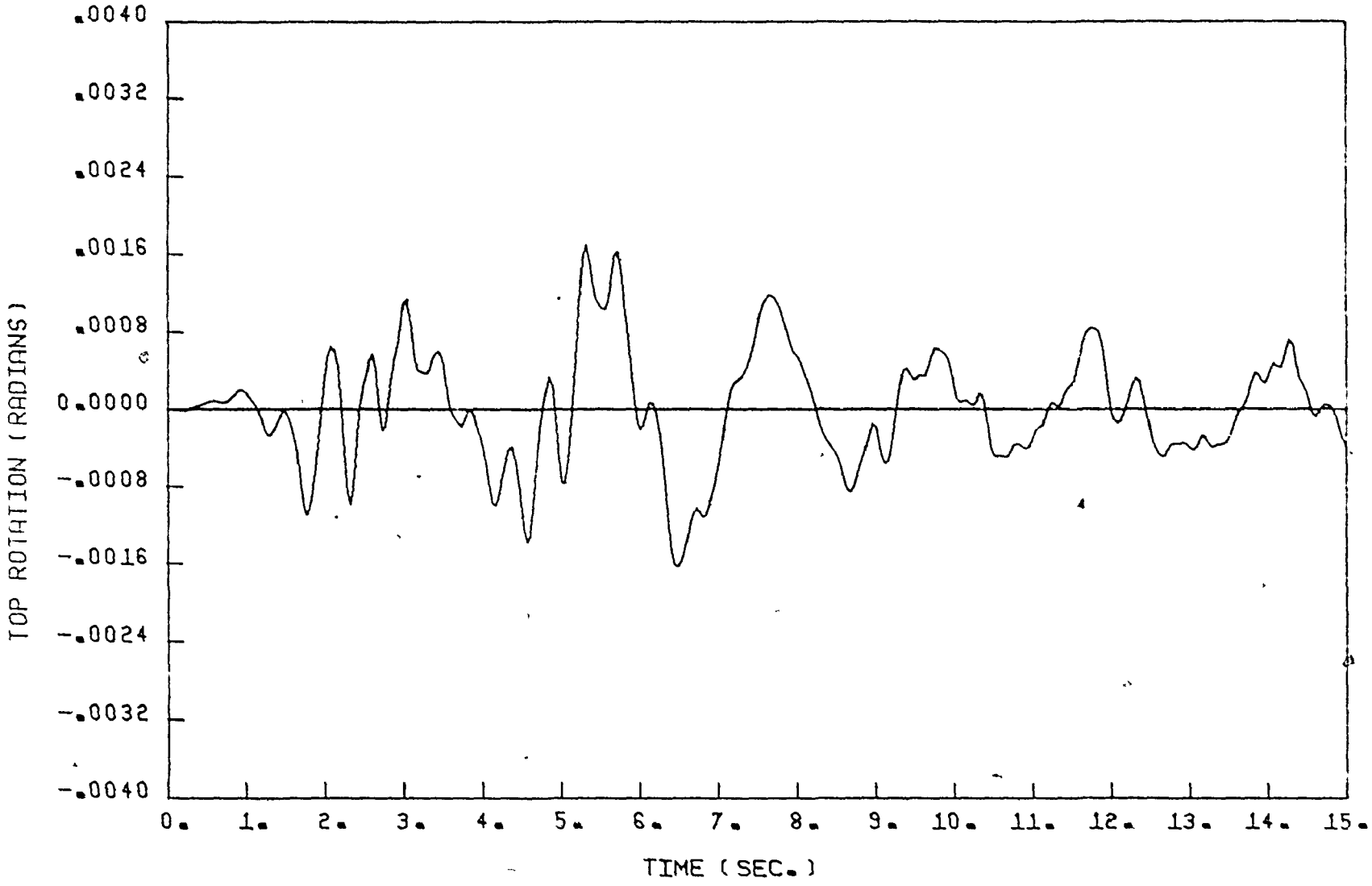

FIGURE 14-b VARIATION OF TOP ROTATION $\bar{\theta}$ WITH TIME

ELCENTRO N-S EXAMPLE STRUCTURE I

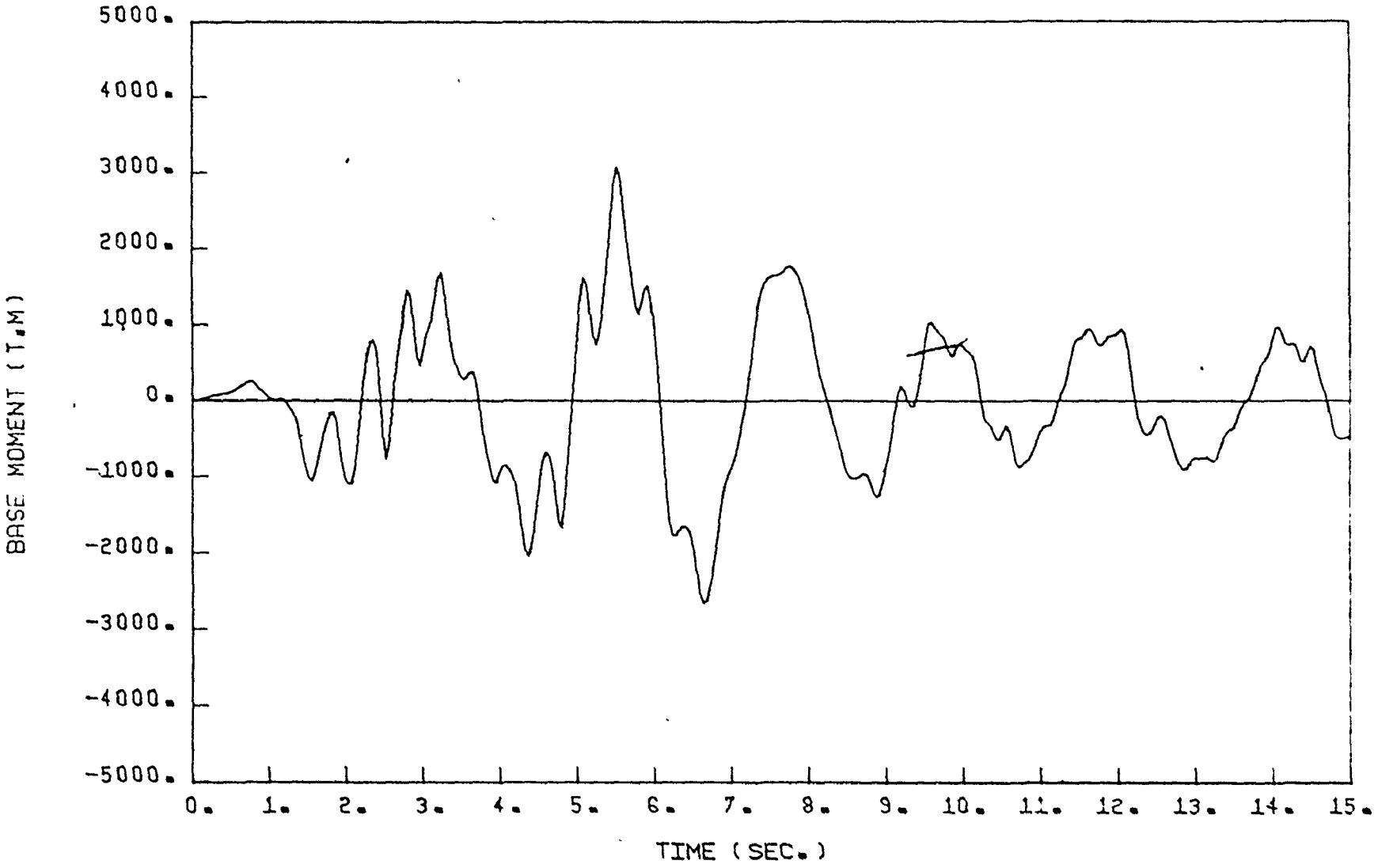

FIGURE 14-c VARIATION OF BASE MOMENT M_W WITH TIME

ELCENTRO N-S EXAMPLE STRUCTURE I

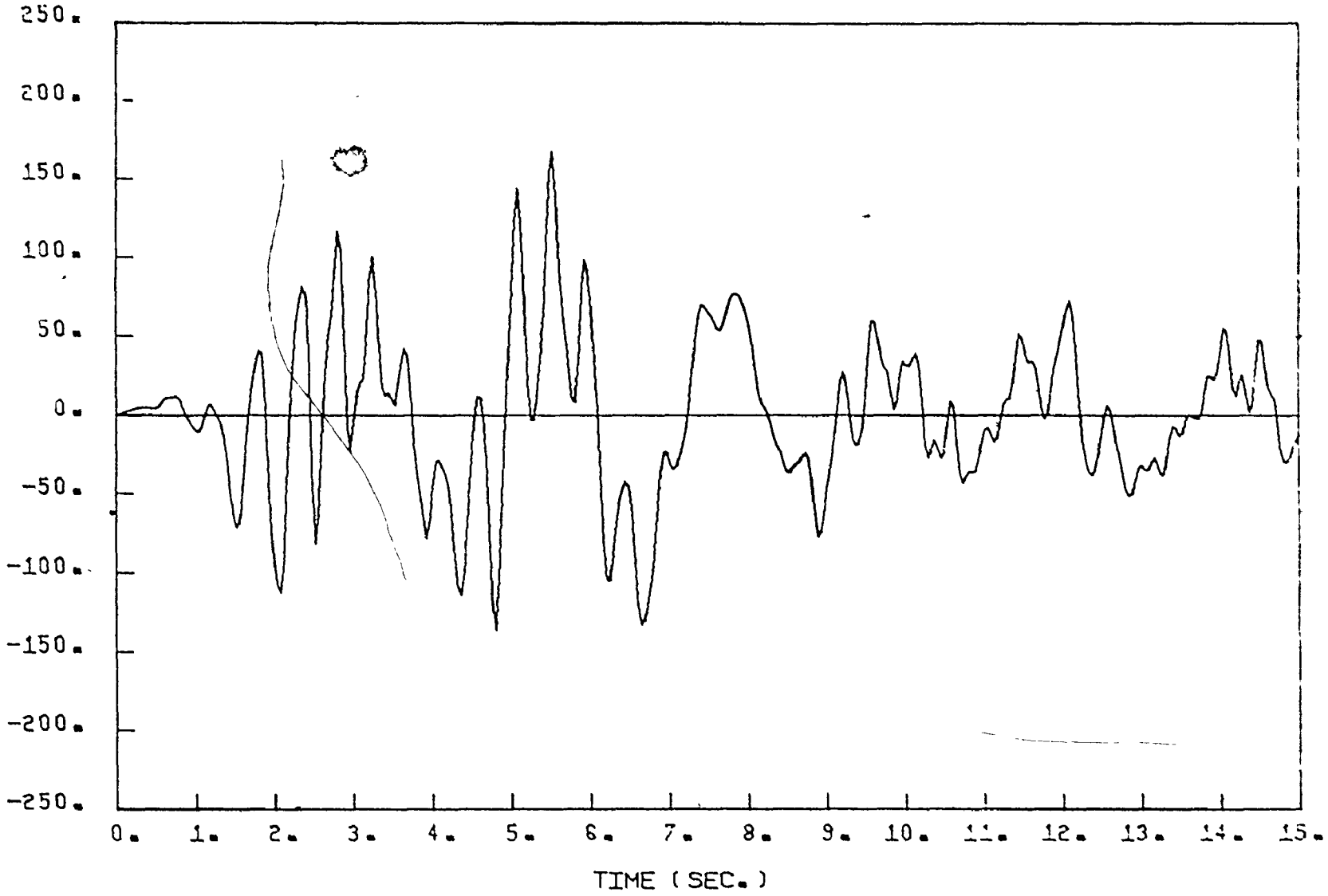

FIGURE 14-d VARIATION OF BASE SHEAR S_W WITH TIME

ELCENTRO N-S EXAMPLE STRUCTURE I

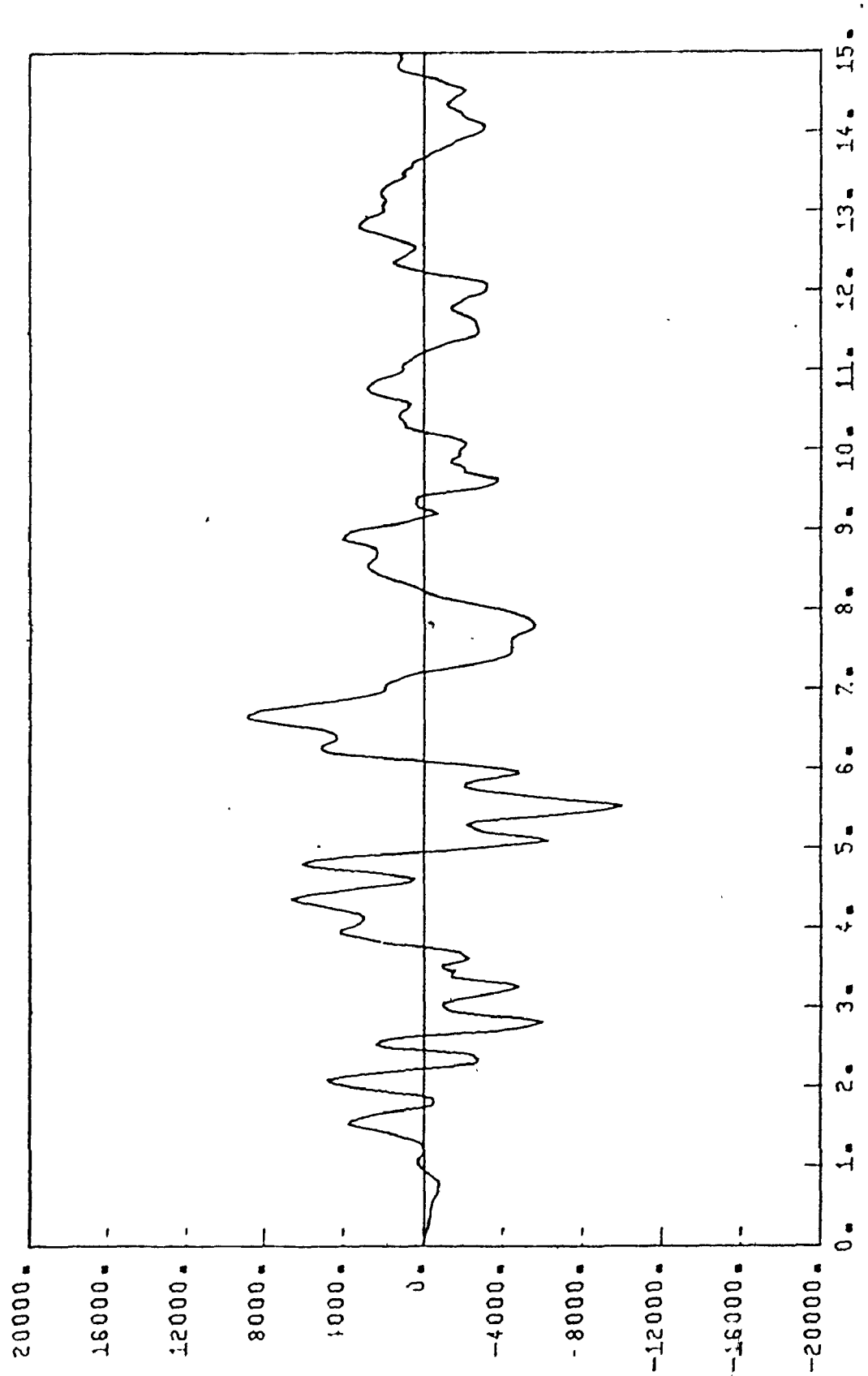

FIGURE 14-e VARIATION OF BASE BIMOMENT B_W WITH TIME
ELCENTRO N-S EXAMPLE STRUCTURE I

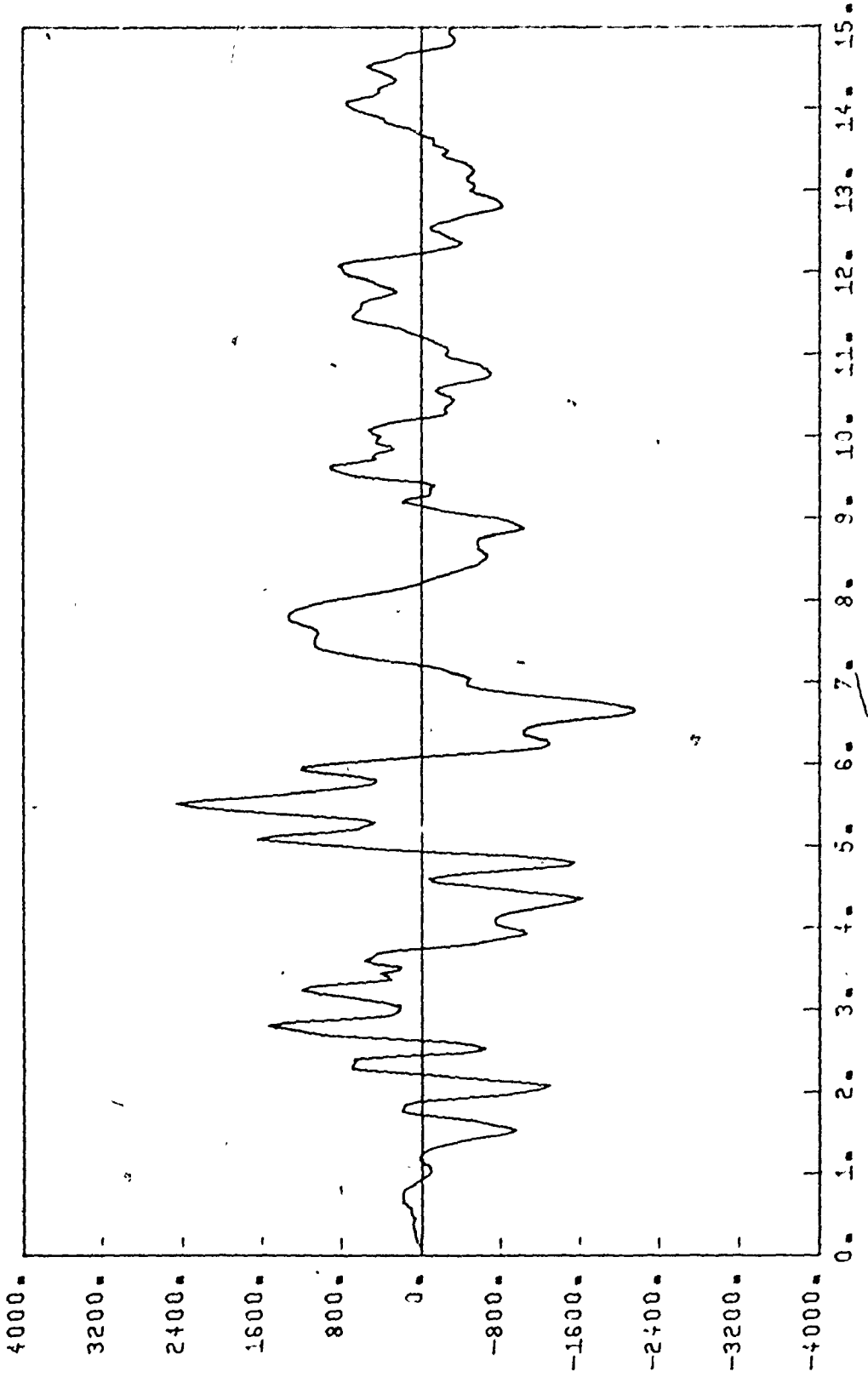

FIGURE 14-1 VARIATION OF BASE TORSION T_W WITH TIME

ELCENTRO N-S EXAMPLE STRUCTURE I

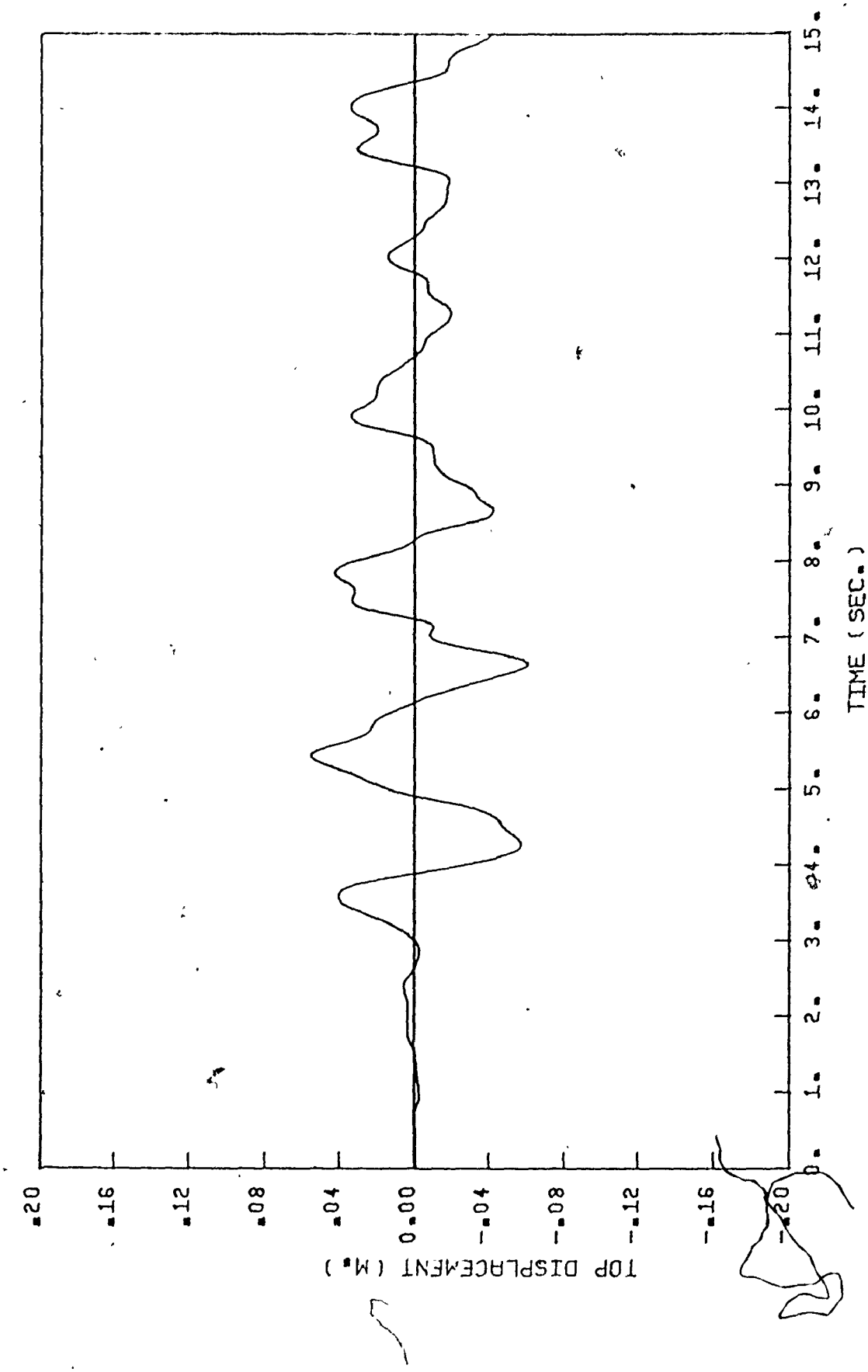

FIGURE 15-a VARIATION OF TOP DISPLACEMENT $\bar{Y}$ WITH TIME

TAFT N21E EXAMPLE STRUCTURE I

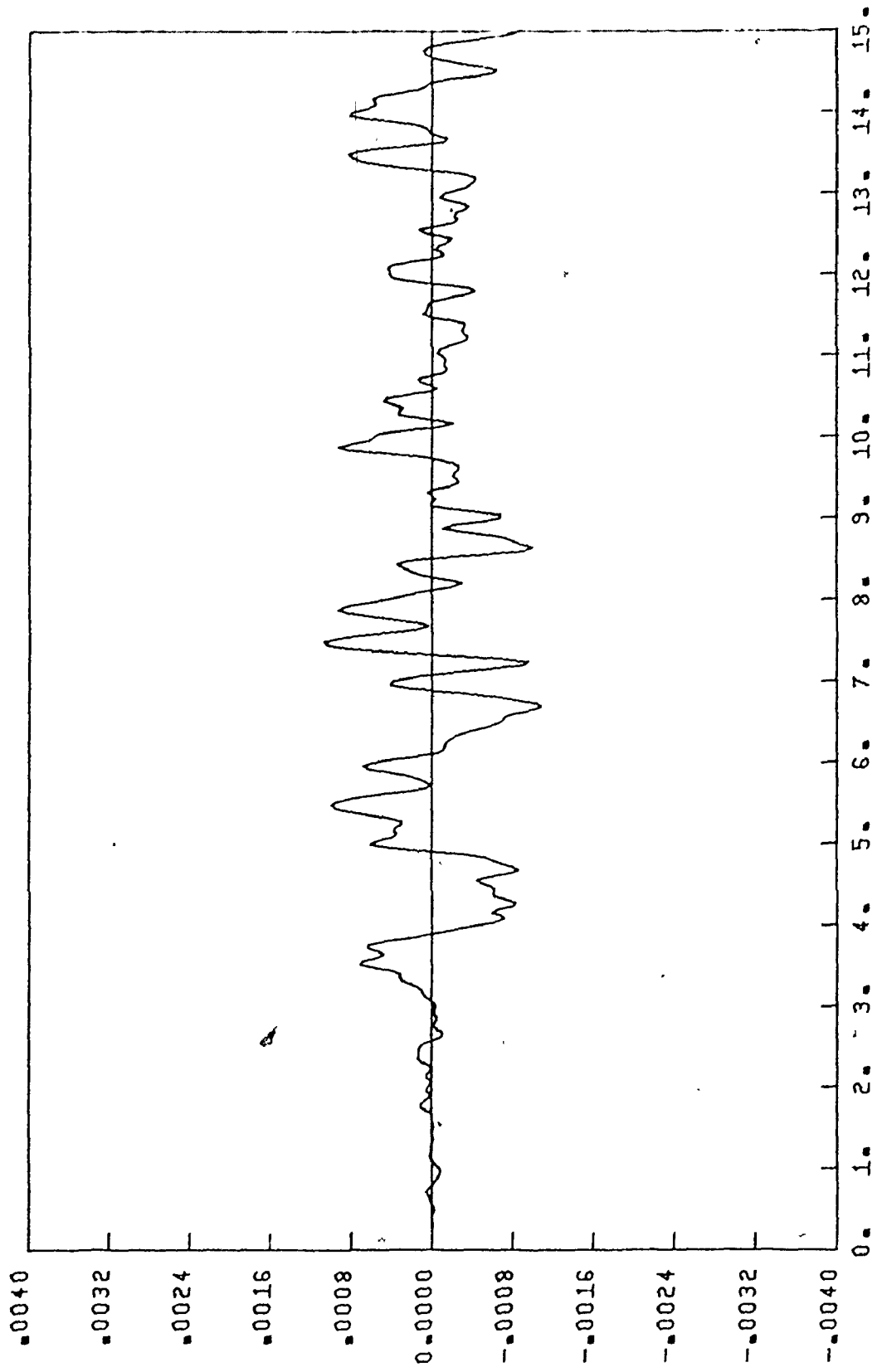

FIGURE 15-b VARIATION OF TOP ROTATION $\bar{\theta}$ WITH TIME

TAFT N21E EXAMPLE STRUCTURE I

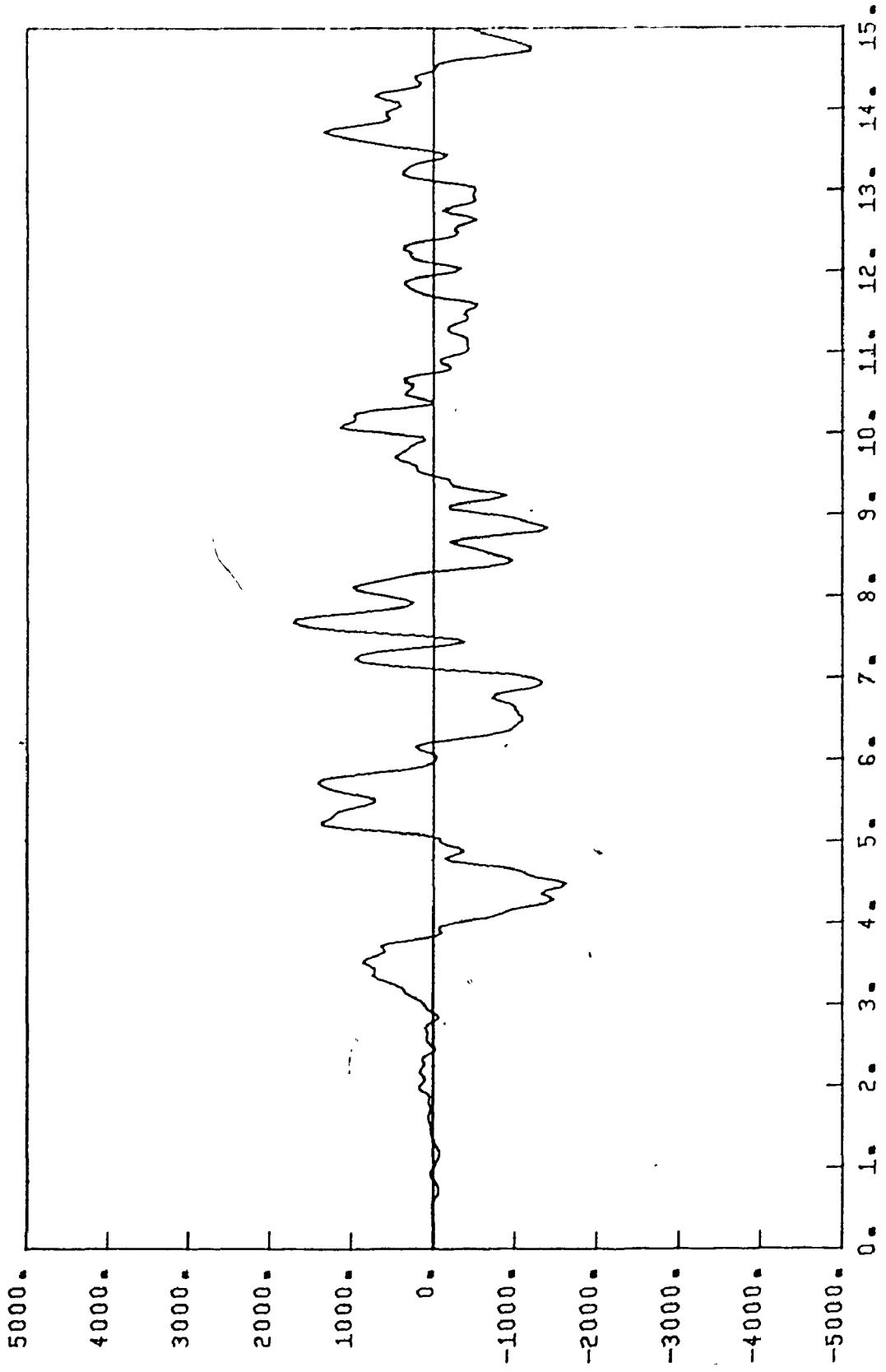

FIGURE 15-c VARIATION OF BASE MOMENT M_W WITH TIME

TAFT N21E EXAMPLE STRUCTURE I

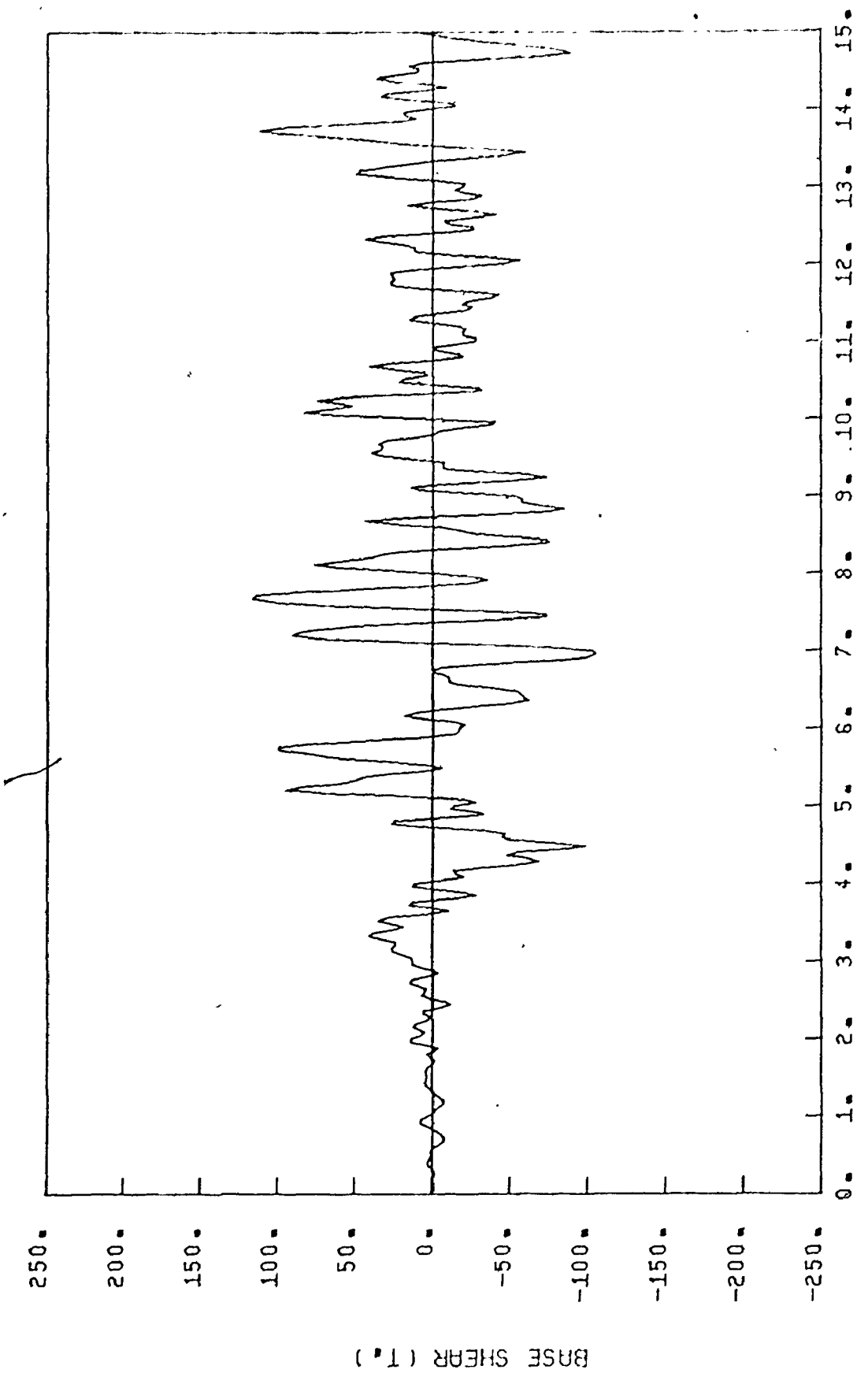

FIGURE 15-d VARIATION OF BASE SHEAR S_W WITH TIME
. TAFT N21E EXAMPLE STRUCTURE I

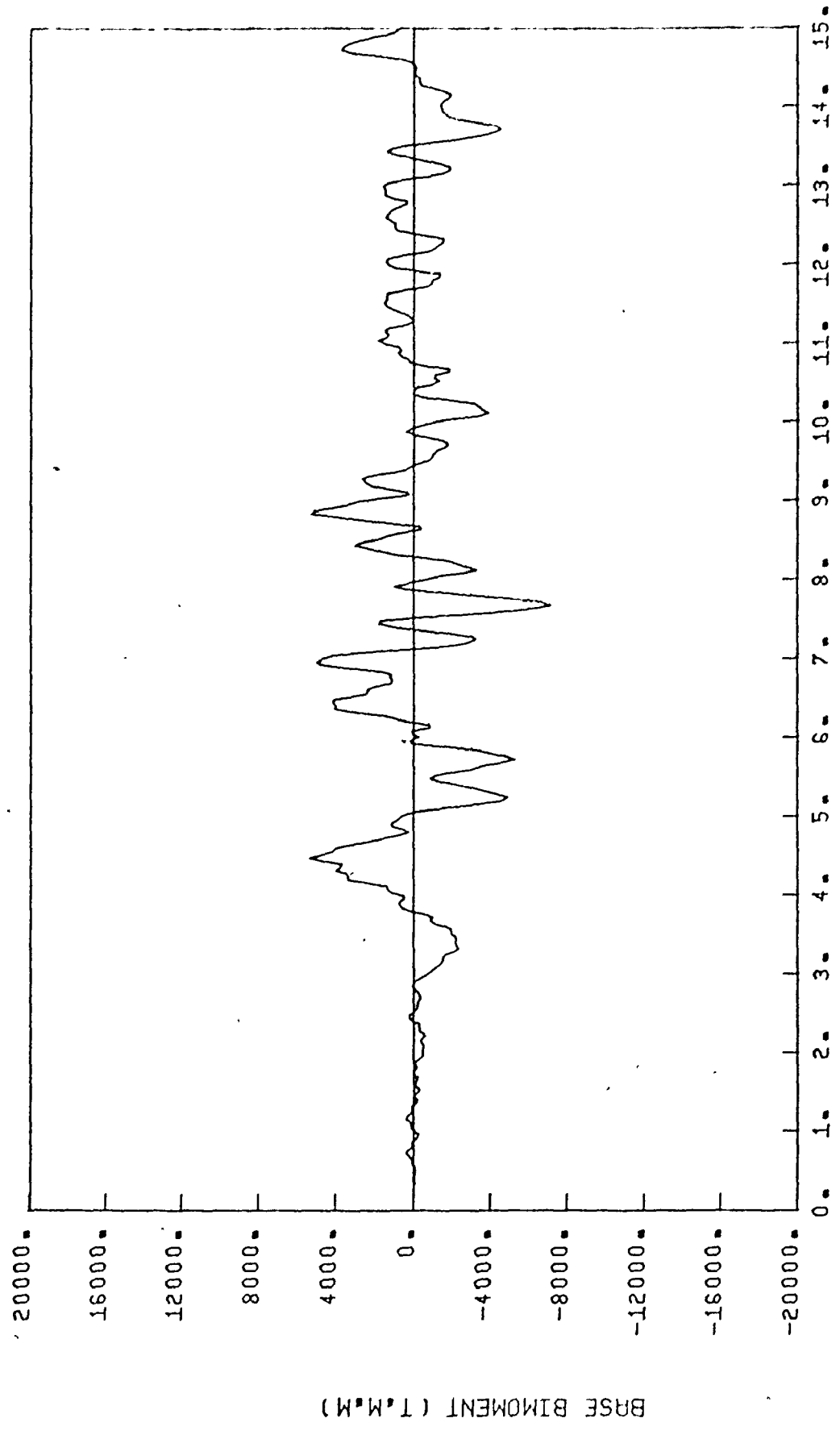

FIGURE 15-e VARIATION OF BASE BIMOMENT B_W WITH TIME

TAFT N21E EXAMPLE STRUCTURE I

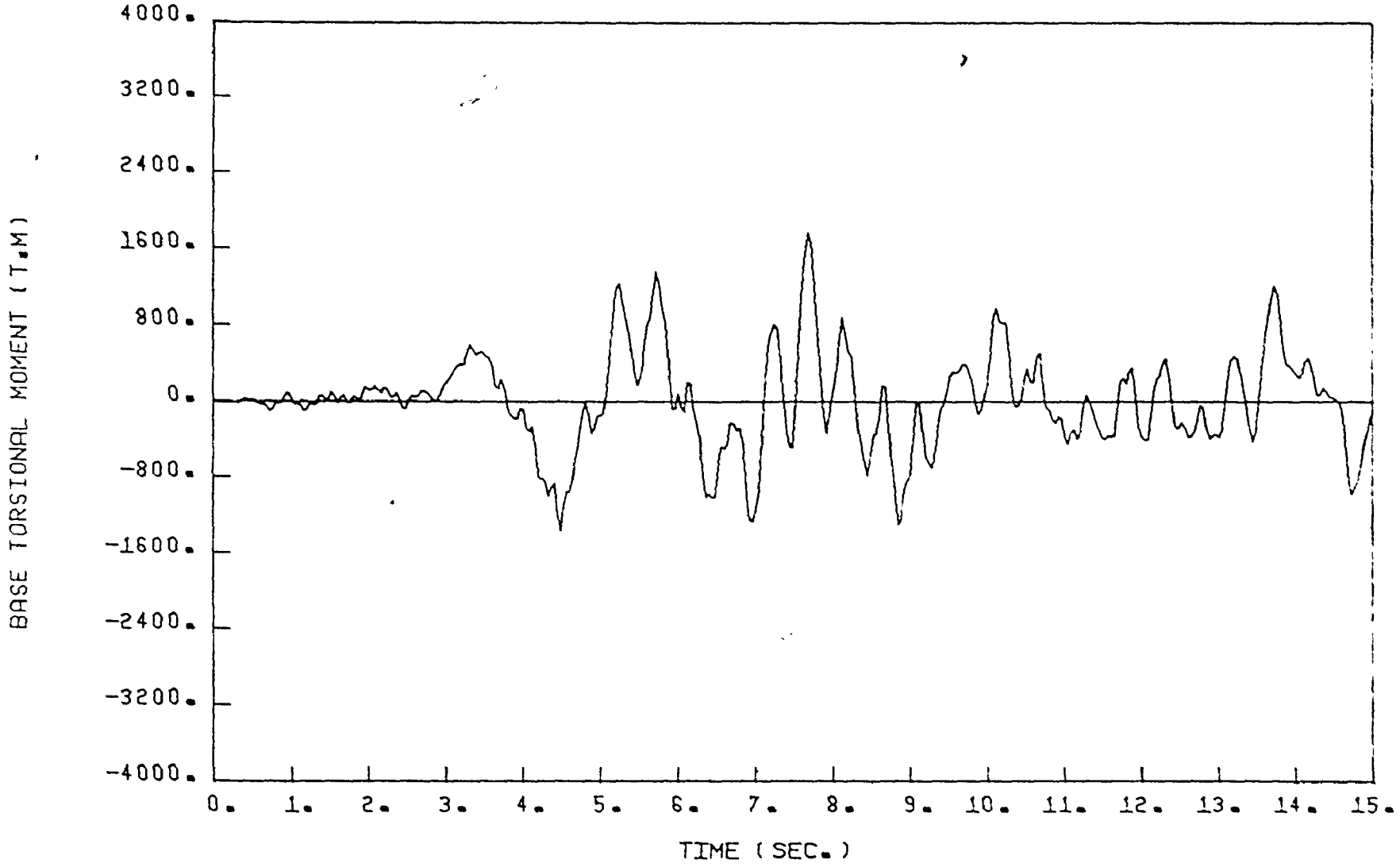

FIGURE 15-1 VARIATION OF BASE TORSION T_W WITH TIME

TAFT N21E EXAMPLE STRUCTURE I

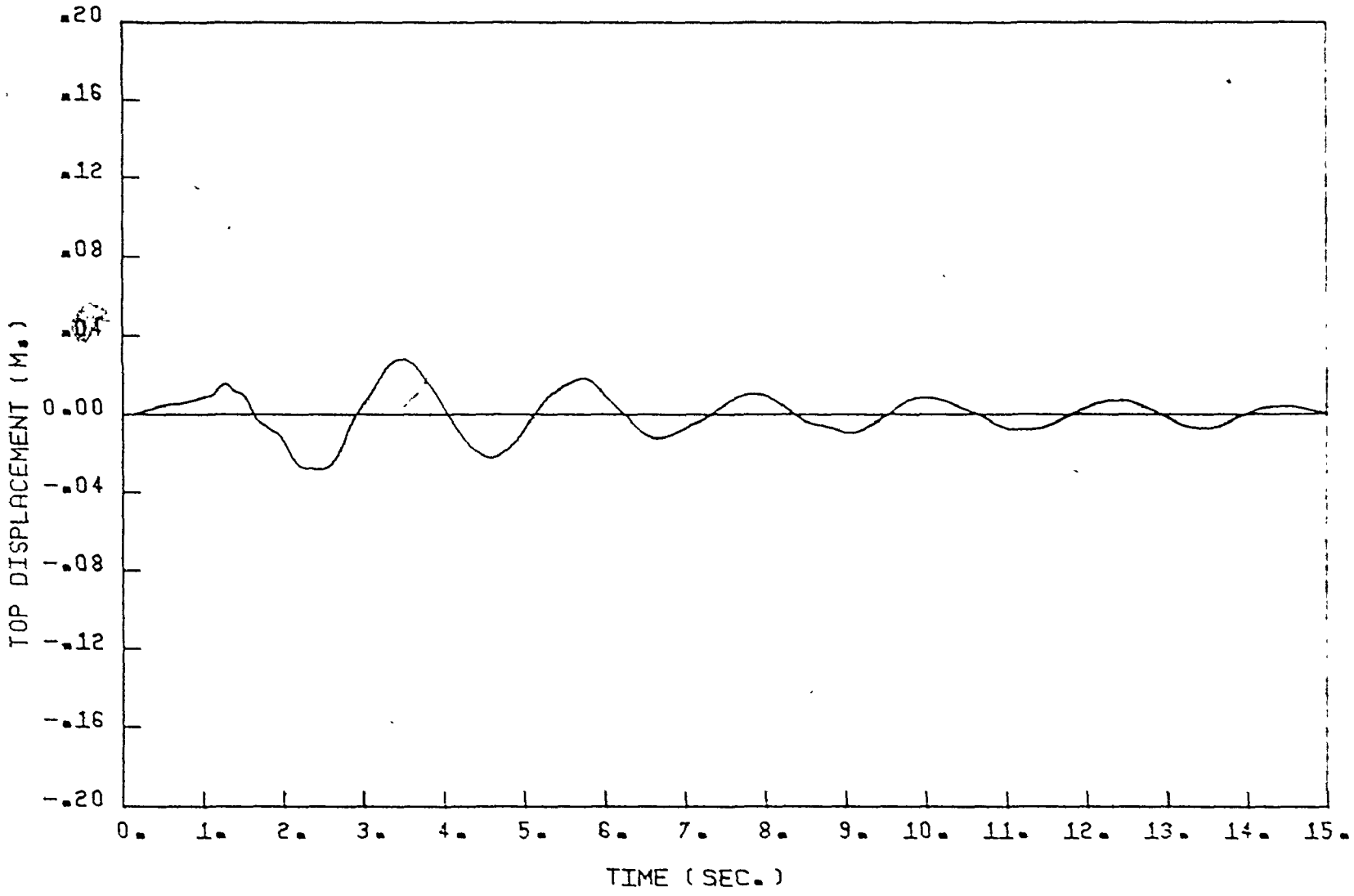

FIGURE 16-a VARIATION OF TOP DISPLACEMENT $\bar{Y}$ WITH TIME

SAN FRANCISCO N10E EXAMPLE STRUCTURE I

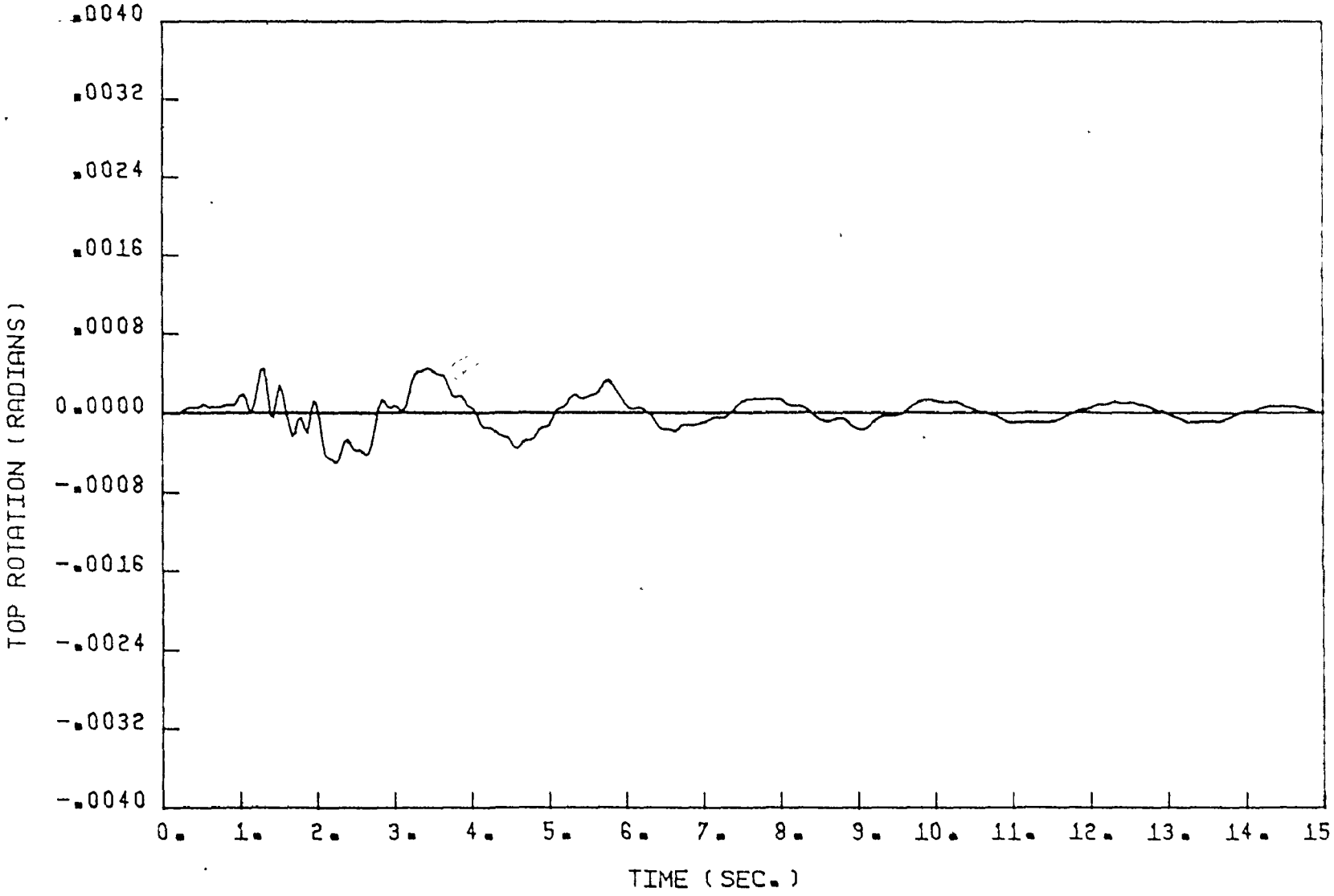

FIGURE 16-b VARIATION OF TOP ROTATION $\bar{\theta}$ WITH TIME

SAN FRANCISCO N10E EXAMPLE STRUCTURE I

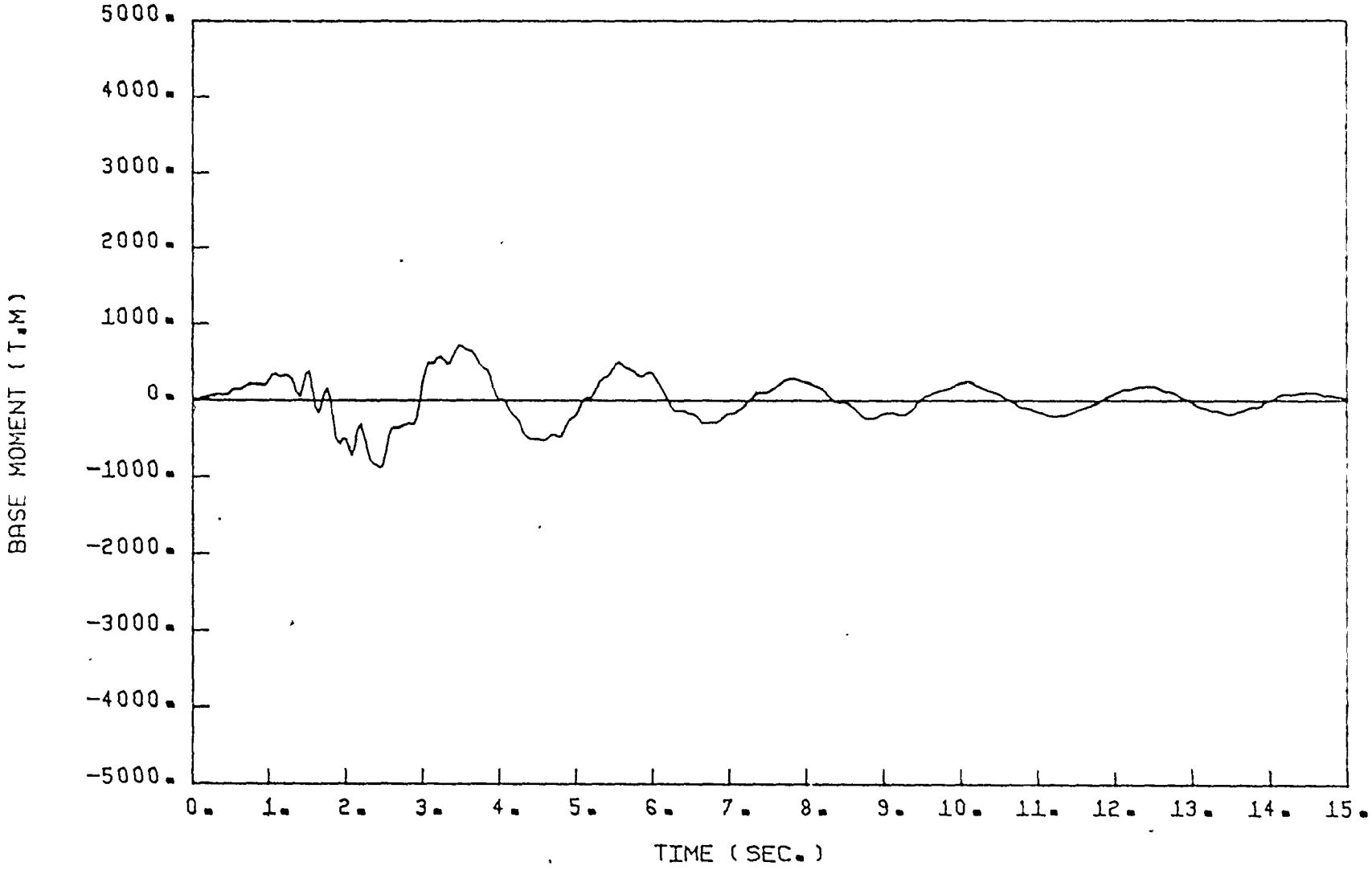

FIGURE 16-c VARIATION OF BASE MOMENT M_W WITH TIME

SAN FRANCISCO N10E EXAMPLE STRUCTURE I

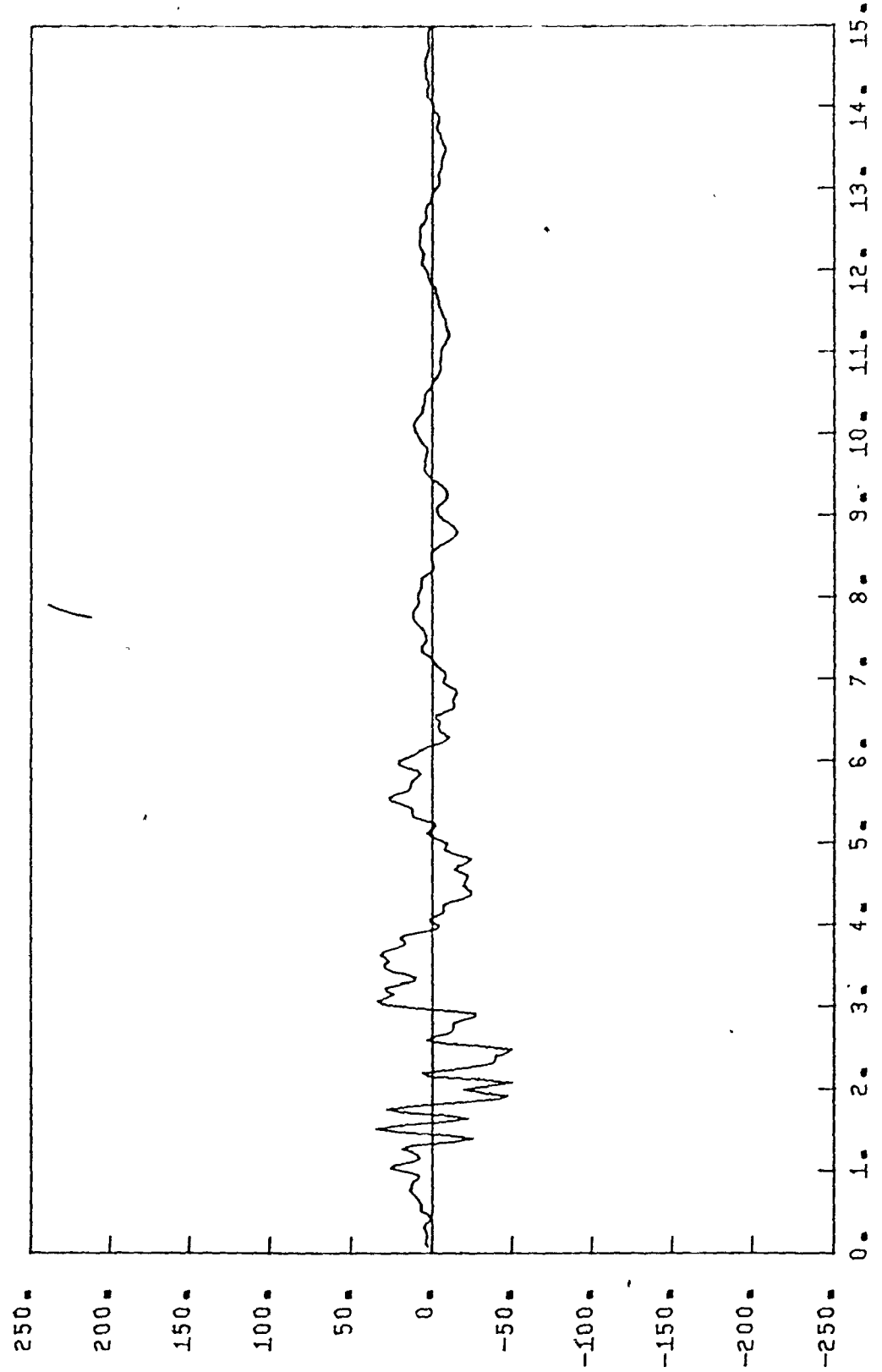

FIGURE 16-d VARIATION OF BASE SHEAR S_W WITH TIME

SAN FRANCISCO N10E EXAMPLE STRUCTURE I

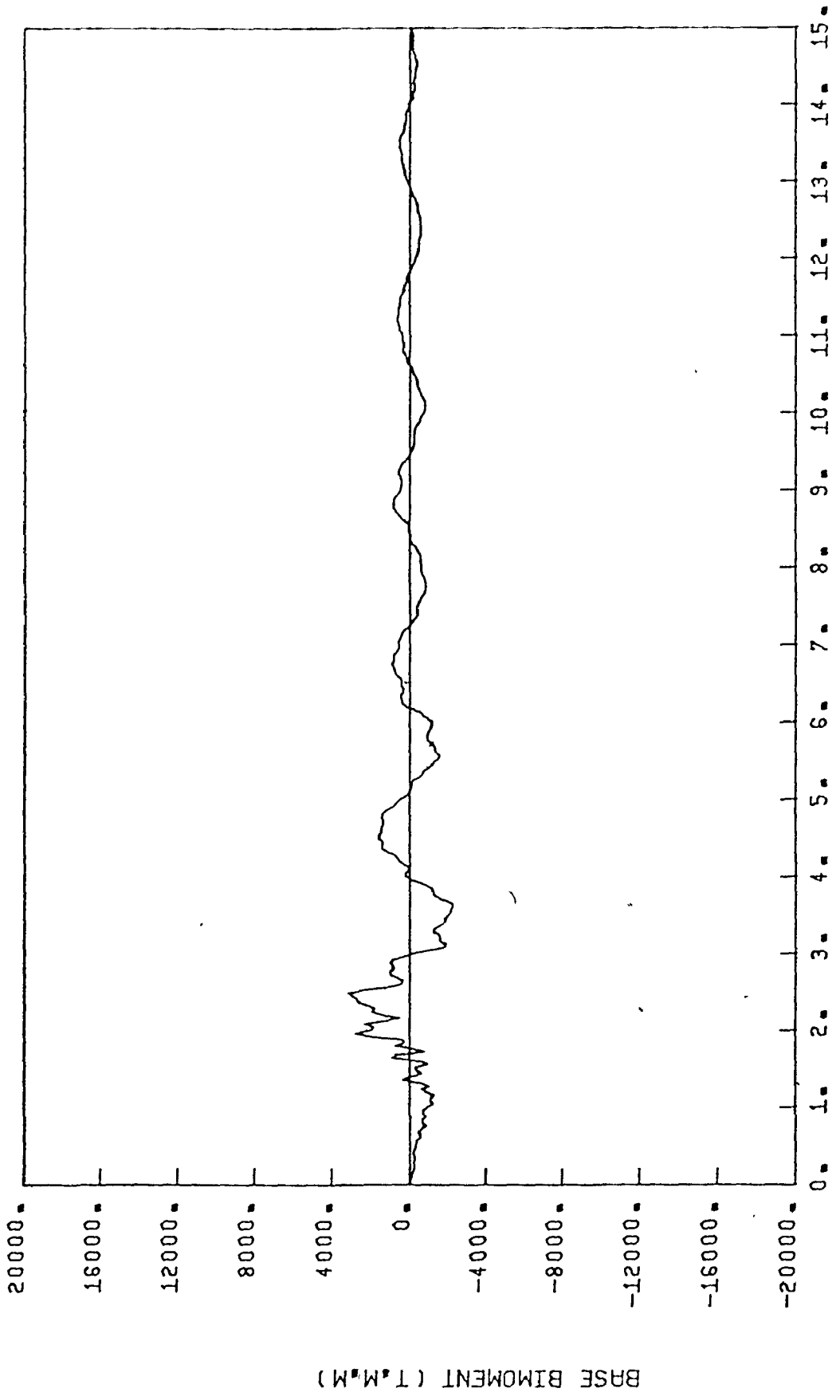

FIGURE 16-e VARIATION OF BASE BIMOMENT B_W WITH TIME
SAN FRANCISCO N10E EXAMPLE STRUCTURE I

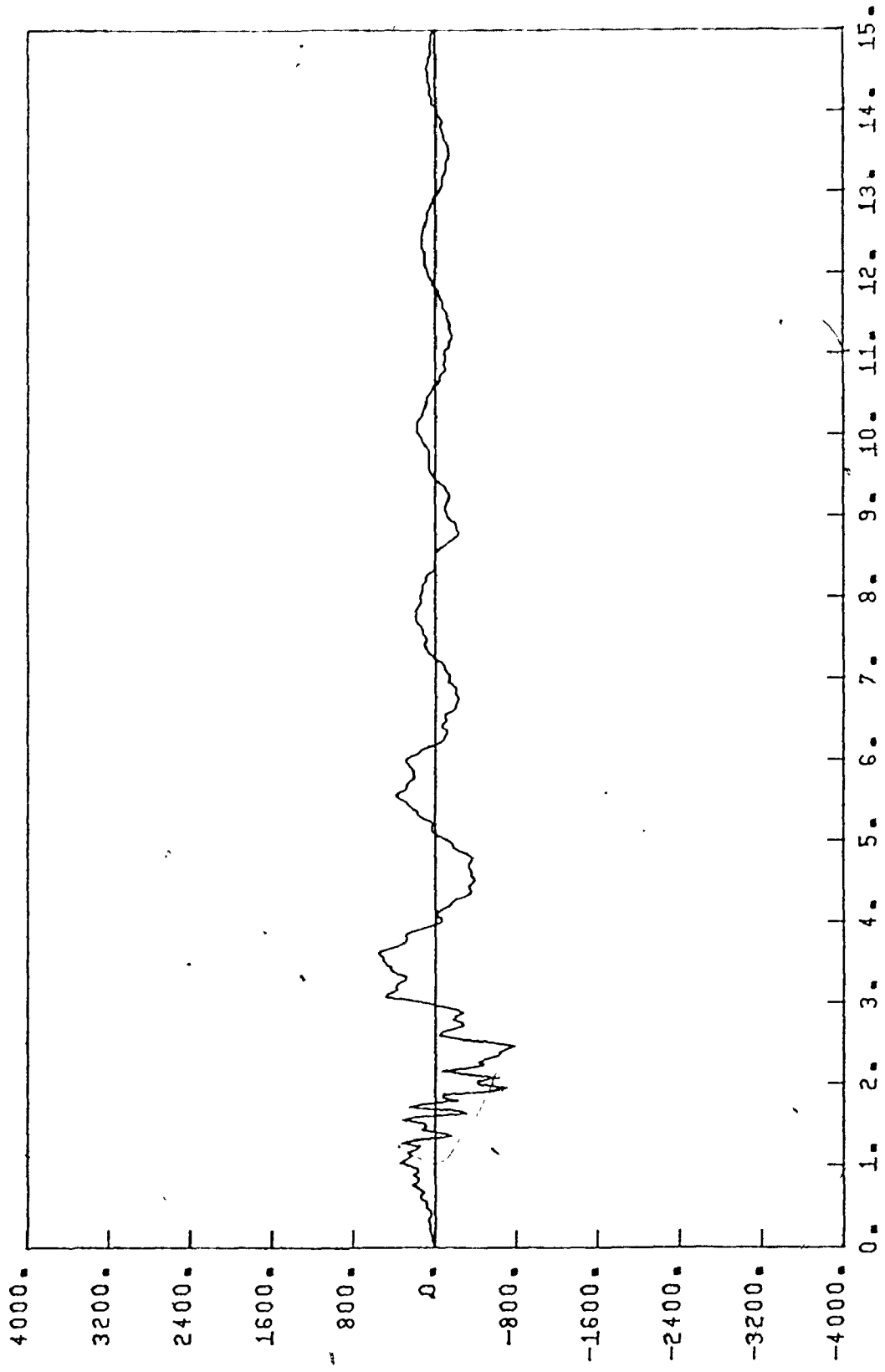

FIGURE 16-1 VARIATION OF BASE TORSION T_W WITH TIME

SAN FRANCISCO N10E EXAMPLE STRUCTURE I

Response Parameter	EL CENTRO N-S		TAFT N21E		SAN FRANCISCO N10E	
	Max. Value	Time(Sec.)	Max. Value	Time(Sec.)	Max. Value	Time(Sec.)
Base Moment [t.m (K. ft)]	3065 (22119)	5.52	1728 (12473)	7.68	888 (6406)	2.44
Base Shear [t (K)]	168 (370)	5.52	116 (256)	7.68	50 (111)	2.08
Base Bimoment [t.m² (K. ft²)]	10016 (237081)	5.52	7193 (170246)	7.68	3145 (74436)	2.48
Base Torsion [t.m (K. ft)]	2464 (17780)	5.52	1770 (12776)	7.68	795 (5740)	2.48
Top Displacement [m (ft)]	0.0987 (0.3237)	5.64	0.0610 (0.2001)	6.68	0.0288 (0.0945)	3.44
Top Rotation [radians]	0.00169	5.32	0.00109	6.68	0.00051	2.24
Design Eccentricity [m (ft)]	14.62 (47.95)	5.52	15.19 (49.82)	7.68	15.73 (51.59)	2.28

Table 11 - Maximum Response Parameters due to various Earthquake Records applied to Example Structure I - Comparison of Results

with factor A of 0.1 g, having an importance factor I of 1.0 and a foundation factor F of 1.0, and using the K factor for a wall-frame system (K = 0.7).

Comparison between the maximum response parameters due to different earthquake records and the stress resultants based on the equivalent static force approach is shown in Table 12. If a modest value of ductility ratio $\mu = 3$ is assumed, one can reduce the base shear response to one third of its value, resulting in a smaller value than that based on the equivalent static force approach. A ductility ratio of 3 may be considered a moderate ductility value that can be expected of a building designed based on a structural K factor of 0.7. Therefore the equivalent static force approach appears to give a conservative design value for the base shear and the base overturning moment.

It is of major interest to interpret the 1975 NBC code provision with respect to torsion in buildings. For this example structure, the core eccentricity being -4.95 m (-16.24 ft) with the width of the building of 16.00 m (52.48 ft), the design eccentricity e_X can be computed by one of the following equations, given in the 1975 NBC code, whichever provides the greater stresses

$$e_X = 1.5\, e_m + 0.05\, D_n \qquad (4.27a)$$

$$e_X = 0.5\, e_m - 0.05\, D_n \qquad (4.27b)$$

The maximum design eccentricity calculated is 8.225 m (26.98 ft). Since the eccentricity exceeds a quarter of the width of the building, the 1975 NBC code provision suggests doubling the effects of torsion,

resulting in an eccentricity of 16.45 m (53.96 ft). The comparison between the design eccentricity computed by the code and the dynamic design eccentricity shows that the code gives similar value to the dynamic analysis after doubling the static effect of this seismic parameter.

The exact static analysis of the wall-frame structures is developed by Mok (20) and an approximate one, suitable for hand computation is presented by Rutenberg and Heidebrecht (24). Solving the same problem statically by the method given in reference (24) for a triangular distributed load resulting for a base shear equal to the maximum dynamic one $[V_W(0,t)]$, the base stress resultants and the top displacement and rotation of the structure are shown in Table 13. This table gives also the corresponding maximum dynamic parameters due to different earthquake records and the magnification (or reduction) factor for each parameter.

The comparison of the dynamically computed maximum displacements and stresses with those computed statically from the National Building Code of Canada or by more exact static analysis (20,24), indicates that the static values of the bending parameters (M_W , $\bar{Y}$) are conservative, while those of the torsion parameters (T_W , $\bar{\theta}$) are underestimated. In other words, the static analysis is conservative whenever torsion is not important, but cannot take into account the magnification effect due to coupling between the Y and θ motions in asymmetric wall-frame building structures.

Design Parameter	Dynamic Response Analysis			Static Analysis of NBC code 1975
	EL CENTRO N-S	TAFT N21E	SAN FRANCISCO N10E	
	Max. Value	Max. Value	Max. Value	
Base Shear	168	116	50	80
[t (K)]	(370)	(256)	(111)	(176)
Base Moment	3065	1728	888	2228
[t.m (K. ft)]	(22119)	(12473)	(6406)	(16077)
Design Eccentricity	14.62	15.19	15.73	16.45
[m (ft)]	(47.95)	(49.82)	(51.59)	(53.96)

Table 12 - Comparison between the Dynamic Response Analysis and the Static Analysis of the 1975 NBC code - Example Structure I

Design Parameter	Dynamic Response Analysis						Static Analysis of Reference (24)
	EL CENTRO *N-S*		TAFT *N21E*		SAN FRANCISCO *N10E*		
	Max. Value	*MF(RF)	Max. Value	MF(RF)	Max. Value	MF(RF)	
Base Shear [*t* (*K*)]	168 / (370)	1.0	116 / (256)	1.0	50 / (111)	1.0	96 / (211)
Base Moment [*t.m.* (*K.* ft)]	3065 / (22119)	0.80	1728 / (12473)	0.65	888 / (6406)	0.77	2183 / (15752)
Base Torsion [*t.m* (*K.* ft)]	2464 / (17780)	2.95	1770 / (12776)	3.07	795 / (5740)	3.18	475 / (3427)
Top Displacement [*m* (ft)]	0.0987 / (0.3237)	0.70	0.0610 / (2.2001)	0.63	0.0288 / (0.0945)	0.68	0.0800 / (0.2624)
Top Rotation [radians]	0.00169	2.09	0.00109	1.95	0.00051	2.10	0.00046

Table 13 - Comparison between the Dynamic Response Analysis and the Static Analysis of Reference (24) - Example Structure I

* MF : Magnification factor = (Dynamic Parameter / Static Parameter) × (Static Shear / Dynamic Shear)
RF : Reduction factor

CHAPTER V

CONCLUSIONS

A research programme has been set up to study the dynamic response of asymmetric wall-frame building structures. In this programme the walls are represented by flexural elements and the frames are represented by shear elements. The analysis is based on the continuous approach. The coupling effect of translational and torsional vibration is included, which has recently drawn a great attention of the researchers. The study includes a dynamic analysis to determine the exact dynamic properties of wall-frame building structures as well as a response analysis to obtain a complete time history response due to Seismic Ground Motion and to compute the maximum design seismic parameters of such structures. The results of this investigation indicate that the following conclusions and recommendations can be made.

1. The natural modes, due to the effect of coupling, consist of both lateral and rotational displacements. For some modes, the deformation consists mainly of lateral displacements with a minor component of rotation of the building. These modes are termed flexural predominant modes. On the other hand, some modes consist mainly of rotation and these modes are called torsional predominant modes.

2. The change of shear and flexural eccentricity has major effect on the coupled natural frequencies of predominant torsional vibration in character and only minor effect on these of predominant flexural vibration in character. It is recommended that the coupled periods be computed for all shear wall-frame structures, even though they appear to be nearly symmetrical. In buildings with small eccentricities the uncoupled periods and mode shapes can provide a good approximation.

3. The study of the natural periods of this type of buildings shows that the formula for period determination as suggested by the 1975 NBC code may lead to errors of 30% or more. A separate calculation for the natural periods is necessary for this type of buildings.

4. The building with large core eccentricity can be treated as a single wall-frame system and the boundary conditions governing its mode shapes are reduced from the 8 boundary conditions of the general case to the 6 boundary conditions of the particular case of interaction of one planar wall with frames in a 2-dimensional wall-frame problem. This treatment is due to the negligible warping torsional stiffness of the core with respect to that of the entire structure.

5. The non-dimensional parameters αH and βH which express the ratio of the frames to the walls in the building, are significant parameters governing the behaviour of the wall-frame structure due to the Y and θ motions, respectively. Buildings which

have predominantly shear walls with little or no frame action will have a low values of αH and βH and will behave essentially as flexural members. As the proportion of frame action increases, αH and βH increase, and the structure behaves more as a shear member. Research on the effect of these parameters on the degree of coupling between the Y and θ motions is needed.

6. The dynamic response being calculated for each mode individually, the total dynamic response is obtained by direct summation of the effect of the modes using equation (3.24). The variation of the modal participaction factor with the modes of vibration enables one to determine the number of modes which must be taken into consideration in the response analysis. It should be pointed out that the torsional to bending natural period ratio is an important parameter affecting the variation of the modal participation factor. Research in this direction is needed.

7. The study on the dynamic response of this type of buildings shows that the eccentricity causes coupling of the forces and displacements; when the ground motion had only a Y-component, the substantial forces and displacements were obtained in other directions as well. The degree of coupling, between the rotation and the displacement, between the torque and the shear and between the bimoment and the bending moment, give a complete understanding of the influence of the eccentricities on the dynamic behaviour of the structure.

8. The comparison of the dynamically computed maximum displacements and stresses with those computed statically from the National Building Code of Canada 1975, indicates that the latter is conservative whenever torsion is not important, but cannot take into account the magnification effect due to coupling between the Y and θ motions in asymmetric wall-frame building structures. Consequently, it is recommended that, in order to ensure safety, that type of buildings in Canadian Zone 3, or its equivalent elsewhere, be designed using the dynamic approach.

9. The method of analysis presented here for asymmetric wall-frame structures are limited to uniform structures. However, in actual tall buildings, the dimensional and structural properties vary along the height. Therefore, this method should be extended to cover non-uniform structures, such as by means of the transfer matrix technique or by other means.

10. The results of this investigation are based on a very limited set of data; the validity for more general situations will require substantial application of this work to a large number of structures and earthquakes.

REFERENCES

1. Baruch, M., Gluck, J. and Mendelson, E., "Normal Modes for Non-symmetric Multi-storey Structures", Proceedings of Institution of Civil Engineers, Vol. 50, February, 1972, pp. 359.

2. Biggs, J.M., "Introduction to Structural Dynamics", McGrall Hill, New York, 1964.

3. Chan, P.C.K., "Static and Dynamic Analysis of Frame-Tube Structures", Thesis submitted in partial fulfilment of the requirements for the degree of Doctor of Philosophy, McMaster University, Hamilton, Ontario, Canada, October, 1973.

4. Clough, R.W., King, I.P. and Wilson, E.L., "Structural Analysis of Multi-storey Buildings", Journal of the Structural Division, A.S.C.E., Vol. 90, No. ST3, June, 1964, pp. 19-34.

5. Coull, A. and Smith, S.B., "Analysis of Shear Wall Structures (A review of Previous Research)", Proceedings of a Symposium on Tall Buildings, University of Southampton, April, 1966, Pergamon Press, pp. 139-155.

6. Fintel, M., et al., "Response of Buildings to Lateral Forces", Journal of the American Concrete Institute, Vol. 68, No. 2, February, 1971.

7. Fleming, J.F. and Romualdi, J.P., "A General Procedure for Calculating Dynamic Response due to Impulsive Loads", Journal of the Franklin Institute, Vol. 275, No. 2, February, 1963.

8. Gluck, J., "Lateral Load Analysis of Asymmetric Multi-storey Structures", Journal of the Structural Division, A.S.C.E., Vol. 96, No. ST2, February 1970, pp. 317-333.

9. Gluck, J. and Gellert, M., "Three Dimensional Lateral Load Analysis of Multi-storey Structures", International Association for Bridge and Structural Engineering, 1972, pp. 77-90.

10. Heidebrecht, A.C. and Raina, R.K., "Frequency Analysis of Thin-Walled Shear Walls", Journal of the Engineering Mechanics Division, A.S.C.E., Vol. 97, No. EM2, April, 1971, pp. 239-252.

11. Heidebrecht, A.C. and Irwin, A.W., "Dynamic Behaviour of Coupled Shear Wall Structures", Proceedings of the First Canadian Conference on Earthquake Engineering Research, Vancouver, B.C., May, 1971.

12. Heidebrecht, A.C. and Stafford Smith, B., "Approximate Analysis of Tall Wall-Frame Structures", Journal of the Structural Division, A.S.C.E., Vol. 99, No. ST2, February, 1973, pp. 199-221.

13. Heidebrecht, A.C. and Stafford Smith, B., "Approximate Analysis of Open-Section Shear Walls Subject to Torsional Loading", Journal of the Structural Division, A.S.C.E., Vol. 99, No. ST12, December 1973, pp. 2355-2373.

14. Heidebrecht, A.C., "Dynamic Analysis of Asymmetric Wall-Frame Buildings", Proceedings of the ASCE National Structural Engineering Convention, New Orleans, Louisiana, April, 1975.

15. Housner, G.W., "Behavior of Structures During Earthquakes", Journal of the Engineering Mechanics Division, A.S.C.E., Vol. 85, No. EM4, October 1959, pp. 109-129.

16. Khan, F.R. and Sbarounis, J.A., "Interaction of Shear Walls and Frames", Journal of the Structural Division, A.S.C.E., Vol. 93, No. ST3, June, 1964, pp. 285-335.

17. Macleod, I.A., "Simplified Analysis for Shear Wall-Frame Interaction", Building Science, Vol. 7, 1972, pp. 121-125.

18. Mendelson, E., "Effect of Earthquake on Multistory Structures", Thesis submitted to the Senate of the Technion-Israel Institute of Technology, in partial fulfilment of the requirements for the degree of Doctor of Science, December, 1970, (in Hebrew).

19. Mendelson, E. and Baruch, M., "Earthquake Response of Non-Symmetric Multistory Structures", The Structural Engineer, Vol. 51, 1973, pp. 61-70.

20. Mok, D., "Static and Dynamic Analysis of Tall Wall-Frame Building Structures", Thesis submitted in partial fulfilment of the requirements for the degree of Master of Engineering, McMaster University, Hamilton, Ontario, Canada, July, 1974.

21. National Building Code of Canada 1975, National Research Council of Canada, Ottawa, Canada, pp. 158-165.

22. Raina, R.K., "Dynamic Response of a Thin-Walled Shear Wall Model", Thesis submitted in partial fulfilment of the requirements for the degree of Master of Engineering, McMaster University, Hamilton, Ontario, Canada, January, 1970.

23. Rosman, R., "Laterally Loaded Assemblies of Walls and Frames in Multistorey Buildings", Acta Technica Academiae Scientiarum Hungaricae Tomus 55, 1966, pp. 117-146.

24. Rutenberg, A. and Heidebrecht, A.C., "Approximate Analysis of Asymmetric Wall-Frame Structures", Building Science, Vol. 10, 1975, pp. 27-35.

25. Rutenberg, A., Tso, W.K. and Heidebrecht, A.C., "Dynamic Properties of Asymmetric Wall-Frame Structures", Submitted for publication, Earthquake Engineering and Structural Dynamics.

26. Stamato, M.C., "Three-Dimensional Analysis of Tall Buildings", ASCE - IABSE Joint Committee on Planning and Design of Tall Buildings, Lehigh University, Bethlehem, Pannsylvania, January, 1972.

27. Stamato, M.C. and Mancini, E. "Three-Dimensional Interaction of Walls and Frames", Journal of the Structural Division, A.S.C.E., Vol. 99, No. ST12, December 1973, pp. 2375-2390.

28. Tso, W.K. and Biswas, J.K. "Seismic Analysis of Multi-Storey Shear Wall Buildings", Dept. Research Report No. 71-5, Department of Civil Engineering and Engineering Mechanics, McMaster University, Hamilton, Ontario, Canada, April, 1971.

29. Tso, W.K. and Asmis, K.G., "Torsional Vibration of Symmetrical Structures", Proceedings of the First Canadian Conference on Earthquake Engineering Research, Vancouver, B.C., May, 1971.

30. Tso, W.K. and Bergmann, R., "Dynamic Analysis of an Unsymmetrical High Rise Building", Proceedings of the Second Canadian Conference on Earthquake Engineering Research, Hamilton, Ont., June, 1975.

31. Winokur, A. and Gluck, J., "Lateral Loads in Asymmetric Multistory Structures", Journal of the Structural Division, A.S.C.E., Vol. 94, No. ST3, March, 1968, pp. 645-656.

32. California Institute of Technology, "Strong Motion Earthquake Accelerograms", Report on Research from Earthquake Engineering Research Laboratory, Pasadena, California, September, 1971.

APPENDIX 1

List of FØRTRAN IV Computer Programmes

Programme 1 : Dynamic Analysis of 2-Dimensional Wall-Frame Building Structures (based on the continuous approach and satisfies 8 boundary conditions).

Programme 2 : Dynamic Analysis of Single Wall-Frame System (based on the continuous approach and satisfies 6 boundary conditions).

Programme 3 : Response Analysis of 2-Dimensional Wall-Frame subjected to Sinusoidal Base Motion (rigorous solution).

Programme 4 : Response Analysis of 2-Dimensional Wall-Frame subjected to Seismic Ground Motion (based on a numerical integration technique).

APPENDIX 2

LIST OF SYMBOLS

a_{Xj}, a_{Yj}, a_X, a_Y, a_m - shear component eccentricities

A_1, A_2, A_3, A_4, A_5, A_2^1 - polynomial constant coefficients

A_m , B_m - arbitrary constants determined by the initial conditions for mode m

Acc (t) - applied ground acceleration function

B_w - Bimoment in the wall

b^2 , c^2 - parameters describing stiffness and mass relationships in the Y and θ directions, respectively

C_{Yn} , $C_{\theta n}$ - mode shape multipliers for mode n

D_n , F_n - characteristic determinants for mode n

e_{Xi}, e_{Yi}, e_X, e_Y, e_m - flexural component eccentricities

EI_{Xi}, EI_{Yi}, $\overline{EI}_X$, $\overline{EI}_Y$ - translational flexural stiffnesses

$EI_{\omega i}$, $\overline{EI}_\omega$ - warping torsional stiffness

F_{om} , P_{om} - modal participation factors for mode m

GA_{Xj}, GA_{Yj}, $\overline{GA}_X$, $\overline{GA}_Y$ - translational shear stiffnesses

GJ_i, GJ_j, $\overline{GJ}$ - St. Venant torsional stiffnesses

G_m - amplitude of $T_m(t)$ for the m^{th} mode of steady forced vibration

H - height of building

I_1 , I_2 - mode shape product integrals

K, K_1, K_2, K_3 - matrix form describing physical and geometrical properties of the stiffning elements.

M_W , M_F - bending moment in flexural and shear components, respectively

Q_n - normalization factor for the coupled shape functions ϕ_{Yn} and $\phi_{\theta n}$, for the n^{th} mode of vibration

r - flexural radius of gyration $= \sqrt{\frac{EI_\omega}{EI_Y}}$

S_W , S_F - shearing force in flexural and shear components, respectively

T_W , T_F - torsional moment in flexural and shear components, respectively

$T_m(t)$ - function determining the temporal variation of the response corresponding to the m^{th} mode of vibration

t - time variable in seconds

w_{Xi}, w_{Yi}, W_X, W_Y - distributed applied lateral loads

$w_{\theta i}$, w_θ - distributed external applied torsional moment

x_K , y_K - X and Y coordinates of element K

X_i , Y_i - lateral displacements of element i

$\bar{X}$, $\bar{Y}$ - lateral displacements of centre of mass

$\bar{x}_c$ - location of the core from the centre of mass in 2-dimensional wall-frame building

Y_0 - excitation displacements amplitude

Z - vertical axis

α , β - parameters describing stiffness relationships in the Y and θ directions, respectively

Δ - longitudinal deformation in the wall

Δt - time interval

ϵ - longitudinal strain in the wall

λ_i - mode shape characteristic parameter

ϕ_{Yn} , $\phi_{\theta n}$ - flexural and torsional shape functions for the n^{th} mode of vibration, respectively

$\overset{N}{\phi}_{Yn}$, $\overset{N}{\phi}_{\theta n}$ - normalized shape functions for the n^{th} coupled mode of vibration, respectively

ρA - mass per unit height of the structure

ρI_m - mass moment of inertia per unit height of the structure

ζ - fraction of critical damping

θ - rotation of the floor cross-section about the centre of mass

ψ_m - phase angle of the m^{th} mode of steady forced vibration

ω_W - principal sectorial area of any point on the cross-section of the wall

ω_n - the n^{th} natural frequency of the free coupled vibration in radians per second

Ω - forcing frequency in radians per second

APPENDIX 3

Response Comparison

Response Parameter	Maximum Value due to		Response Spectrum
	Response Analysis	Response Spectrum	Response Analysis
Base Moment [$t.m$ ($K.ft$)]	4326 (31218)	6290 (45388)	1.45
Base Shear [t (K)]	226 (497)	216 (475)	0.95
Base Bimcment [$t.m^2$ ($K.ft^2$)]	12690 (300355)	16400 (388163)	1.29
Base Torsion * [$t.m$ ($K.ft$)]	277 (1999)	281 (2028)	1.01
Top Displacement [m (ft)]	0.1539 (0.5048)	0.1594 (0.5228)	1.03
Top Rotation [radians]	0.002836	0.002400	0.85

Table 14 - Comparison between the maximum response parameters obtained from the Dynamic Response Analysis and those computed by the Response Spectrum Technique.

By comparing these results it can be seen that the proposed method yields results which compare very well with those obtained by the response spectrum technique.

* The Base Torsion is computed at the centre of mass.